A Remark on Solvent Power of Various Solvents for High Polymers

By Toru KAWAI

(Received January 23, 1953)

The process of the interaction of long chain molecules with low molecular weight solvent molecules, which includes solubility, swelling, and plasticization, is of great importance both to research and to industry. The definition of solvent power still lacks precision; namely, the term of "good" or "bad" solvent has been employed vaguely in the discussions of viscosity, osmotic pressure, swelling, and other measurements.

The empirical parameter μ, which was introduced by Huggins[1] in his statistical treatment of high polymer solutions is well used as a measure of thermodynamic interaction between polymer and solvents. Although this parameter μ can be considered as a measure of solvent power, it cannot always explain the experimental results of viscosity, osmotic pressure, and swelling measurements. Indeed, systematic study, choosing various liquids for one polymer substance, reveals that the second virial coefficient in osmotic pressure expression represented by power series expansion in polymer concentrations, intrinsic viscosity and swelling ratio do not always show a good correspondence to the μ values. In this paper we shall analyse the meaning of μ in a more improved and empirically satisfying approximation, considering principally the volume effect of the solvent, and shall examine some experimental results in the light of this procedure.

Analysis of Parameter μ

From the well-known Flory-Huggins' theory of high polymer solutions the partial molal free energy of solvent is expressed by

$$\Delta\bar{F}_1 = RT\{\ln(1-v_2)+(1-1/x)v_2+\mu v_2^2\} \quad (1)$$

where v_2 is volume fraction of polymer, and x the volume ratio of polymer molecule to solvent molecule (number average). With the use of Eq. (1) justified to a large measure by experiment, a more careful consideration of the parameter μ is desirable. In the initial statistical treatment of Huggins,[1] μ consisted of a term $1/z'$, introduced from the calculation of the entropy of mixing (z': effective co-ordination number in hypothetical lattice sites[1]), to which was added a contribution from the heat of mixing. As mentioned in the later sections, the necessity of choosing unreasonably low values of z (co-ordination number) to fit the data has lead to abandonment of this original interpretation, but the separation of μ into entropy and heat terms is of quite general validity, and we may write[2]

$$\mu = \mu_S + \mu_H \quad (2)$$

Let us first consider μ_S for athermal solutions. In Table 1 the expressions of μ_S are summarized, being calculated from the results of the statistical evaluation of the entropy of dilution by several authors[1][3][4][5].

Table 1

Theoretical Expression of μ_s by Several Authors

Authors	$\Delta\bar{S}_1$	μ_S
Flory[3]	$-R[\ln(1-v_2)+v_2]$	0
Huggins[1]	$-R[\ln(1-v_2)-(1-1/x)(Z'/2)\ln\{1-)2v_2/Z')\}]$	$(1-1/x)/Z'$
Miller[4]	$-R[\ln(1-v_2)-(Z/2)\ln\{1-(2/Z)v_2(1-1/x)\}]$	$(1-1/x)^2/Z$
Guggenheim[5]	$-R[\ln(1-v_2)-(Zq_1/2)\ln\{1-(2/Zq_2)(x_2-x_1)v_2/x_2)\}]$ $(q=[x(Z-2)+2]/Z)$	$(1-1/x)^2/Z \quad (x_2 \geqslant x_1)$

Except Flory's original formulation[3], the theoretical expressions of μ_S are nearly equal to $1/z$. Experimentally μ_S falls between 0.3 and 0.5, far too high to be explained as merely $1/z$. This discrepancy is well interpreted in the following sections by consider-

1) M. L. Huggins, *Ann. N. Y. Acid Sci.*, 43, 1 (1942).
2) Within the accuracy of experiments μ is nearly independent on polymer concentration for many systems, but the μ_S or μ_H is not constant except in very dilute range. Therefore, our discussion is limited to that of high dilution.
3) P. J. Flory, *J. Chem. Phys.*, 9, 660 (1941).
4) A. R. Miller, *Proc. Camb. Phil. Soc.*, 35, 109 (1942); ibid., 39, 54, 131 (1943).
5) E. A. Guggenheim, *Proc. Roy. Soc.*, A183, 203 (1944).

CHEMISTRY HALL LIBRARY

ing chiefly the effect of segment size.

In the case when the heat of dilution is not zero, we must consider the problem of the preferential ordering induced in the solution by difference in the interaction energy. However, it was shown by Orr[6] and Guggenheim[7] that this effect does not introduce a serious error for high polymer solutions, and therefore, we shall neglect this effect for the time being. Thus we must consider the nature of μ_S and μ_H separately, in considerable detail, examining error due to over-simplified approximations or inadequate assumptions in the existing theories, which are not always applicable to the actual systems.

The Effect of Segment Size

In the majority of the existing theories of high polymer solutions, it has been assumed that the unit segment of polymer chain and solvent molecule are the same in shape and size. It requires that a section of the polymer chain which occupies a volume equal to that of one solvent molecule is also not very different in shape from the solvent molecule, and that it is equally free to occupy any one of $(z-1)$ cells in purely stereometric mean without considering the flexibility of the polymer chain. Considering the effect of flexibility of the chain also in addition to the above hindrance, perhaps steric in nature, Flory[8] modified his initial formulation of the entropy of dilution. If the solvent molecule is very small, or if there are limitations on the tortuosity which the chain may comfortably assume, then the size of the section of the chain which is free to orient itself at random, irrespective of the orientation of the preceding sections, may be equivalent to the volume occupied by several solvent molecules. Thus, he constructs a new lattice in which one cell will accomodate either β solvent molecules or one segment of the polymer chain, and obtains the same results as that of the writer[9] when the volume of "segment" is larger than that of solvent molecule as mentioned later. In the earlier papers[9][10], the writer calculated this effect of size and shape of solvent molecule and polymer "segment", and the result obtained may be written (Eqs. (9) and (11) in reference 9),

when $V_1 > V_2$,

$$\Delta\bar{S}_1 = -R\{(V_1/V_2[\ln v_1 + (1+1/x)v_2 + \mu_S v_2^2] + [1-(V_1/V_2)](\ln v_1 + v_2)\} = R[(V_1/V_2x)v_2 + (1/2 - \mu_S V_1/V_2) v_2^2 + \cdots\cdots] \quad (3)$$

when $V_1 < V_2$,

$$\Delta\bar{S}_1 = -(RV_1/V_2)[\ln v_1 + (1-1/x)v_2 + \mu_S v_2^2] = R(V_1/V_2)[v_2/x + (1/2 - \mu_S)v_2^2 + \cdots], \quad (4)$$

where V_1 and V_2 are molal volumes of solvent molecule and polymer "segment" respectively. Here, we assume the "segment" as a unit submolecule which must be determined by steric factor only[11], and is characteristic to the polymer chain without regard to the types of the solvent, whereas Flory[8] assumed it as a section of the polymer chain which occupies a volume equal to the solvent molecule. Considering that the above approximation of Flory may not be allowed when the section of the polymer chain extremely differs in shape from the solvent molecule the validity of the usual expression of the entropy of mixing, $\Delta S = -R[N_1 \ln v_1 + N_2 \ln v_2]$, fails when the section of polymer chain and the solvent molecule are extremely different in shape from each other even if the molal volumes are the same (See Eq. (8) in reference (9).) It is therefore evident that our assumption on the "segment" is more reasonable than that of Flory. Furthermore, it may be proper that this effect of segment size is separated from the effect of flexibility of the chain as in our treatment. Thus, we can improve the degreeof approximation because the term $(1-2\mu_S)$ may be considered as a probability factor modifying the purely random probability of finding adjacent polymer segments, whereas the Flory's modification was applied to his first approximation treatment[3] of high polymer solutions, which is an obvious oversimplification, as Flory himself recognized. It must be noted here that all the factors except the effect of the "segment" size are involved in μ_S in our treatment, because this treatment is proved to be very useful although it must be regarded as semi-empirical, and the theoretical limitations for further analysis of μ_S are increasingly apparent. In these factors, however, the effect of flexibility of the polymer chain is supposed to play the most important role, and hereafter, we are to employ f instead of μ_S which

6) W. J. C. Orr, *Trans. Faraday Soc.*, **11**, 320 (1944).
7) E. A. Guggenheim, *Proc. Roy. Soc.*, A**183**, 213 (1944).
8) P. J. Flory, *J. Chem. Phys.*, **10**, 51 (1942).
9) T. Kawai, This Bulletin, **25**, 336 (1952).
10) T. Kawai, This Bulletin, **24**, 269 (1951).

11) The types of the hypothetical lattice sites are determined by the stereometric relation between the solvent and the polymer (the shape and size of the solvent molecule and the polymer "segment"). However, the "segment" should be determined uniquely by the stereometric factors of the polymer molecule itself.

was usually employed and which involved the effect of segment size. This parameter f corresponds to the μ_S value theoretically estimated when the polymer segment and the solvent molecule are the same in shape and size (its value is nearly equal to $1/z$)[12], and depends upon properties (mainly flexibility) of the polymer chain alone. Thus, Eqs. (3) and (4) may be rewritten when $V_2<V_1$,

$$\Delta\bar{S}_1=R[(V_1/V_2x)v_2+\{1/2-(fV_1/V_2)\}v_2^2+\cdots\cdots] \quad (5)$$

when $V_2<V_1$,

$$\Delta\bar{S}_1=R[(V_1/V_2)\{v_2/x+(1/2-f)v_2^2+\cdots\cdots\}] \quad (6)$$

Application of The Above Treatment to The Osmotic, Viscosimetric and Swelling Measurements

We are going to examine the effect of segment size mentioned above on the results of the measurements of osmotic pressure, viscosity, and swelling ratio. Combining the expression of the partial heat of dilution of the solvent,

$$\Delta\bar{H}_1=KV_1v_2^2 \quad (7)[13]$$

with Eqs. (5) and (6), the usually employed μ may be expressed by

$$\mu=fV_1/V_2+KV_1/RT, \quad (8)$$

when, $V_2<V_1$ and

$$\mu=1/2-(V_1/V_2)(1/2-f)+KV_1/RT, \quad (9)$$

when $V_2>V_1$.

Osmotic Pressure: The second virial coefficient, A_2, in osmotic pressure expression represented by power series expansion in polymer concentrations, may be given as follows;

when $V_2<V_1$,

$$A_2=(RT/\rho^2V_1)(1/2-\mu)=(RT/\rho^2\{1/2V_2-f/V_1+K/RT\} \quad (10)$$

when $V_2>V_1$,

$$A_2=(RT/\rho^2\{1/2-f)/V_2+K/RT\} \quad (10)$$

(ρ is density of the polymer). Therefore, the order of magnitude of the A_2, values (accordingly the slope of the line drawn through points of π/C plotted against C) obtained in a series of measurements with a polymer substance and different solvents, may not always agree with that of the $(1/2-\mu)$ values. One of such examples was reported in an earlier paper.[14]

Viscosity: The intrinsic viscosity of dilute solutions of a given high polymer varies with the nature of the solvent. For flexible linear polymers, this variation of intrinsic viscosity may, according to Flory[15], be treated as a swelling phenomenon, and be interpreted in terms of the interaction between solute and solvent molecules, although only the long range interferences between segments belonging to remotely connected portions of the chain were considered in his treatment. In an earlier paper[16] the writer formulated exactly the relation between intrinsic viscosity and the thermodynamic parameter μ. This formulation was exactly equivalent to that for swelling phenomenon. Thus, we shall confine ourselves to show that the above treatment, in which the effect of "segment" size has been considered, can be applied to the formula of swelling equilibrium.[17]

Swelling:—According to Flory-Rehner,[18] when solvent in gel is in equilibrium with excess solvent, the condition attained is that the partial molal free energy of the solvent in the gel equals zero;

$$\Delta\bar{F}_{1g}=\Delta\bar{F}_{1m}+\Delta\bar{F}_{1el}=RT\{\ln(1-v_{2g})+v_{2g}+\mu_g v_{2g}^2\}+RT(\rho V_1/M_c)v_{2g}^{1/3}=0 \quad (12)$$

, where ΔF_{1m} is the osmotic and ΔF_{1el} the elastic contribution to the partial molal free energy. The notation of this equation is similar to what is usually employed.

Here, applying the above effect of "segment" size to Eq. (12), there is obtained

$$\ln(1-v_{2g})+v_{2g}+f(V_1/V_2)v_{2g}^2+(KV_1/RT)v_{2g}^2+AV_1v_{2g}^{1/2}=0 \quad (13)$$

when $V_2<V_1$, and

12) B. H. Zimm, *Am. Chem. Soc.*, Meeting Sept. 1947.

13) For application to the case in which strong mutual energy exists between unlike pairs, the constant K is employed here in a rather empirical meaning, instead of the form $\Delta\bar{H}_1=V_1[(\Delta E_1/V_1)^{1/2}-(\Delta E_2/V_2)^{1/2}]^2$ ($\Delta E_i/V_i$: cohesive energy density).

14) K. Ishikawa and T. Kawai, *J. Chem. Soc. Japan* (Ind. Chem. Section), **55**, 73 (1952).

15) P. J. Flory, *J. Chem. Phys.*, **17**, 103 (1949).

16) T. Kawai, This Bulletin, **25**, 341 (1952).

17) Yamaguchi deduced analogous results concerning the relation between intrinsic viscosity and the nature of solvents from an entirely different procedure (B. Yamaguchi and T. Oki. Paper read at the rheological meeting held by the Chemical society, the High Polymer Society, and the Physical society, on 4th, Dec. 1952, in Tokyo.)

18) P. J. Flory and J. Rehner Jr., *J. Chem. Phys.*, **11**, 512 (1943).

$$(V_1/V_2)[\ln(1-v_{2g})+v_{2g}+fv_{2g}^2]+(KV_1/kT)v_{2g}^2+AV_1v_{2g}^{1/3}=0 \quad (14)^{19)}$$

, when $V_2>V_1$.

Hence,

$$\mu_g=(V_1/V_2)f+KV_1/RT$$

, when $V_2<V_1$, and (15)

$$\mu_g={}^1/_2-(V_1/V_2)({}^1/_2-f)+KV_1/RT$$

, when $V_2>V_1$. (16)

Therefore, when $V_2>V_1$, volume swelling ratio ($={}^1/v_{2g}$) is a function of $({}^1/_2-\mu_g)/V_1$, and is independent upon V_1. When $V_2<V_1$, volume swelling ratio may be determined in somewhat different manner from the case when $V_2>V_1$. These problems will be discussed in the next section in more detail, being compared with experimental results.

Comparison with Experimental Results

Eqs. (13) and (14) will be tested from the measurement of the swelling of Boyer and Spencer[20] on styrene-divinylbenzene gels, which is one of the systematic studies in a large number of liquids differing widely in chemical type and in solvent power for a gel sample. In Table 2, one of their experimental results is analysed, attempting to show the better correspondence of the observed volume swelling ratio ${}^1/v_{2g}$ with $({}^1/_2-\mu_g)/V_1$ calculated from the above procedure, rather than with the parameter μ_g which have been usually interpreted in terms of the Flory-Rehner theory.

Table 2

Swelling of 0.0333% Divinyl Benzene Gels in Various Solvents at 23°C.

Solvents	Volume Swelling Ratio	μ_g	$(1/2-\mu_g)/V_1 \times 10^4$	$(1/2-\mu_g+\Delta\mu)/V_1\times 10_4$	V_1
Phenyl Cyclohexane	18.57	0.417	4.85	6.02(14)	171
sym-Tetrachloroethane	23.92	0.417	7.83	9.72 (1)	106
Styrene	21.96	0.424	6.61	8.35 (5)	115
Phenyl Acetylene	22.43	0.426	6.73	8.54 (4)	110
o-Xylene	20.98	0.427	6.03	7.69 (7)	121
m-Xylene	20.02	0.433	5.45	7.07 (9)	123
p-Xylene	19.63	0.436	5.18	6.80(11)	124
Toluene	20.72	0.440	5.63	7.51 (8)	107
Trichloroethylene	21.84	0.444	6.23	8.45 (6)	89.9
Thiophene	22.99	0.450	6.31	8.83 (2)	79.3
cis-Dichloroethylene	22.49	0.453	6.19	8.82 (3)	75.9
Cyclohexanone	19.08	0.453	4.53	6.45(13)	104
Tetrahydrofuran	21.0	0.455	2.18	3.00	217
Dimethylfuran	18.00	0.458	2.87	5.71(16)	104
sym-Triethylbenzene	13.72	0.458	2.27	3.35(18)	103
Perchlorethylene	18.31	0.459	3.99	5.93(15)	120.9
Pyridine	19.82	0.464	4.46	6.94(10)	80.7
Ethylidene Chloride	18.41	0.469	0.83	1.37	372
trans-Dichloro-1-nitroethane	19.24	0.469	3.70	6.08(12)	83.8
Nitrobenzene	15.72	0.475	2.44	4.39(17)	103
Aniline	11.99	0.503	−0.33	1.86(19)	91.4
Diethyl Carbonate	10.79	0.503	−0.25	1.40(20)	122
Ethyl Chloroacetate	10.29	0.510	−0.94	0.94(22)	106
r-Valerolactone	10.96	0.510	−1.10	1.10(21)	91.0
Propylene Oxide	12.7	0.590	−14.4	−1.01	69.4
Ethyl Laurate	65.3	0.570	−2.63	−11.5	266

The order of magnitude of the volume swelling ratios for the liquids given in Table 2 does not always correspond to that of the μ_g valves[21]. On the other hand, the order of their magnitude shows a better correspondence with that of the $({}^1/_2-\mu_g)/V_1$ values. (The larger the $({}^1/_2-\mu_g)/V_1$ values, the greater

19) Speculation of the "network" theory of Flory-Rehner leads to the conclusion that ΔF_{el}, the elastic contribution to the partial molal free energy, should be expressed by the form $AV_1v_{2g}^{1/3}$, where A is a constant characteristic to the network structure, rather than by the form $(\rho V_1/Mc)v_{2g}^{1/3}$, which involves Mc explicitly.

20) R. F. Boyer and R. S. Spencer, *J. Polymer Sci.*, 3, 97 (1948).

21) In many cases, the molal volumes of solvents do not differ very much from each other, and in such cases, the order of magnitude of the volume swelling ratios agrees with that of the μ_g values.

the solvent power, whereas the smaller the μ_9, the greater the solvent power.)

However, the regularity of this correspondence fails for a few liquids which are given under the line of ethylchloroacetate in Table 2. These discrepancies are completely removed by applying the following correction. In an earlier paper[22] it was pointed out that the values of μ_9 calculated from swelling measurements are usually larger than those of μ obtained by osmotic measurements, and that, generally, the magnitude of these discrepancies is about 0.02[22] (which was determined approximately from many experimental results). These corrected values, $(1/2-\mu_9+\Delta\mu)/V_1$, are given in the fourth column in Table 2, where the number in the parentheses shows the order of magnitude of these values. A satisfactory correspondence is obtained between the volume swelling ratio and these values, whereas such a complete correspondence fails for the μ_9 values. Now, there are three exceptional cases of tetrahydrofran, ethyl laurate and ethyliden chloride, in which the V_1 values are much larger than in the other cases. This exception may be well interpreted by Eq. (15), although the solvent power of these three liquids cannot be compared with that of the other liquids due to the uncertainty of the V_2 value[23].

This paper was read at the Meeting of Soc. of High Polymer, Japan, in Kanazawa, on 8th Nov., 1952.

The author expresses his apprecation to Professor H. Maeda and K. Makishima for their encouragement and support of this work.

Laboratory of Textile Chemistry,
Tokyo Institute of Technology, Tokyo

22) T. Kawai, This Bulletin, **21**, 691 (1951). Probably, these discrepancies are due to over-simplification in the network theory of Flory (See P. J. Flory, *J. Chem. Phys.*, **18**. 108 (1950).

23) In the writer's opinion, the V_2 values should be determined through systematic study of experimental results, employing Eqs. (15) and (16). In this experiment of Boyer and Spencer, available data is too scanty to discuss quantitatively the case of $V_2>V_1$. From Table 2, the value of V_2 of this polymer is supposed to be about 100. It must be noted, however, that Eq. (16) may hold approximately even in the range $V_1>V_2$ so long as the difference between V_1 and V_2 is not considerably large, because the μ value should, according to Eqs. (15) and (16), decrease as V_1 increases ($V_1<V_2$), and become equal to that calculated from Eq. (1) when $V_1=V_2$, and then increases ($V_1>V_2$).

Studies of Molecular Structures by Electron Diffraction. I. The Molecular Structure of Monofluoro- and Monobromobenzenes

By Tooru YUZAWA (†) and Mashio YAMAHA

(Received February 26, 1953)

The molecular structures of monofluoro- and *o*-difluorobenzenes with regards to the C-F distance from the resonance theory were investigated by Dr. H. Oosaka[1] using electron diffraction method. Recently a new apparatus which is capable of giving photographs of large scattering angle diffraction pattern has been constructed in our laboratory. We have reinvestigated the molecular structure of monofluorobenzene and also investigated the structure of monobromobenzene and determined the lengths of C-F, C-Br and C-C bonds using this new apparatus.

Experimental

The new apparatus is of the vertical hot cathode type, and the accelerated electron beam from the cathode is focused by an electromagnetic coil. The camera length is about 91 mm. The wave length of the electron beam is 0.062~0.054 Å, which is calibrated by the gold photographs.

Monofluorobenzene (boiling point: 85.0°C.) was synthesized[2] by the following reaction:

$$C_6H_5NH_2+HBF_4+NaNO_2 \xrightarrow[\text{ice cold}]{HCl} C_6H_5N_2BF_4 \xrightarrow{heat} C_6H_5F+N_2\uparrow+BF_3\uparrow.$$

Commercial monobromobenzene was purified by distillation. (Boiling point: 154.0°C.).

Results and Discussion

The theoretical intensity curves for several assumed molecular models have been calculated by the formula[3],

$$I=k\sum_i\sum_j Z_iZ_j/r_{ij}\cdot\exp(-b_{ij}q^2)\cdot\sin qr_{ij},$$

where $q=10s/\pi, s=(4\pi\sin\theta/2)/\lambda$, θ the scattering angle, and λ the wave length of the beam. The thermal vibration factore $\exp(-b_{ij}q^2)$ is ignored here[4].

In Table 1 are shown the assumed interatomic distances of the molecular models with marks from A to H for fluorobenzene and from J to O for bromobenzene. The coplanarity of the benzene ring and the attached halogen atom is assumed for all models. The visual intensity curves of ten or more photographs of each substance are compared with the theoretical curves in Figs. 1 and 2. The q-values at the measured maxima and ratios $q/q_{obs.}$ with the deviations of the theoretical q-values from the observed are listed in Tables 2 and 3 for each substance.

Table 1

Assumed Molecular Models Corresponding Interatomic Distances (cf. Figs. 1 and 2)

	C—C	1.38	1.40	1.42 (Å)
C—F:	1.27 (Å)	A	D	
	1.31	B	E	(H)
	1.35	(C)	F	
C—Br	1.86	J	L	(N)
	1.88	K	M	O

In order to determine the consistent molecular models, we have compared the shapes and q-values of maxima of theoretical curves. and found the following characteristic features

For monofluorobenzene, 1) the 7th maximum is influenced by C—C distance variation, 2) the 4th and the 6th maxima, and the separation between the 3rd and the 4th change by C—C and C—F distances, and 3) the shape of the 9th and the 10th maxima has the characteristic feature for C—F variation, and it also depends slightly on the thermal vibration of the molecule (See Fig. 1).

For monobromobenzene, 1) generally, the q-values of intense maxima shift sligtly by the variation of C—C distance, and 2) the 6th, 8th and 11th maxima as well as the shape of the 4th maximum change with C—Br (See Fig. 2).

These considerations lead us to the conclusion that:

1) H. Oosaka, This Bulletin, **15**, 31 (1940). cf. C. Finbak & O. Hassel, *Arch. Math. Naturvidenskab*, 45, No. 3,8 (1941).

2) "Organic Synthesis" XIII, p. 46.

3) R. Spurr and V. Schomaker, *J. Am. Chem. Soc.*, **64**, 2393 (1942). cf. L. Pauling and L. O. Brockway, *J. Am. Chem. Soc.*, **57**, 2684 (1935).

4) The influence of various thermal vibrations is small as will be seen in our next report on difluorobenzenes (3).

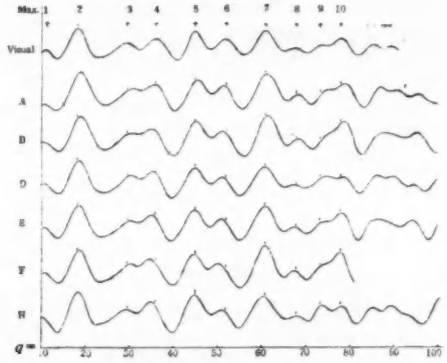

Fig. 1. Theoretical and Visual Intensity Curves for Monofluorobenzene.
The measured q-values of maxima are shown by arrows and dots on each curve. (These are the same in Fig. 2.)

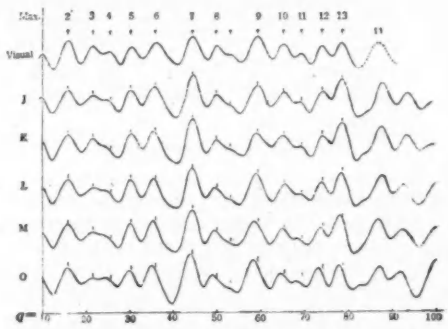

Fig. 2. Theoretical and Visual Intensity Curves for Monobromobenzene

Table 2

Observed q-values and the Comparison of Measured and Theoretical Values for Monofluorobenzene.

Models		A		B		D		E		F		
Max.	$q_{obs.}$	q/q_0	dev. (q's)	q/q_0	dev. (q's)	q/q_0	dev. (q's)	q/q_0	dev. (q's)	q/q_0	dev. (q's)	wt.
1	11.05	—	—	—	—	—	—	—	—	—	—	
2	18.05	1.042	+0.75	1.042	+0.75	1.036	+0.65	1.025	+0.45	1.019	+0.35	1
3	29.35	1.048	+0.41	1.024	+0.7	1.031	+0.9	1.028	+0.8	1.024	+0.7	1
4	35.80	0.997	−0.1	0.986	−0.5	0.989	−0.4	0.972	−1.0	0.964	−1.3	2
5	44.80	1.018	+0.8	1.011	+0.5	1.009	+0.4	0.998	−0.1	0.996	−0.2	2
6	51.90	0.990	−0.5	0.983	−0.9	0.981	−1.0	0.976	−1.2	0.970	−1.5	1
7	60.66	1.012	+0.9	1.011	+0.6	0.996	−0.2	0.996	−0.2	0.996	−0.2	2
8	67.62	1.012	+0.8	1.012	+0.7	1.004	+0.3	0.999	−0.1	0.998	−0.1	1
9	diffuse											
10	77.31	1.023	+1.4	1.017	+0.9	1.015	+0.7	1.009	+0.3	1.001	−0.3	1
*												
mean av.		1.017_8		1.010_7		1.007_5		1.000_2		0.995_2		
av. dev.		0.014_9		0.013_4		0.015_2		0.016_0		0.014_8		
wt. mean av.**		1.015_5		1.008_1		1.004_9		0.997_0		0.993_1		
mean sq.av. dev.		0.78		0.63		0.58		0.68		0.76		

* See Fig. 1. for outer halos.

** Used weights for each maximum are shown in the last column. In these average values the contribution of the C-C variation is predominant.

Table 3

Observed q-values and the Comparison of Measured and Theoretical Values for Monobromobenzene.

Models		J		K		L		M		O	
Max.	$q_{obs.}$	q/q_0	dev. (q's)	q/q_0	dev. (q's)	q/q_0	dev. (q's)	q/q_0	dev. (q's)	q/q_0	dev. (q's)
2	15.97	1.005	+0.08	0.996	−0.07	0.996	−0.07	0.989	−0.17	0.989	−0.17
3	21.56	1.020	+0.4	1.007	+0.14	1.011	+0.24	1.009	+0.19	1.011	+0.24
4	25.65	—	(−0.6)	—	—	—	—	—	(−0.8)	—	—
5	30.40	1.007	+0.2	1.005	+0.15	0.997	−0.1	0.993	−0.2	0.987	−0.4
6	35.97	0.997	−0.12	0.988	−0.42	0.990	−0.37	0.988	−0.42	0.979	−0.8
7	44.47	1.005	+0.2	1.002	+0.1	0.997	−0.12	0.996	−0.2	0.991	−
8	49.95	1.001	+0.15	0.999	−0.05	0.994	−0.3	0.989	−0.5	0.979	−0.8
	shelf										

9	59.44	$1.003_4+0.06$	$0.994-0.3$	$0.991-0.5$	$0.986-0.8$	$0.982-1.1$
10	65.30	$1.006+0.4$	$0.997-0.2$	$0.999-0.05$	$0.992-0.5$	$0.989-0.8$
11	69.40	$0.996-0.3$	$0.994-0.4$	$0.994-0.4$	$0.987-0.9$	$0.984-1.1$
*						
mean av.		1.004_4	0.997_8	0.996_6	0.992_3	0.989_0
av. dev.		0.004_7	0.004_2	0.001_6	0.004_9	0.005_6
mean sq. av. dev.		0.24	0.24	0.28	0.48	0.74

* See Fig. 2 for outer halos.

C—F = 1.30±0.03 Å for monofluorobenzene, C—Br = 1.86±0.02 Å for monobromobenzene, and C—C = 1.39±0.02 Å for the both.

This C—F length of monofluorobenzene is shorter than the previously reported value 1.34 Å[1], but is more accurate since the outer halos are taken into account in this case. We are investigating the carbon-halogen distances of various halogenated benzenes containing fluorine atom. For instance, the value 1.30 Å for C—F bond are obtained for *m*- and *p*-difluorobenzenes[5].

The Pauling formula, which shows the shortening of the bond length in the molecule with resonance structures, is

$$R = R_s - (R_s - R_d)(3x/2x+1),$$

where x is the double bond character, R_s and R_d are the interatomic distances[6] for a single and double bond respectively, and R is the resultant intermediate distance. The values of x estimated from our observed bond lengths are 29% for C—F of monofluorobenzene and 25% for C—Br of monobromobenzene. If we use the corrected values of R_s, 1.355 Å for C—F and 1.883 Å for C—Br, which are the length of the normal single bond proposed by Pauling and Schomaker[7], we obtained 16.9% for C—F and 13.3% for C—Br.

Summary

The molecular structures of monofluorobenzene and monobromobenzene have been investigated by the electron diffraction method. The C—F and C—Br distances in each molecule have been determined as 1.30±0.03 A and 1.86±0.02 Å respectively. These distances are shorter than the case in which the bonds have the normal single bond characters. The double bond characters for these bonds have been calculated and obtained 16.9% for C—F and 13.3% for C—Br, in which we have considered the corrected single bond lengths in both cases.

Acknowledgment

We would express our deep gratitude to the late Professor H. Oosaka for his guidance, especially for having suggested to us the study of this problem; to Mr. M. Tanaka, Director of Kichô Shindôsho Factory, for having offered to us very useful material for the construction of the apparatus; and also to Mr. S. Uchida for his kind help in its actual construction.

Department of Chemistry, Faculty of Science, Tokyo University of Education, Tokyo

5) Published shortly (we have investigated for p- and o-fluorochlorobenzenes, p-fluorobromobenzene and m- and p-difluorobenzenes).

6) L. Pauling, "The Nature of the Chemical Bond" p. 175 (1940).

R_s=1.41Å, 1.91Å for C-F, C-Br respectively, and R_d=1.21Å, 1.81Å for C=F, C=Br respectively.

7) L. Pauling and V. Schomaker, *J. Am. Chem Soc.*, **63**, 37 (1941).

$R_{AB}=R_A+R_B-\beta|x_A-x_B|$, values for C-F, C-Br bonds are as follows:

R_C=0.77Å*, R_F=0.72Å, R_{Br}=1.14Å*, x_C=2.5, x_F=4.0, x_{Br}=2.8, β=0.09. C-F: 0.77+0.72−0.09(4.0−2.5)=1.355Å, C-Br: 0.77+1.14−0.09(2.8−2.5)=1.883Å.

*) proposed by Pauling and Huggins.

New Colorimetric Microdetermination of Vanadium in Natural Waters*

Ken SUGAWARA, Motoharu TANAKA and Hideo NAITÔ

(Received March 2, 1953)

I. General description

A new colorimetric method of the determination of vanadium was established which allows to separate and determine a few μg. of this element with a two figure accuracy from a bulk of water as large as 20 liters.

The procedure consists of three main steps: (1) Coprecipitation of the element with ferric hydroxide. (2) Separation of vanadium from the coprecipitant and other accompanied elements. (3) Final colorimetry of vanadium oxinate in amyl alcohol.

The concentration by coprecipitation saves much time, which is required in the ordinary evaporation method, and avoids at the same time loss of vanadium into a large bulk of residue, produced when the latter method is applied.

The intense coloration of vanadium oxinate in amyl alcohol makes the determination of a few μg. of the element possible[1], a quantity lying close to the limit in the current phosphotungstovanadate method[2].

II. Procedure

Step 1. Take a sample of 5 to 20 liters depending upon the probable content of vanadium. Acidify with hydrochloric acid, add ferric nitrate solution to give a solution containing 10 mg. of iron per liter and then 1 cc. of 1 *M* sodium hypochlorite solution per one liter. While warming on a water bath the solution is neutralized with 2 *N* ammonium hydroxide to bromthymol blue or bromcresol purple and then filtered.

Step 2. Ignite the paper and its contents in a platinum crucible. The ash is ground with 3 g. of anhydrous sodium carbonate in an agatemortar, transferred in a platinum crucible and fused for 40 to 60 minutes by a full burner. The cake obtained is transferred into a small beaker and the crucible is rinsed with hot water. Add 2 to 5 drops of hydrogen peroxide, then 30 to 40 cc. of water in order to digest the entire mass. When digestion is complete, the contents of the beaker are filtered through a small filter paper of fine texture which is previously washed with 20% hot solution of sodium carbonate. Wash the residue with hot 2% sodium carbonate solution.

Step 3. The joint filtrate is neutralized to *p*-nitrophenol by sulfuric acid in expelling the liberated carbon dioxide. Add 2.5 cc. of 4 *N* sulfuric acid in excess and set the solution aside to cool to room temperature. Add 1 cc. of 5% malonic acid solution and 0.5 cc. of 2% oxine solution. The whole is transferred into a separatory funnel and mixed with 4 cc. of 4 *N* sodium acetate for buffer with constant stirring. Add 3 cc. of chloroform, shake for one minute and the layers are left to separate. The chloroform layer is drawn off into a platinum crucible. Add 1 cc. of chloroform to the funnel to wash its stem. Then 2 cc. of chloroform and 0.2 cc. of oxine solution are added. Shake vigorously. After leaving it to stand still, the chloroform layer is drawn out into the platinum crucible. Two to three extractions are sufficient to remove all the oxinate when the last chloroform extract remains faintly yellowish due to oxine itself.

Step 4. Add 1 g. of sodium carbonate to the united chloroform extract, evaporate to dryness at a lower temperature on a water bath. The residue is heated by a burner in order to destroy the organic matter and finally fused by a full burner.

Step 5. The melt is digested with water, filtered and neutralized to *p*-nitrophenol. Adding 1 cc. of 4 *N* sulfuric acid, the solution is once heated to boil and left with immersing in cold water. The volume of the solution is made up to 70 to 100 cc. Add 0.5 cc. of the oxine solution and 6.0 cc. of 2 *N* ammonium hydroxide with constant stirring. In case any white precipitate is formed, the solution should be diluted till it dissolves. Transfer the solution into a separatory funnel, add 10 cc. of benzene and shake vigorously for one minute. Two benzene extractions remove ferric oxinate completely.

Step 6. The remaining aqueous layer is mixed with 4 cc. of sodium acetate solution and 4.5 cc. of 4 *N* sulfuric acid, whereby the *pH* is adjusted to about 4.

Add 0.2 cc. of the oxine solution and extract with amyl alcohol. The extraction is repeated till the final fraction bears no perceptible coloration. The united extract is transferred into a

* The following two methods have been proposed for similar purposes; (1) M. Ishibashi, T. Shigematsu and Y. Nakagawa, *Bull. Inst. Chem. Research*, Kyoto Univ., Kyoto Japan. **24**, 68 (1951), (2) J. M. Bach and R. A. Treiles, *Bol. obras sanit. nacion Buenos Aires*, 5 127 (1941); *Chem. Abstracts*, **36**, 859 (1942); ibid., **35**, 545 (1941). In the former vanadium is coprecipitated with ferric cupferronate and determined by the current phosphotungstovanadate method, while in the latter the oxinate is extracted by isoamyl alcohol.

1) E. Sudo, *J. Chem. Soc. Japan*, **72**, 817 (1951).

2) E. B. Sandell, "Colorimetric Determination of Traces of Metals" Interscience Publishers Inc. New York, p. 607 (1950).

10 cc. measuring flask and diluted to the mark with amyl alcohol. Then the optical density of the solution is determined by the spectrophotometer at wavelength of 475 mμ.

III. Discussion

1) Ferric hydroxide as coprecipitant.—The recovery of vanadium in the coprecipitation with ferric hydroxide is practically 100% at the *pH* ranges of bromthymol blue and bromcresol purple. The following experiment showed this.

Various amounts of iron and vanadium were added to dilute hydrochloric acid solution, neutralized with ammonium hydroxide to different kinds of indicator whose *Hp* ranges differ. The vanadium content of the formed precipitate was determined (See Table 1).

Table 1

Optimum *pH* Range for the Coprecipitation of Vanadium with Ferric Hydroxide

Indicator	*pH* range	V added μg.	V found μg.	Error %
Methyl orange	3.1–4.5	27.9	26.0	−6.8
Bromcresol purple	5.2–6.8	27.9	28.0	+0.4
Bromthymol blue	6.0–7.6	27.9	28.1	+0.7
Phenolphthalein	8.0–9.8	27.9	26.7	−4.3
Ammonia in excess		27.9	26.4	−4.7

It is also notable that five dissolution-precipitations of the precipitate did not give any loss.

2) Amount of iron required for the complete precipitation of vanadium.—Seven mg. of iron per liter is sufficient to precipitate 0–27.9 μg. of vanadium and an amount up to 150 mg. gives no interference. Table 2 shows it.

Table 2

Coprecipitation of Vanadium with Ferric Hydroxide

Fe added mg.	V added μg.	V found μg.	Error %
150	0	< 1.0	
150	27.9	26.8	− 3.9
100	27.9	27.6	− 1.1
50	27.9	27.6	− 1.1
10	27.9	28.1	+ 0.7
10	27.9	28.3	+ 1.4
10	27.9	28.0	+ 0.4
7	27.9	27.9	0.0
7	27.9	28.1	+ 0.7
5	27.9	26.2	− 6.1
5	279	239	−14.3
2	27.9	17.8	−36.2
0	27.9	1.3	−95.4

3) Separation of iron from vanadium.—Oxine gives colored compounds with various kinds of elements other than vanadium, which can be extracted by organic solvents. Thus careful separations of these elements are required to precede a successful determination of vanadium.

Iron is the first to be considered, its separation being caused at two different stages in the writers' procedure; (1) leaching process of the melt of carbonate fusion and (2) oxinate extraction by benzene.

According to E. B. Sandell the recovery of vanadium at (1) is complete for silicate materials. The writers confirmed it on melts particularly rich in iron as shown in Table 3

Table 3

Separation of Vanadium from Iron in Step (1)

Fe added mg.	V added μg.	V found μg.	Error %
50	27.9	27.7	−0.7
50	27.9	27.6	−1.1
150	0	<1.0	

In order to check the point (2), the following experiment was done.

Different amounts of iron and vanadium were added to a series of 50 cc. waters, containing 3 g. of sodium carbonate, which were divided into four groups to be treated in different ways. Group 1. After being neutralized with sulfuric acid to phenolphthalein, oxine was added and the formed ferric oxinate was separated by shaking with benzene. Groups 2 and 3. After being neutralized with sulfuric acid, 1 cc. and 0.5 cc. of 2 *N* sodium carbonate solution were added respectively and then oxine. The formed oxinate was

extracted by benzene. Group 4. 1 cc. of 4 *N* sulfuric acid was added in excess after it was neutralized. Oxine was then added and the solution was made alkaline with 6 cc. of 2 *N* ammonium hydroxide. The formed oxinate was extracted. The residual solutions from the four different treatments were regulated to *pH* 4 with a mixture of sulfuric acid and sodium acetate, then extracted by amyl alcohol. Vanadium was determined in the extract. Table 4 shows the result in which Group 4 gives the best result.

Table 4

Separation of Vanadium from Iron in Step (2)

	Fe added μg.	V added μg.	V found μg.	Error %
Group 1	0	55.8	55.0	− 1.4
	0	0	<1.0	
	100	55.8	47.3	−13.7
Group 2	0	55.8	55.1	− 1.3
	100	0	<1.0	
	100	55.8	55.1	− 1.3
	100	55.8	61.3	+ 9.9
Group 3	100	55.8	54.0	− 2.9
	100	55.8	55.0	− 1.4
Group 4	100	55.8	56.0	+ 0.4
	100	55.8	55.9	+ 0.2
	100	55.8	55.8	0
	100	55.8	56.3	+ 0.9

4) Interference by other elements.—Aluminum, manganese and silicon are other elements which are usually encountered in tural waters and coprecipitated with iron, thus probably causing some interference.

Aluminum.—A greater part of aluminum moves into the filtrate, when the melt from carbonate fusion is leached and expected to be extracted by organic solvents, in forming oxinate at a *pH* range 4.5—9.8[3]. The oxinate formation, however, can be avoided by masking the element with malonic acid in a slightly acidic solution. The following experiment shows it.

A series of acid solutions containing various amounts of vanadium, 10 mg. of aluminum and 50 mg. of iron was treated with ammonium hydroxide. The precipitates obtained were processed following the steps 2—6 in the procedure to determine vanadium. The result is given in Table 5.

Manganese.—Manganese is reduced by hydrogen peroxide to form precipitate in step 2 of the procedure. In case the manganese content is large, there may form a large bulk of precipitate with a considerable retention of vanadium. However it was shown that an amount of manganese up to 50 mg. does not matter as shown in Table 5.

Table 5

Interferences by Aluminium and Manganese

		Fe added mg.	V added μg.	V found μg.	Error %
Al	10 mg.	50	0.0	<1.0	
	„	„	27.9	27.7	−0.7
	„	„	11.2	10.9	−2.7
	„	„	5.6	5.5	−1.8
Mn	5 mg.	10	27.9	27.9	0
	50	„	27.9	26.4	−5.4

3) E. Sudo, *J. Chem. Soc. Japan*, **72**, 718 (1951).

Table 6

Examples of Application

Description	Sample taken	V added	V found
Ground water rich in silicate from a well in the campus of Nagoya University (126 mg. SiO_2/L)	10 L		13.7 μg.
	10 „	11.2 μg.	24.6 „
Surface water of Lake Yogo-ko, Shiga Pref. (Aug., 1951)	20 „		8.9 „
Surface water of Lake Kizaki-ko, Nagano Pref. (Dec., 1952)	20 „		3.9 „
A spring water from Higashiyama area, Nagoya City	20 „		0.8 „
Bottom deposits of Lake Yogo-ko	24.7 mg.		0.018%*
	24.7 „		0.017 „
	24.7 „		0.018 „

* by the current phosphotungstovanadate method.

Silicon.—Silicon in the water is coprecipitated with iron and separates as jelly, when the melt from carbonate fusion is leached and neutralized, thus any vanadium is probably retained. However the retention does not occur so long as the silica content of the water does not exceed 126 mg. per liter: an analysis of a 10 liter sample of well water originally containing 1.26g. of SiO_2 and 13.7 μg. of vanadium, with an additional 11.2 μg. of the latter element, gave a satisfactory vanadium value, 24.6 μg. (See Table 6).

5) Colorimetry.—The following is notable concerning the colorimetry of vanadium oxinate in amyl alcohol.

a) The Lambert-Beer's law is strictly obeyed from 0.00 up to 10.0 μg. of vanadium per ml. In case the optical density at 475 mμ is measured, using "Coleman model 14 Universal spectrophotometer", the following relation holds good;

$$X=\frac{E-0.023}{0.0117}$$

where X—the amount of vanadium in μg. per 10 ml. of amyl alcohol
E—the optical density when an accessory "round cuvette", with effective cell thickness 13.06 mm., is used

b) The color developed undergoes no measurable change within 24 hours.

c) The recovery of vanadium by extraction depends largely on the quality of amyl alcohol. Hence a careful purification of amyl alcohol is needed and a preliminary test of its quality by extracting a known amount of vanadium is recommended.

6) Appilcation to silicate materials.—The present method, originally developed for water analysis, may be applied to common silicate materials. An example of its application to the bottom deposits of Lake Yogo-ko, Shiga Prefecture, is given in comparing with the value for the same sample by the current phosphotungstovanadate method at the bottom of Table 6, in which some data for terrestrial waters are collected.

The writers wish to express their deepest thanks to the Trustees of the Elizabeth Thompson Science Fund who decided to donate a grant for supplying the Faculty of Science, Nagoya University, with a universal type Coleman spectrophotometer by the aid of which the present research was accomplished.

Chemical Institute, Faculty of Science, Nagoya University

The Crystal Structure of Chlorodinitro-triammine-cobalt. III.

By Yoshimichi TANITO, Yoshihiko SAITO and Hisao KUROYA

(Received March 18, 1953)

Introduction

In the absorption spectra of aqueous solution of chlorodinitrotriammine-cobalt III, $[Co(NH_3)_3(NO_2)_2Cl]$, the third absorption band was found at $\lambda=2500$Å with log $\varepsilon=4.4$[1], and therefore, it has been postulated that two of the negative radicals are co-ordinated in trans-positions with respect to each other. Since there are three negative ligands in the molecule, there remain the following two possibilities about the configuration of this molecule as shown in Fig. 1.

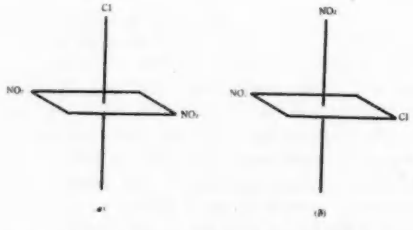

Fig. 1 Two possible forms of $[Co(NH_3)_3(NO_2)_2Cl]$, having two negative radicals in *trans* positions.

1) M. Kobayashi, A. Hagitani, and I. Mita: *J. Chem. Soc. Japan*, **58** (1937) 391.

In order to decide between (a) and (b) we have attempted to investigate the crystal structure of this compound by means of X-rays.

Unit Cell and Space Group

Chlorodinitro-triammine-cobalt (III) was prepared from trinitro-triammine-cobalt (III) and hydrochloric acid according to the method described by Jörgensen.[2] The crystals for this work were grown by slow evaporation of saturated aqueous solution containing a small amount of acetic acid at about 20° C. in a dessicator containing calcium chloride.

They are dark red tetragonal bipyramids, the effective dimensions of which are 0.4 mm. in each dimensions.

Making use of these crystals, oscillation photographs were taken around the [110] and [001] axes.

The unit cell dimensions were found from high order reflections. They are:

$$a=9.87\pm0.02\ \text{Å},\quad c=16.51\pm0.05\ \text{Å}.$$

The unit cell contains eight formula units. The calculated density is 1.961 g./cc., whereas the observed value was 1.952 g./cc. determined at 10°C. by the pyknometer method.

The Laue symmetry was found to be C_{4h}-$4/m$.

The systematic absences are: (hkl) present only with $h+k+l$=even, $(hk0)$ present only with $h=2n$, $k=2n$, and $h+k=4n$, and $(00l)$ present only with $l=4n$, so that the space group is C_{4h}^{6}-$I4_1/a$.

The intensities of the diffraction maxima were estimated visually by comparison with a time-exposure calibrated standard and converted into structure amplitudes in the usual way, which were later placed on an absolute scale by comparison with the calculated values.

Analysis

The space group $I4_1/a$ possesses sixteen general positions, and since the unit cell contains eight units of $[Co(NH_3)_3\ (NO_2)_2\ Cl]$, it may be concluded that 16 N (nitro), 16 N (ammonia), and 32 O probably lie in general positions, while the other 8 Co, 8 Cl and 8 N ammonia) must occupy special positions.

The possible eight fold special positions for these Co, Cl and N atoms are: $(00z)$, etc., which lie on two fold axes, sets of symmetry centres at (0, 1/4, 1/8), etc., or (0, 1/4, 5/8) etc., or otherwise, two sets of four fold positions at (000), $(00\frac{1}{2})$, etc., in the four fold inversion axes.

It is quite natural to assume an octahedral co-ordination around a cobalt atom as shown in Fig. 1.

Since the symmetry $\bar{1}$ and also $\bar{4}$ cannot be achieved by any octahedral arrangement of the ligands around a central atom, it may be concluded that the cobalt atom lies on a two-fold axis, having two NO_2 and two NH_3 groups in trans-positions with respect to each other, and a Cl atom and one NH_3 group being on the two-fold axis (Fig. 1 (a)).

A trial model of a molecule was derived from the knowledge of interatomic distances and bond angles found in our previous works on cobaltic complexes.[3][4][5] The approximate coordinates for those atoms which lie on the symmetry axis were easily deduced from packing considerations.

A Patterson projection P (xy) was synthesized, from which the azimuthal orientation of the complex molecule could be readily deduced.

Approximate coordinates for all the atoms were then written down, and the structure amplitudes for about 60 planes $(hk0)$ and $(h0l)$ were calculated. The agreement was reasonably good, and enabled a start to be made with the process of refinement by means of Fourier syntheses. These parameter values were used for a calculation of the signs of the $F(hkl)$ values, the origin of coordinates being shifted on a center of symmetry at (0, 1/4, 1/8).

Successive refinement of these parameter values was made by two dimensional Fourier syntheses $\rho(xy)$ and $\rho(xz)$. Then Fourie syntheses along lines parallel to the c-crystal axis were made at the values of x and y obtained from the two-dimensional projection. It was found that the maxima on these lines were sharp, and by taking these new maxima as new z-coordinates and then repeating the process of structure amplitude calculation and Fourier syntheses, refinement was achieved fairly rapidly. After five stages of these refinement processes all the $F(hkl)$ values were involved in a final set of line syntheses. One of the results is shown in Fig. 2. Finally, all the structure amplitudes were inserted as terms of a three-dimensional Fourier syntheses which was computed in sections perpendicular to c axis at the values obtained in the line syntheses for Co, $O_{(1)}$ and $O_{(2)}$. The result is shown in Fig. 3. The final parameter values obtained from these Fourier syntheses are listed in Table 1.

2) S. M. Jörgensen: *Z. anorg. Ch.* **7**. 310 (1894); **13**, 180 (1897).

3) Y. Tanito, Y. Saito and H. Kuroya: This Bulletin, **25**, 188 (1952).

4) Y. Tanito, Y. Saito and H. Kuroya: This Bulletin, **25**, 328 (1952).

5) A. Nakahara, Y. Saito and H. Kuroya: This Bulletin, **25**, 331 (1952).

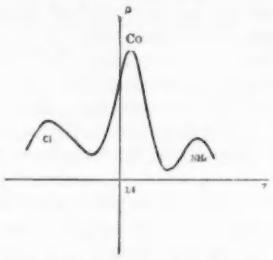

Fig. 2 Electron density along a two-fold axis, showing positions of Cl, Co and NH_3

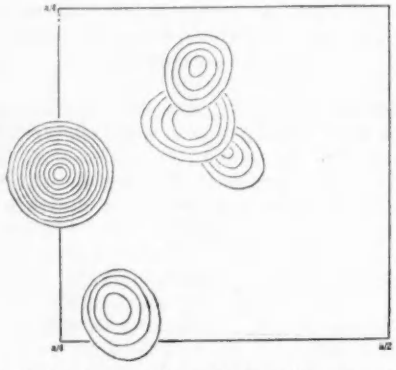

Fig. 3 Superposition of three-dimensional Fourier sections for [Co $(NH_3)_3$ $(NO_2)_2$ Cl]. Those for Cl and NH_3 (1) are not shown, which lie above and below Co respectively. The electron-density contours are drawn to an arbitrary scale.

Table 1.
Parameter Values Found for [Co $(NH_3)_3$ $(NO_2)_2$ Cl] (Values in fractions of the cell dimensions)

	x	y	z
Co	0	0	0.267
Cl	0	0	0.128
N (1) (ammonia)	0	0	0.382
N (2) (ammonia)	0.077	−0.186	0.267
N	0.187	0.075	0.267
O (1)	0.215	0.180	0.304
O (2)	0.275	0.015	0.230

The atomic scattering factors used in computing the structure amplitudes were those given in the International Tables. The value of B in the temperature factor was given the value 2.5 Å^2.

The figure of merits $\Sigma||F_o|-|F_c||/\Sigma|F_o|$ is 0.26 for all the (hkl) data, for which only observed 330 reflections up to $\sin\theta/\lambda=0.49$ have been included. Fig. 4 gives a general indication of the agreement between the calculated and experimental F values.

Description of the structure

The crystal consists of [Co $(NH_3)_3$ $(NO_2)_2$ Cl] molecules and Fig. 5 gives a perspective drawing of the structure. Interatomic distances and interbond angles are listed in Table 2.

A molecule of [Co $(NH_3)_3$ $(No_2)_2$ Cl] is illustrated in Fig. 6. It has a two fold axis of symmetry. Two nitro-groups and two ammonia molecules, NH_3 (2), are co-ordinated to a cobalt atom in trans-positions respectively. These four nitrogen atoms form a square around a cobalt atom within experimental

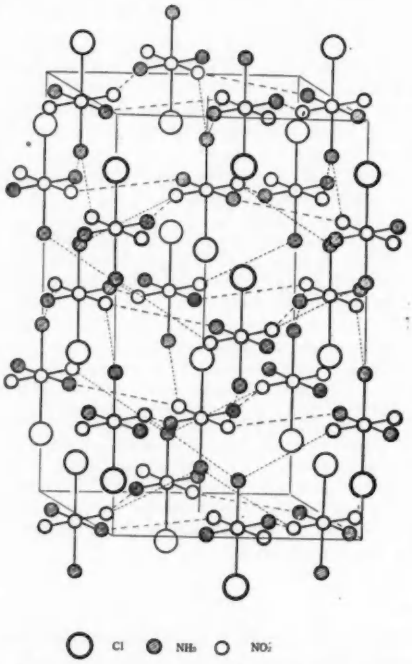

Fig. 5 A perspective drawing, showing the packing of the molecules in [Co $(NH_3)_3$ $(NO_2)_2$ Cl]. Circles are not drawn strictly to scale. Oxygen atoms are omitted.

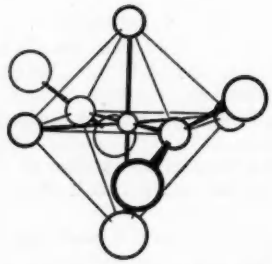

Fig. 6 The molecule of chlorodinitro-triammine-cobalt (III).

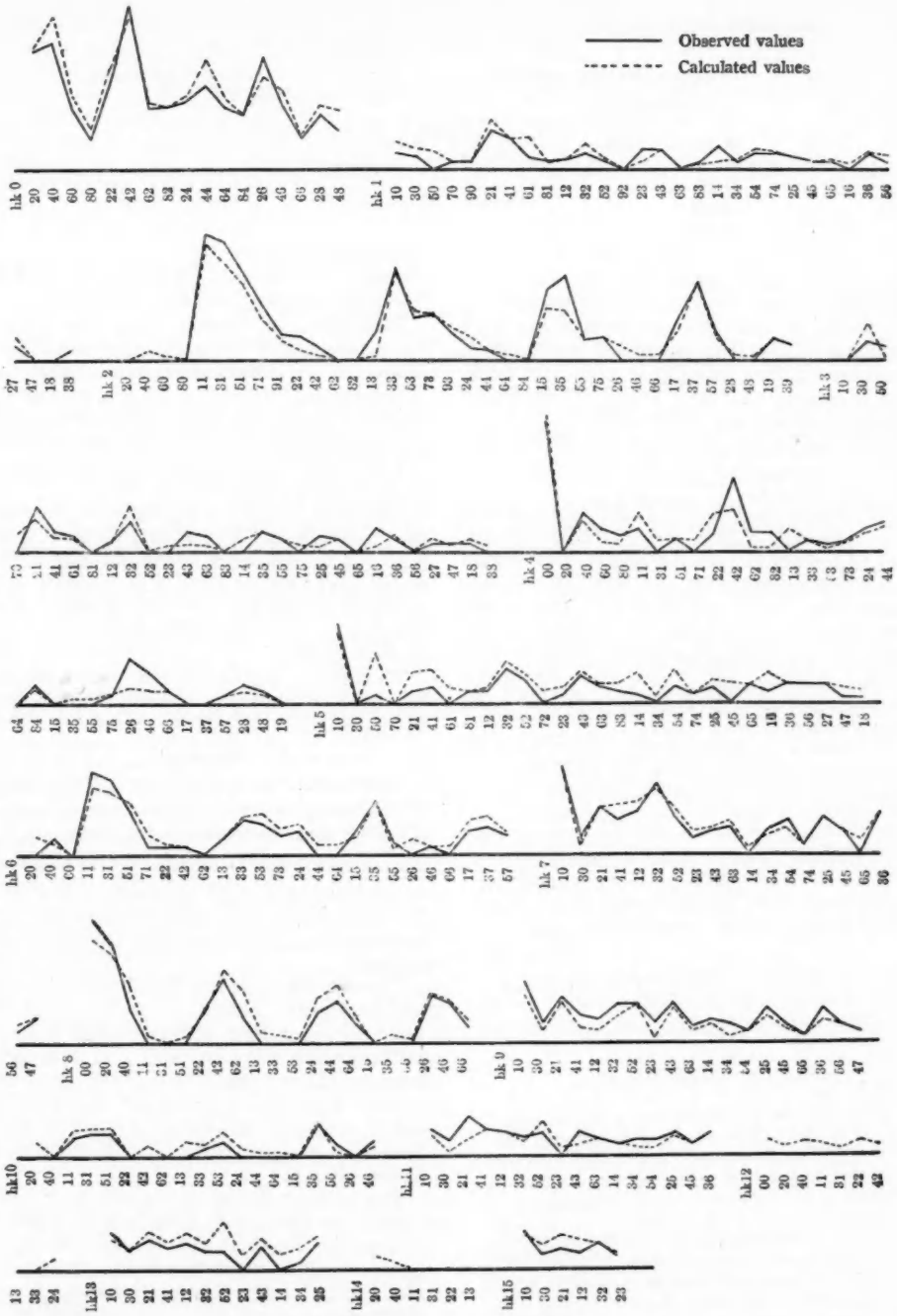

Fig. 4 Observed and calculated *F*'s

Table 2
Calculated Interatomic Distances and Bond Angles (Values in A Maximum errors about ±0.05 A and ±4°.)

	within a molecule			between molecules	
Co	N (1) (ammonia)	1.90	O (1)	N (2) (ammonia)	2.84
	Cl	2.30	O (2)	N (1) (ammonia)	2.75
	N (2) (ammonia)	1.99	N (1) (ammonia)	Cl	3.68
	N	1.99		Cl	3.99
N	O (1)	1.24	Cl	Cl	4.24
	O (2)	1.22			
O (1)	O (2)	2.12			
∠ ONO		119°			

errors, being 1.99 Å apart from it. On a line through a cobalt atom and perpendicular to the plane of four nitrogen atoms are a Cl atom and a NH_3 (1) group at 2.30 Å and 1.90 Å respectively, thus forming a distorted octahedron around a metal atom. These interatomic distances are in good agreement with those found in the structures of [Co $(NH_3)_3$ $(NO_2)_3$], [$Coen_2$ Cl_2] $Cl \cdot HCl \cdot 2H_2O$ and [Co $(NH_3)_3$ H_2OCl_2] Cl.[3][4][5]

The shape and size of the nitro-groups (N . . . O=1.24, 1.22 Å and ∠ONO=119°) are also in agreement with our previous results as well as with those in the case of KNO_2 recently determined very accurately.[3] The plane containing a nitro-group is inclined at an angle of about 34.8° with the plane of four nitrogen atoms. Thus there exist two kinds of molecules in the crystal, each being the mirror image of the other.

The closest approach of molecules is between NH_3 of one molecule and O of a nitro-group of the other. The unusual short NH_3 . . . O distances of 2.75 and 2.85 Å suggest probable hydrogen bonding between molecules.

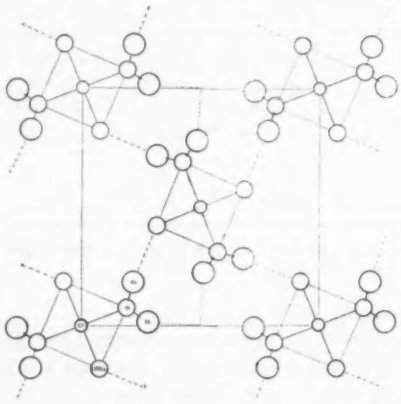

Fig. 7 Portion of the structure projected upon a plane perpendicular to [001], showing NH_3 . . . O linkages. Broken lines represent linkages in the layer, and dotted lines indicate those between layers.

Such hydrogen bonds were also found in the structure of trinitrotriammine-cobalt (III).[3] Molecules are arranged approximately in a layer parallel to (001) which is shown in Figs. 5 and 7. Each layer comprises equal numbers of two kinds of molecules above-mentioned.

The main forces acting between molecules in the layer seem to be NH_3(2) . . . O(1) interactions which are indicated in the figure by broken lines. These (001) layers are held together by hrdrogen bonds between NH_3 (1) of one layer and O (2) of a nitro-group of the molecule belonging to the adjacent layer. These bonds are also shown by dotted lines in Figs. 5 and 7.

Thus each molecules are bound together by these two kinds of hydrogen bonds, forming a three-dimensional net work.

Summary

The crystal structure of [Co $(NH_3)_3$ $(NO_2)_2$ Cl] is tetragonal, with eight formula units in a cell of dimensions $a=9.87$ Å and $c=16.51$ Å.

The space group is C_{4h}^6-$I4_1/a$. The determination of atomic parameters was made by three dimensional Fourier syntheses. The configuration of the complex molecule is described.

Two nitro-groups are found to be in trans-positions with respect to each other. The main forces acting between these molecules in the crystal seem to be O . . . H-N bonds between the oxygen atoms of the nitro-group and the ammonia of the other. Molecules are linked together by these hydrogen bonds, forming a compact three-dimensional network in the crystal.

The authors desire to express their hearty thanks to Professor I. Nitta and Professor R. Tsuchida for their kind advice and encouragement throughout this work. Part of the cost of this study has been defrayed from the research grant from the Ministry of Education.

Institute of Polytechnics, Osaka City University, Osaka

6) G. B. Carpenter: *Acta Cryst.* 5, 132 (1952).

Surface Chemistry of Synthetic Protein Analogues. II. Temperature Dependence of the Force-Area Relations of Some Polypeptides Monolayers and Thickness of the Monolayer*

By Toshizo ISEMURA and Kozo HAMAGUCHI

(Received March 20, 1953)

Introduction

Previously, the authors studied the various kinds of the behavior of the monolayers of some synthetic polypeptides as the model of natural proteins.[1] The polypeptides were of non-ionic side chains from four to ten carbon atoms in length. The force-area relations of the films were first investigated. From the results obtained, it was concluded that poly-DL-α-aminocaproic acid resembles exceedingly natural proteins among others. It has the side chains of four carbon atoms and its limiting area occupied by the film at zero compression was ca. 15 Å^2 per amino-acid residue. On the other hand, it was found that a plateau which is a part of high compressibility appears in the force-area (F-A) curves of the monolayers of polypeptides of longer side chains such as poly-DL-α-aminocaprylic acid, poly-DL-α-aminocapric acid, poly-DL-α-aminolauric acid and poly-γ-benzyl-DL glutamate. The F-A curves of these polypeptides monolayers were quite different in shape from those of natural proteins. The end of the plateau was always about 15 Å^2 per residue with all these films mentioned above. This area corresponds to the area per residue calculated from X-ray data of close packed chains of polypeptide of β-keratine type. (when the side chains were compressed away from the surface and the backbones were closely packed.). The resemblance between F-A curves of the protein monolayer and that of synthetic polypeptide of short side chains such as poly-DL-α-aminocaproic acid is due principally to the fact that natural proteins have on the average the side chains of effective length of three carbon atoms or less.

In the previous paper, the appearance of the plateau in the F-A curve was attributed to the reorientation of the polymer molecule caused by the compression of monolayer. To prove our supposition, the energy required for reorientation was evaluated and the thickness of the monolayer before and after transition was determined. In the course of experiments, it was found that the plateau of the F-A curves moves to the lower pressure region with the rise of temperature. From the relation of temperature and the pressure of transition from one state of the film to the other reoriented state, the heat of transition was estimated by the aid of two-dimensional equation of Clapeyron-Clausius.

On the other hand, these polypeptides films were transferred on the optical guage made of the built-up film of barium stearate under the spreading pressures under and above the transition pressure using the various piston oils. Then, the thickness of the built-up film of these polypeptides films was measured optically.

From the experimental results, our views of the reorientation at the plateau in F-A curve were justified for the most part.

Experimental Methods

Surface pressure was measured by the hanging plate method as reported in the previous paper. Distilled water was used as substrate, for the monolayer of these polypeptides is scarcely affected by the acidity or basicity of the substrate, as reported in the previous paper. To regulate the temperature of the substrate in the trough, the glass hose was dipped in the trough, through which water at constant temperature was circulated from a thermostat.

The films of these polypeptides were built up on the optical guage made of barium stearate multilayers by Langmuir-Blodgett's technique[2,3]

* This paper was presented before the "Symposium on the Studies on Protein Structure" which was held under the auspices of the Chemical Society of Japan, in Oct. 31-Nov. 1, 1952.

1) T. Isemura and K. Hamaguchi, This Bulletin, **25**, 40 (1952). T. Isemura, K. Hamaguchi, H. Tani. J. Noguchi and H. Yuki, *Nature*, **168**, 165 (1951).

under various spreading pressures of piston oils such as castor oil, tricresyl phosphate and some piston oils of low spreading pressure. Piston oils of low spreading pressure were prepared by mixing ethyl myristate with liquid paraffin[4] and their spreading pressure was measured by film balance beforehand for use. The thickness of the films of these polymers was determined optically by Blodgett's method.[3]

Poly-DL-α-aminocaproic acid film could not be transferred on the optical guage by dipping the plate vertically into the water covered with monolayer. However, it was transferred if the plate was inserted into the aqueous phase at an angle of 15° with the water surface and then withdrawn holding the plate at the same inclination. Polypeptide films other than that of poly-DL-α-aminocaproic acid were built up in the usual manner.

Results

The observed force-area relations at various temperatures are shown in Figs. 1–4.

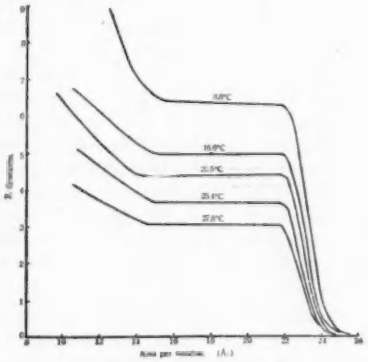

Fig. 1.—Poly-DL-α-aminolauric acid

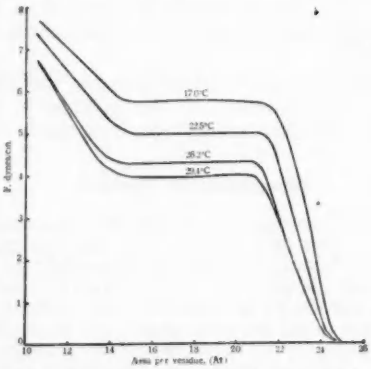

Fig. 2.—Poly-DL-α-aminocapric acid

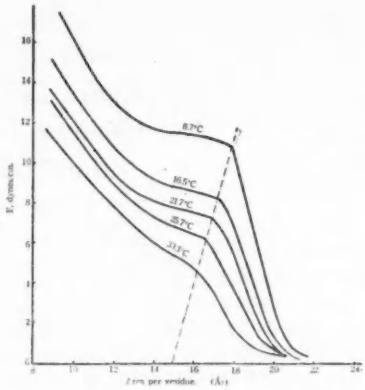

Fig. 3.—Poly-DL-α.aminocaprylic acid

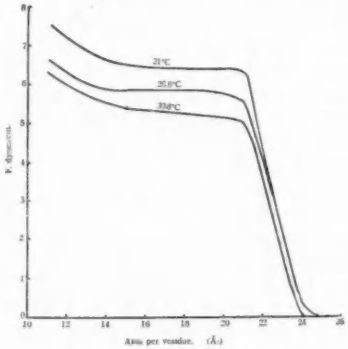

Fig. 4.—Poly-γ-benzyl-DL-glutamate

The force-area relation of the polymer film of short side chains such as poly-DL-norleucin was hardly influenced by the change of temperature. However, the force-area curves of the surface films of the polymers with longer side chains, such as poly-DL-α-aminolauric acid, poly-DL-α-aminocapric acid, poly-DL-α-aminocaprylic acid and poly-γ-benzyl-DL-glutamate were profoundly affected by the change of temperature. The plateau which appears in the F-A curves of monolayers of these polymers, passes to the lower pressure region with the rise of temperature of the substrate water. Nevertheless, the area at which the plateau begins to appear and the area at the end of the plateau, where the surface pressure begins to increase again were always nearly the same and independent of temperature. Moreover, the area of the end of the plateau was constant, namely, 15 Å^2 irrespective of the kind of polypeptides. The behavior of the monolayer of poly-DL-α-aminocaprylic acid was somewhat different from that of three other polypeptides. Although the plateau passes to the lower pressure region with the rise of temperature, the plateaus are not parallel to the area axis. In this case, their inclinations increase gradually and the area at which the plateau begins to appear, shifts to a

2) K. B. Blodgett, *J. Am. Chem. Soc.*, **57**, 1107 (1935).
3) K. B. Blodgett and I. Langmuir, *Phys. Rev.*, **53**, 909 (1938).
4) Norris and Taylor, *J. Chem. Soc.*, **1938**, 1719.

smaller area with the rise of temperature. The F-A curves of the monolayer of poly-DL-α-aminocaprylic acid may be an intermediate case between monolayers of polypeptide of shorter side chains and those of longer side chains.

The thickness of the built-up films of these polypeptides are shown in Table 1. The observed thickness h_3 indicated in the Table is not the value actually observed but the thickness which the built-up film should have, if the deposition ratio were unity. For comparison, the calculated thickness is also shown in the Table. h_1 is the thickness obtained by dividing the density of the polypeptide with the area per amino-acid residue at the spreading pressure of the piston oil used, which can be estimated from F-A curve. h_2 is the thickness of the film estimated by using the molecular model by Stuart, when the polypeptide chain is of β-keratine type and is compressed closely so as to project the side chains of the one side of the backbone and to push the side chains of the other side into the water.

Table 1.

Polypeptides	Spreading Pressure F (dynes/cm.)	Thickness (Å) calculated h_1	calculated h_2	observed h_3
Poly-DL-α-aminocaproic acid	3.1	10.7	11.7	11.1
Poly-DL-α-aminocaprylic acid	5.8	10.1	—	9.0
	9.5	15.0	16.4	15.6
Poly-DL-α-aminocapric acid	3.1	9.6	—	9.4
	9.5	24.0	21.3	22.7
Poly-DL-α-aminolauric acid	3.1	9.6	—	9.5
	5.8	23.9	26	20.7

Discussion

In the previous paper, the appearance of the plateau in the F-A curve was attributed to the reorientation of the polymer molecule caused by compression of monolayer. If we assume that both films before and after reorientation are two different surface phases, the surface pressure at which the plateau appears in the F-A curve, is the pressure of a phase transition. If this transition pressure was plotted against the temperature, straight lines were obtained for every polypeptide as shown in Fig. 5. dF/dT was readily evaluated from this figure. Inserting this value into two-dimensional Clapeyron-Clausius' equation, the change of enthalpy by the phase transformation of the film at any temperature can be evaluated as follows:

$$\Delta H^S = T \cdot \Delta A \frac{dF}{dT}$$

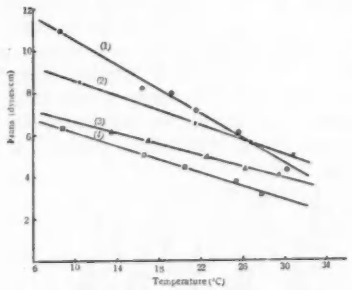

Fig. 5.—Transition pressure-temperature relation (1) Poly-DL-α-aminocaprylic acid; (2) poly-γ-benzyl-DL-glutamate; (3) Poly-DL-α-aminocapric acid; (4) Poly-DL-α-aminolauric acid.

where F is the surface pressure of transition, ΔH^S the change of heat content per ground mole of the surface film, T transition temperature and ΔA the change of area per mole of ground molecule. If we assume a relation between the internal energy of surface film and its heat content, namely

$$H^S = U^S + FA,$$

we can estimate the change of internal energy of surface film as follows

$$\Delta U^S = \Delta H^S - F \cdot \Delta A.$$

The calculated changes of enthalpy and changes of internal energy of the phase change of the polypeptide monolayers are shown in Table 2.

Table 2.

	ΔH^S (cal./ground mole)	ΔU^S (cal./ground mole)
Poly-DL-α-aminolauric acid	567 (25.4°C)	608
Poly-DL-α-aminocapric acid	395 (26.2°C)	440
Poly-DL-α-aminocaprylic acid	285 (25.4°C)	302
Poly-γ-benzyl-DL-glutamate	498 (21.6°C)	565

The difference of internal energy between both states before and after the phase transformation decreases with the length of the side chains of the polypeptide. From the figures in the Table, it may be expected that the energy required for the phase transformation must be very small if the side chains were of four carbon atoms or less. This is caused perhaps by the following reasons. The ratio of two axes of the cross section of the polypeptide molecule perpendicular to the direction of the main chain is not widely different from unity. The thermal energy will readily exceed the energy needed for the transformation. In fact, no plateau was found in the F-A curve of polypeptides of side chains of four carbon atoms such as poly-DL-α-aminocaproic acid, copolymer of glycine-alanine and natural proteins. A report on the monolayer of the copolymer of glycine-alanine, will be given in the following paper in some details. In the cases of polypeptides of short side chains and proteins, the difference of energy between two states may be negligible and reorientation of the molecule occurs without any difficulty. After the reorientation is completed, the film just becomes incompressible and the surface pressure rises suddenly even with a small decrease of area.

It is very interesting that the heat content of the condensed phase of the film is more than that of the expanded phase, contrary to many usual cases met in three dimensions. In the case of polypeptide film, the more condensed phase is of high entropy. The order of the reoriented, condensed film may be worse than that of the film lying flat on the substrate. The order of magnitude of ΔU^S is far less than that of any kind of bonding such as hydrogen linkage. So, the energy change found in the present case is insufficient to break such linkages and may be spent principally for the reorientation.

Recently, Dervichian reported[5] that the plateau would appear in the force-area curve when the film of natural proteins, such as, serum albumin and egg albumin, was compressed relatively rapidly and continuously. Howover, the plateau would disappear from F-A curve if the film was compressed intermittently. He explained his experimental result as follows. There are some modifications in protein film and the transformation between them takes some time, and so, the surface pressure rises if the film is rapidly compressed, before a modification of larger area is transformed to a modification of smaller area.

5) D. G. Dervichian, *Kolloid-Z.*, **126**, 15 (1952).

If our views of reorientation of polypeptide films are accepted and it is assumed that it needs some time for reorientation of the side chains even in the polypeptides of short side chains such as natural proteins, the facts found by Dervichian can be readily explained.

The film of poly-DL-α-aminocaprylic acid gives an intermediate film between that of poly-DL-α-aminocaproic acid or natural proteins and that of the polypeptides which show a distinct plateau in the F-A curve. In this case, the plateau found in F-A curves are not completely parallel to the area axis but somewhat inclined. The less inclined the plateau is, the lower the temperature is. In other words, the more compressible the film at the plateau is, the lower the temperature is. Moreover, the area at which the transformation begins, moves to the smaller area with the rise of temperature, while the area at which the film begins to transform is almost entirely independent of temperature with the polypeptide film of side chains longer than eight carbon atoms or more in length. The points at which the transformation begins to occur lie nearly on a straight line which intercepts the area axis at about 15 Å^2, as shown in Fig. 3. It may be inferred that the plateau will completely disappear from the F-A curve at about 46°C. and it may be presumed that F-A curve of the film becomes that of poly-DL-α-aminocaproic acid.

As previously mentioned, the plateau appears even in the F-A curve of natural proteins, if the film is compressed rapidly and continuously, for it takes some time to reorient such short side chains found in proteins. In our present experiment, when the area occupied by the film is decreased intermittently. Accordingly, it seems reasonable that the polypeptide such as poly-DL-α-aminocaproic acid which resembles protein shows no plateau in F-A curve.

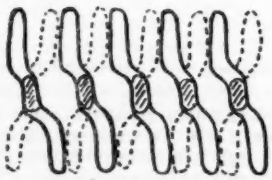

Fig. 6.—Close packed state of DL-polypeptide

To prove our supposition on the reorientation of the polymer, the determination of the thickness of the monolayer is the most direct method. It is expected that a distinct difference will be found between the thickness of monolayers built up at the pressure of more than the pressure at which the plateau ap-

pears and that built up at the pressure less than the transition pressure. And this is the case. After the reorientation was completed, the film assumed the shape shown in Fig. 6. With proteins and synthetic polypeptides of short side chains, only the built-up film of this orientation may be obtained. Whereas, with polypeptide films of longer side chains the other type of built-up film in which the side chains lie flat was also obtained.

With poly-DL-α-aminocaproic acid, the thickness of the film was 11.1 Å at pressure as low as 3.1 dynes/cm. In this case, the observed thickness, h_3, is in good agreement with h_1 and h_2. It suggests that the reorientation of the film is already completed. With poly-DL-α-aminocaprylic acid film, the thickness of the monolayer built up at 5.8 dynes/cm. (this pressure is less than the transition pressure) was 9.0 Å, whereas the thickness of the monolayer built up at 9.5 dynes/cm. (this pressure is more than the transition pressure) was 15~16 Å. This value is in good agreement with h_2. Although similar results were obtained with the monolayers of poly-DL-α-aminocapric acid and poly-DL-α-aminolauric acid, the thickness of the monolayer built up at the pressure higher than the transition pressure was nearly equal to but slightly less than the thickness evaluated by using Stuart models.

(for the most part.) These results support our views on the reorientation of the side chains of polypeptide.

Summary

In the force-area curves of the monolayer of synthetic polypeptides of longer side chains, a plateau which is a region of very high compressibility appears. The appearance of the plateau can be attributed to the reorientation of the polymer molecule at the interface. The pressure at which the plateau appears, decreases with the rise of temperature. From the temperature dependence of this pressure, the heat of transformation was evaluated.

The polypeptides of shorter side chains of four carbon atoms or less in length scarcely need any energy for reorientation. Accordingly, no plateau was found with these polypeptides. The thickness of the monolayer of these polypeptides at the pressure above and under the transition pressure was determined optically by Langmuir-Blodgett technique. The thickness of the monolayer observed was compared with that calculated by using Stuart model (for the most part.) Our views on the reorientatoin of the film were ascertained.

The authors wish to express their sincere thanks to Dr. H. Tani and Mr. H. Yuki in the Faculty of Science, Osaka University and to Dr. J. Noguchi at Kanazawa University who gave them the valuable samples of synthetic polypeptides. The authors' thanks are also due to Mr. R. Onishi for his assistance. A part of the expense for the experiment has been defrayed from a grant given by the Ministry of Education to which the authors' thanks are due.

The Institute of Scientific and Industrial Research, Osaka University, Sakai, Osaka

---

Studies on the Molecular Structures of Gaseous Acetamide and N-methylacetamide by Electron Diffraction

by Masao KIMURA and Michiro AOKI

(Received April 1, 1953)

Introduction

In many problems of the structure of protein, it is essential to determine the probable dimension of the polypeptide chain. Recently Corey and Donohue carried out X-ray diffraction experiments on DL-alanine, L-threonine, β-glycylglycine and N-acetylglycine, and suggested the probable dimension of the polypeptide chain to be as follows[1]: C=O 1.23 Å, C-N 1.32 Å, αC—C 1.53 Å, αC—N 1.47 Å, $\angle$NCO 122°, $\angle\alpha$CCO 121°, $\angle$CNαC 120° and $\angle$CαCN 110°. In the present investigation the molecular structure of gaseous acetamide, units of the polypeptide chain, and of gaseous N-methylacetamide, the simplest

1) R. B. Corey, J. Donohue, *J. Am. Chem. Soc.*, **72**, 2399 (1950).

molecule with a peptide linkage, were determined by electron diffraction and were compared with the result obtained from the X-ray diffraction experiments of some proteins.

Senti and Harker[2] determined the structure of acetamide using X-ray diffraction by crystal to be as follows: C=O 1.28 Å, C—N 1.38 Å, C-C 1.53 Å, ∠NCO 122° and ∠CCO 129°. No reports have ever been published regarding the structure of N-methylacetamide.

Experiment

The boiling points of acetamide and N-methylacetamide are 222°C and 206°C respectively. These compounds were vaporized by the use of a high temperature nozzle shown in Fig. I. The temperature of vapors could easily be raised up to 200°C by heating a nichrome wire coiled around a sample holder. The amount of the vapor could be regulated by a needle.

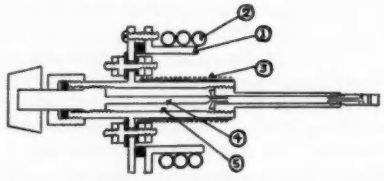

Fig. 1.—Diagram of the high temperature nozzle: (1) camera; (2) pipe coiled for coiled pipe for water cooling through which water is flowed; (3) nichrome wire; (4) needle; (5) sample holder.

The positions of maxima and minima of halos were estimated visually and were listed in Table 1. The visual curves are shown in Fig. 2V and Fig. 3v.

2) F. Senti, D. Harker, *J. Am. Chem., Soc.*, **62**, 2008 (1940).

Table 1

Observed Values for Acetamide and N-methylacetamide*.

Max.	Min.	q		Max.	q	
		Acetamide	N-methylacetamide		Acetamide	N-methylacetamide
	2	15.36	14.14	6	53.23	53.30
2		19.40	18.65	7	61.54	60.15
	3	24.01	24.33	8	68.18	69.14
3		27.81	27.97	9	77.03	76.76
	4	31.96	31.45	10	84.67	86.15
4		36.35	35.31	11	93.00	94.13
	5	40.56	40.75	12	100.55	
5		44.37	44.26			
	6	49.16	49.27			

* The observed values for the 1st maximum and the 7th, 8th, 9th, 10th, 11th and 12th minima were inaccurate and were not listed in this table. These values were not used for quantitative comparison.

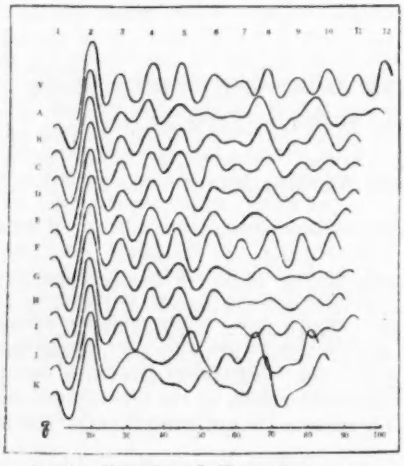

Fig. 2.—Visual and theoretical curves for acetamide.

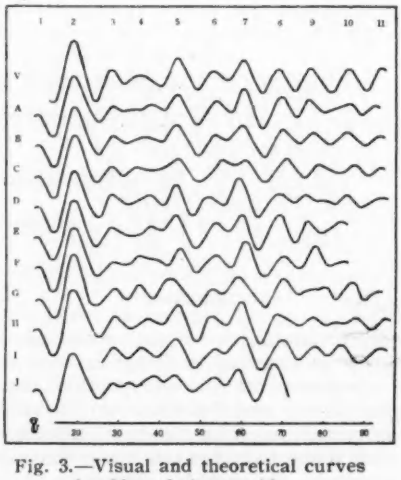

Fig. 3.—Visual and theoretical curves for N-methylacetamide.

The theoretical intensity curves,

$$I(q)=\sum_{i}\sum_{\neq j}(Z_iZ_j/r_{ij})\exp(-a_{ij}q^2)\sin(\pi qr_{ij}/10)$$

were computed for various models and were compared with the visual curve. Here notations have their usual significances and $\exp(-a_{ij}q^2)$ is a factor relating to the intramolecular vibration.

Because the theoretical intensity curves for acetamide were not affected appreciably by vibrations, a_{ij}'s could be taken as zero. For N-methylacetamide, the rotational vibration about carbon nitrogen bond cannot be neglected, therefore a a_{ij}'s were taken as either zero or 0.0004 for both C—C pair and C—O pair (Fig. 4).

Table 2
Models Assumed for Acetamide

model	C—N (Å)	C=O (Å)	C—C (Å)	∠NCO (degree)	∠CCO (degree)
A	1.37	1.25	1.54	122	120
B	„	1.23	1.54	124	122
C	„	1.21	1.54	126	120
D	„	„	1.52	124	124
E	„	„	1.57	126	118
F	„	1.21	1.54	128	120
G	„	„	„	124	120
H	„	„	„	126	118
I	„	1.19	1.54	126	124
J	1.38	1.28	1.53	122	129
K	1.32	1.23	1.53	122	121

Table 3
Models Assumed for N-methylacetamide

model	C—N (Å)	∠CNC (degree)	
A	1.45	115	trans
B	„	„	trans, vibrating
C	„	110	trans, rigid
D	„	120	trans, rigid
E	1.49	115	trans, rigid
F	1.39	„	trans, rigid
G	1.45	115	cis, rigid
H	„	„	twisted by 30 degrees from trans
I	„	„	free rotating
J	1.47	120	trans

Acetamide.—It was assumed that C-H 1.09 A, N-H 1.02 Å, ∠CCH 109°28′, ∠CNH 107° and that C, C, N and O atoms are coplaner. Because of many parameters involved, first the C—N distance was kept at 1.37 Å and the theoretical intensity curves were computed for various values of C-C, ∠NCO and ∠CCO, where the C=O distance was presumed to be 1.25 Å, 1.23 Å, 1.21 Å or 1.19 Å. Some of them are reproduced in Fig. 2.

(a) *Case of* C=O 1.25 Å: The theoretical curve for the model having the values of C-C 1.54 Å, ∠NCO 122° and ∠CCO 120° (Fig. 2A) did not agree with the visual curve, because the 6th and 7th maxima were too low; the 9th maximum appeared as a shelf and the q values of maxima were smaller than those in the visual curve. Even if different values were used for C—C, ∠NCO and ∠CCO with the values of model A, the 7th maximum disappeared and the theoretical curve in agreement with the visual curve could not be obtained.

(b) *Case of* C=O 1.23 Å: For the model having C—C 1.54 A, ∠NCO 124° and ∠CCO 122° (Fig. 2B), the theoretical curve obtained was similar in shape to the visual curve, except that the positions of maxima and minima disagreed with the observed values. If we assumed 1.57 Å for C—C distance, which was longer than the value of model B, the 8th, 9th and 11th maxima became higher, while the 6th and 7th maxima became lower. If we assumed 1.52 Å for C—C distance, which was shorter than the value of model B, the 6th, 7th, 8th, 10th, 11th and especially the 9th maxima became too low. These two theoretical curves appeared to be worse than the curve for model B. If C—C distance, ∠NCO and ∠CCO were varied properly, in the only case of about 1.52 Å, the theoretical curve could be obtained with the features similar to the visual curve. But the positions of maxima and minima shifted to q values smaller than the observed one.

(c) *Case of* C=O 1.21 Å: For the model having C—C 1.54 Å, ∠NCO 126° and ∠CCO 120° (Fig. 2C)~124°, the theoretical curves showed good agreement with the visual curve in features and the positions of maxima and minima. In order to determine the acceptable range of parameters, C—C, ∠NCO, and ∠CCO, their values were varied from the values of model C. When ∠NCO and ∠CCO were kept at the value of model C and C—C distance was assumed to be 1.52 Å, no good theoretical curve could be obtained. But in this case, if ∠NCO and ∠CCO were varied properly, an acceptable theoretical curve could be obtained, for example, as shown in the curve of ∠NCO 124° and ∠CCO 124° (Fig. 2D). When ∠NCO and ∠CCO were kept at the value of model C and C—C distance was assumed to be 1.57 A, no curve could be obtained in agreement with the visual curve, even though we took any value of ∠NCO and ∠CCO (for example Fig. 2E). When C—C and ∠CCO were kept at the value of model C and ∠NCO was larger or smaller by two degrees than the angle of model C, acceptable theoretical curves could not be obtained as shown in Fig. 2F or G respectively. Finally if C—C and ∠NCO were kept at the value of model C and ∠CCO was smaller by two degrees than the angle of model C, no acceptable theoretical curve (Fig. 2H) could be obtained. In this case if ∠CCO was 126°, the theoretical curve was entirely similar to that of model H and therefore could not be accepted.

(d) *Case of* C=O 1.19 Å: For the model having C—C 1.54 Å, ∠NCO 126° and ∠CCO 124°, the theoretical curve (Fig. 2I) could be obtained in agreement to some extent with the visual curve, but it cannot be accepted as a better model from the point of view of the relations of the 8th and 9th, or of the 10th and 11th maxima.

Even though C—C, ∠NCO and ∠CCO were varied properly, satisfactory theoretical curves could not be obtained.

According to the results of interpretation outlined above, if we assume 1.37 Å for C—N distance, the value of 1.21 Å is the best and the values of 1.23 Å—1.19 Å are acceptable for C=O distance. For other parameters, ∠NCO, ∠CCO and C—C distance, fairly wide ranges of values are permissible to obtain theoretical curves similar to the visual one. Thus ∠NCO 128°~132°, C—C 1.50 Å~1.56 Å and ∠CCO 118°~126° may be adopted as the widest range of the values. Furthermore quantitative comparison with the visual curve was made for the positions of maxima and minima in several better theoretical curves.

Thus the structure of acetamide was determined as follows:

C=O	1.21 Å±0.02 Å,	∠NCO	125°±3°
C—N	1.36 Å±0.02 Å,	∠CCO	122°±4°
C—C	1.53 Å±0.03 Å,		
C—H	1.09 Å (assumed),	∠CCH	109°28′ (assumed)
N—H	1.02 Å (assumed),	∠CNH	107° assumed)

and C, C, N and O atoms assumed lying in one plane.

The structure obtained by Senti and Harker and the probable dimension of a polypeptide chain given by Corey and Donohue give theoretical curves shown in Fig. 2J and K respectively. They disagree definitely with the visual curve.

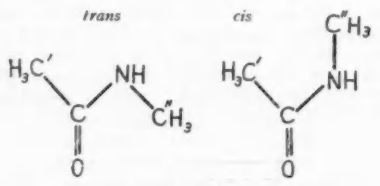

Fig. 4.—N-methylacetamide

N-methylacetamide. The photograph was analysed assuming a molecular structure similar to acetamide obtained above and using second C″—N distance, ∠C″NC and a rotational angle of the methylgroup about C″—N bond axis as parameters.

In the case of the trans configuration (Fig. 4), the theoretical curve having the values of C″—N 1.45 Å and ∠CNC 115° agreed to some extent with the visual curve, but the 4th and 11th maxima did not agree with those of the visual curve (Fig. 3A). If we took into account the rotational vibration of methyl group about C″—N bond axis, the theoretical curve was in satisfactory agreement with the visual curve (Fig. 3B). When C″—N was kept at 1.45 Å and ∠CNC was varied to 110° (Fig. 3C), even if we took the vibrational effect into account, no acceptable theoretical curve could be obtained. when C″—N was kept at 1.45 Å and ∠CNC was varied to 120° (Fig. 3D), the 7th maximum seemed to be too high compared with the 6th. But this model should not be discarded, entirely because, if the vibration is taken into account, the theoretical curve becomes more similar to the visual one than the theoretical curve for model 3D.

When ∠CNC was kept at the value of model A and C″—N distance was varied to 1.49 Å or 1.39 Å, the theoretical curves were obtained as shown in Fig. 3E and F respectively. Both curves are unacceptable.

In the case of the cis configuration (Fig. 4), the theoretical curve Fig. 3G was obtained using the same value of C″—N distance and ∠C″NC as model A. The curve was not in agreement with the visual one in regard to the positions of the 5th, 6th, 7th and 10th maxima and the feature of the 4th maximum. It could not be revised even if we took into account the rotational vibration of a methyl group. In the theoretical curve (Fig. 3H) computed for the model with the methyl group twisted by 30 degrees from the *trans* configuration, the 6th and 8th maxima shifted to smaller values and the similarity to the visual curve became worse in the feature of the curve. But the theoretical curves for the models with the methyl group twisted within about 30 degrees, could not be discriminated from the visual one. Further the theoretical curve for the model whose methyl group rotates freely about C—N bond axis (Fig. 3I), does not better account for the visual one than the curves for the *trans* configuration, but this also cannot be discarded.

According to the result mentioned above, it is most probable that N-methylacetamide has the trans configuration and its methyl group oscillates about C—N bond axis. But the structures whose methyl group rotates freely may also be probable. The conclusion from the measurement of dipole moment in solution[3] is that N-methylacetamide has the *trans* configuration. Further from the viewpoint of steric repulsion, the *trans* configuration is more favorable than the *cis* configuration.

with the known structure of acetamide the structure of N-methylacetamide was determined as follows:

C″—N	1.44 Å±0.04 Å
∠C″NC	117°±5°

trans configuration.

The theoretical curve for N-methylacetamide was computed using the structure of a polypeptide chain obtained by Corey and Donohue an' is shown in Fig. 3J. It could be distinguished definitely from the visual curve.

Discussion of Results

Our results differ definitely from the values

3) S. Mizushima, T. Shimanouchi, S. Nagakura, K. Kuratani, M. Tsuboi, H. Baba, O. Fujioka, *J. Chem. Soc. Japan* **71**, 32 (1950); *J. Am. Chem. Soc.*, **72**, 3490 (1950).

obtained by Senti and Harker, but do not differ very much from the probable dimension of a polypeptide chain proposed by Corey and Donohue. The result obtained by Senti and Harker seems to be not very accurate. It has already been mentioned that the probable dimension of a polypeptide chain obtained by Corey and Donohue does not give a satisfactory theoretical curve.

The discrepancy between the results obtained by us and by Corey and Donohue may be supposed to be due to the difference in materials used and in the states of aggregation. Namely, Corey and Donohue used as samples β-glycylglycine, N-acetylglycine and so on while we used acetamide and N-methylacetamide morover they determined the crystal structures, while we determined the structures in the gaseous state.

As it is unlikely that the former difference will give rise to an appreciable change in the molecular structure, it will be more adequate to consider that the latter is the main cause of the difference between the results obtained by us and by Corey and Donohue, i.e. to suppose that the hydgrogen bond, which is absent in the gaseous state but exists in the crystalline state, plays a major role

Acetamide will have the resonance structures shown by

$$CH_3\text{-}\overset{\overset{O}{\|}}{C}\text{-}NH_2 \text{ (A)} \quad \text{and} \quad CH_3\text{-}\overset{\overset{+}{}}{C}\overset{\overset{O^-}{|}}{=}NH_2 \text{ (B)}$$

as the extreme cases, hence by the hydrogen bonds the contribution of the structure (B) becomes greater in the crystal line state than in the gaseous state. As a result, C=O distance will tend to be longer and C—N distance to be shorter in the crystal.

The change in the structure of acetamide due to the formation of a hydrogen bond is supported by another fact. N-methylacetamide in dilute benzene solution shows an infrared absorption maximum of C=O vibration at 1700 cm^{-1} in extreme dilution, but its wave number shifts to 1640 cm^{-1} as the concentration increases[3] owing to the hydrogen bond between solute molecules.

Summary

1) The molecular structures of acetamide and N-methylacetamide were determined using electron diffraction by gases. The results were compared with the values obtained from X-ray diffraction by crystals.

2) C=O distance is longer in the crystalline state than in the gaseous state, while C—N distance is shorter in the crystalline state than in the gaseous state. This is due to the hydrogen bond which is absent in the gaseous state but exists in the crystalline state.

We wish to express our sincere thanks to Professor S. Mizushima and Professor Y. Morino of Tokyo University who supplied us with the sample of N-methylacetamide used in this experiment. We also wish to thank Professor M. Kubo of Nagoya University for his helpful advice.

Department of Chemistry,
Faculty of Science,
Nagoya University

Studies of Molecular Structures by Electron Diffraction. II. The Structures of *o*-,*p*-Fluorochrolobenzene and *p*-Fluorobromobenzene

By Hajime Oosaka† and Yûmi Akimoto

(Received May 1, 1953)

Introduction

Recently the molecules of fluorine substituted benzene derivatives have been the subjects of several investigations. Early electron diffraction results on fluorobenzene and *o*-difluorobenzene by the visual method was reported by one of the authors.[1] The quoted bond lengths, C—F, have been 1.34±0.04 Å and 1.35±0.03 Å respectively. A little later a discrepant result was reported by Finbak and Hassel[2] who found 1.31±0.03Å for the C—F distance in fluorobenzene by the sector method.

It was, therefore, decided to carry out the

1) H. Oosaka, This Bulletin, **15**, 31 (1940).

2) C. Finbak and O. Hassel, *Arch. Math. Naturvidenskab.* XLIV (1941); O. Hassel and H. Viervoll, *Acta Chim. Scand.*, **1**, 149 (1947).

extensive measurement on the various fluorobenzene derivatives. Not long afterward, some of our collaborators have reported the result of reinvestigation of fluorobenzene.[3] And, in this paper, the molecular structures of *o*-, *p*-fluorochlorobenzene and *p*-fluorobromobenzene are to be reported as a second part of this series.

Materials

Each fluorobenzene derivative was prepared from corresponding nitroaniline by the successive diazotations. All steps are too familiar to describe in detail but the step, Schiemann reaction, where a fluorine atom is introduced into the aromatic nucleus.

Schiemann Reaction.[4]—(The following procedures are common to the three compounds mentioned above.)

(A) Preparations of Diazonium Fluoborates.—To a mixture of 100 cc. of 40% fluoboric acid and 50 cc. of water is added 0.25 mole of well ground corresponding halogenated aniline. The solution (or suspention) is cooled to 5°C., and a saturated solution of 17.3 g. (0.25 mole) of sodium nitrite is added slowly, the temperature being kept under 20°C. The precipitate is washed with cold water, cold methanol and ether successively. The yields are 92% (o-$BF_4N_2ClC_6H_4$), 89% (p-$BF_4N_2ClC_6H_4$) and 93% (p-$BF_4N_2BrC_6H_4$).

Meigs[5] reported that the temperature of the reacting mixture may rise to 30°C. without ill effect during the diazotation of aniline in fluoboric acid solution. Carrying out the diazotations for several numbers of compounds,[6] we extended Meigs' conclusion over nearly all monohalogenoaniline. Table 1 serves to confirm this conclusion by showing the yields obtained under several different temperatures, in case of the diazotation of *p*-fluorochloroaniline, as an example.

Table 1
Temperature Effect for the Diazotation of *p*-chloroaniline

Sample	Temp. of bath (°C)	Max. temp. of reacting mixture (°C)	Yield (%)
1	15	30	78.5
2	7	18	88.7
3	0 (ice)	10	86.1
4	−10 (ice-NaCl)	0	84.7

All the other halogenated anilines can be treated likewise: there are no troubles up to 20°C. However, in case of nitroanilines, the reacting mixture must be kept under 7°C, because considerable decomposition occurs even at about 10°C. A more severe condition is necessary in case of tetrazotation: decomposition begins at about −8°C.

(B) Decompositions of Diazonium Fluoborates.—Decompositions were carried out according to the direction of Organic Reactions.[4] The yields were 68% (o-$FClC_6H_4$), 72% (p-$FClC_6H_4$), and 74% (p-$FBrC_6H_4$).

Each sample was distilled before use.

Experimental

Electron diffraction photographs of *p*-fluorochlorobenzene were taken in the apparatus of Brockway type with the camera distance of 13.4 cm. For the other two compounds a new camera, previously described,[3] was used.[7] About eight photographs were taken for each compound under different conditions, and were measured visually in the usual way. The electron wave length was determined to be 0.052~0.064 Å by caribration against gold leaves.

Theoretical intensity curves were calculated by the following equation.

$$I(s)=\sum_i\sum_j Z_iZ_j \exp(-a_{ij}s^2)\frac{\sin sl_{ij}}{sl_{ij}}$$

where $s=(4\pi/\lambda)\sin\theta/2$, l_{ij}: the distance between the i-th and j-th atoms, Z: the atomic number, a: the coefficient of thermal vibration, λ: the wave length, and θ: the scattering angle. (For *p*-fluorobromobenzene and *o*-fluorochlorobenzene, modified parameter $q(=(40/\lambda)\sin\theta/2)$ was used in place of s.[8])

For hydrogen, an effective value, 1.25, was used in order to approximate better to its low-angle scattering relative to carbon and halogen atoms.

***p*-Fluorochlorobenzene.**—In computing theoretical intensity curves, assumptions were made as below: (1) C—C=1.40 Å, (2) C—H=1.04 Å, (3) ∠H—C—C=∠Hal.—C—C=120°, (4) the molecule has a planar skeleton. The parameter values were made for fourteen models over the following ranges: C—Cl=1.66~1.72 Å, C—F=1.27~1.41 Å. All interactions involving hydrogen atoms were included, except H—H terms. The thermal term was neglected since the high-angle scattering region hardly contributed to the determination of parameters. Typical curves are shown in Fig. 2, and the values of the parametersin Fig. 1.

Curve C is inconsistent with the experimental data for lack of max. IV. Curves G and H can be rejected because max. III is too large. In

3) T. Yuzawa and M. Yamaha, in press.
4) A. Roe, "Organic Reactions" Vol. V, Chap. IV. p. 193.
5) Meigs, U. S. pat. 1,916, 327 (C.A., **27**, 4539 (1933)).
6) *p*-Fluoroaniline, *o*-,*m*-,*p*-chloroaniline, *o*-,*p*-bromoaniline, *p*-iodoaniline and *o*-,*m*-,*p*-nitroaniline were diazotized for this purpose. Tetrazotations were carried out also.
7) Because of the accomplishments of a new apparatus and calculation tables in q scale in the midst of our research, such disorepances were introduced unavoidably.
8) R. Spurr and V. Schomaker, *J. Am. Chem. Soc.* **64**, 2693 (1942).
9) On account of possible majority of thermal vibration on Br··F, some additional curves were calculated with suitable values of a_{ij} for all terms, but the resulting changes were insignificant but for max. IX.

curve F, max. III is larger still compared with max. II. Curves A and B are borderline cases since max. VI is too weak as compared with max. V. Furthermore, curve B can probably be eliminated because of the disappearance of shelf II.

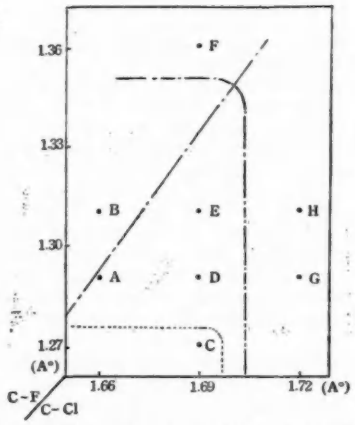

Fig. 1.—Parameter chart for *p*-fluorochlorobenzene

The position of the letters indicate the parameters of the models for which intensity curves were computed. The dashed and dotted lines indicate where particular features of the intensity curves were sufficiently different from the visual curve to make them unacceptable.

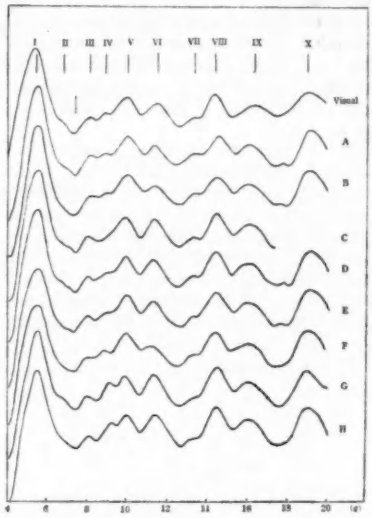

Fig. 2. Theoretical intensity curves for *p*-fluorochlorobenzene.

The best agreement with the observed pattern would be given by a model located about the midway between D and E. Finally we have C—F=1.30±0.03 Å, and C—Cl=1.68±0.02 Å. (The quantitative comparisons are in Table 2.)

Table 2

p-Fluorochlorobenzene

Max.	Min.	Obs. (s)	$s_{c.}/s_{o.}$ A	D	E
I		5.381	1.022	1.025	1.022
II		(6.778)			
	III	7.336	0.988	0.993	0.988
III		8.082	1.007	0.994	0.992
IV		8.890	1.006	1.000	0.996
V		9.935	1.006	0.997	1.000
VI		11.509	0.984	0.980	0.973
VII		(13.398)	(0.996)	(0.988)	(0.985)
VIII		14.381	1.008	1.001	1.000
IX		16.349	0.984	0.979	0.981
X		19.016	1.003	1.003	1.001
Average, 9 features			1.001	0.997	0.995
Mean deviation, $\bar{\Delta}$			0.011	0.009	0.010
Mean square root, $(\Delta^2)^{1/2}$			0.012	0.013	0.014

***p*-Fluorobromobenzene.**—Theoretical curves were calculated over the following parameter ranges: C—Br=1.84~1.90 Å, C—F=1.27~1.33 Å. The assumptions were made just as those of fluorochlorobenzene. Typical ones of these curves are shown in Fig. 4, and the values chosen for the parameters in Fig. 3.

In order to avoid laborious computation in a literal treatment of the thermal factors, a_{ij} was neglected over all models and a procedure was

adopted wherein two curves were plotted for several models. The light curves represent only the scattering due to non hydrogen distances and the bonded C—H distances; in addition to these terms, the heavy curves include the non-bobded C···H and Hal.···H terms. The heavy curves are significant for small q and the light curves for large q.

Curve A may be excluded because of the intense max. III. Dislocation of max. V eliminated curve J and put curve I on a borderline. For the remaining curves, there are not any sufficient reasons to eliminate them qualitatively. Indeed curves F, G and H lack max. VI, and curves B, C and F show max. XI distinctly. However, they are too weak to be decisive criteria hence the thermal effects may weaken these tendencies.

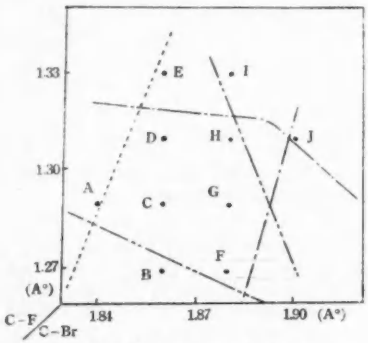

Fig. 3.—Parameter chart for *p*-fluorobromobenzene.

The quantitative comparisons are tabluated in Table 3. As the final result we obtain C—F = 1.30 ± 0.03 Å and C—Br = 1.87 ± 0.02 Å.

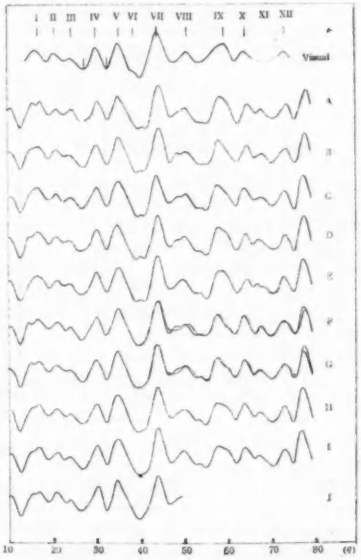

Fig. 4.—Theoretical intensity curves for *p*-fluorobromobenzene.

Table 3

p-Fluorobromobenzene

Max.	Min.	Obs. (q)	c_o/q_o		
			C	D	G
I		16.68	0.999	1.006	1.006
II		20.86	1.006	1.016	1.006
III		24.61	(0.980)	(0.980)	(0.976)
	IV	27.46	(0.977)	(0.970)	(0.984)
IV		30.08	1.007	1.004	1.004
	V	33.03	0.993	0.990	0.984
V		35.59	0.986	0.986	0.992
VI		(38.8)			
VII		44.42	0.999	1.008	1.000
VIII		51.35	0.993	0.985	0.993
IX		59.99	(0.958)	(0.963)	(0.953)
X		64.60	1.003	1.001	1.000
XI		73.76	1.003	1.002	1.002
Average, 9 features			0.999	1.000	0.999
			1.001	**1.002**	**1.000**
Mean deviation, Δ			0.005	0.008	0.005
Mean square root, $(\Delta^2)^{1/2}$			0.007	0.010	0.007

	B	E	F	H
Average, 9 features	1.003	1.001	0.998	0.998
	1.006	**1.002**	**1.001**	**0.999**
Δ	0.010	0.009	0.008	0.007
$(\Delta^2)^{1/2}$	0.011	0.012	0.010	0.008

Black style numerals indicate the values obtained from temperature-factored curves.

***o*-Fluorochlorobenzene.**—In this case, we cannot always assume the coplanarity of all atoms. Using the sector method, Bastiansen and Hassel[10] concluded that the forces acting between C-halogen atoms tend to bring the halogen atoms out of the plane of the benzene ring. However, as opposed by Morino,[11] this result is inconceivable theoretically.

No matter which they may be, in computing theoretical intensity curves this problem has no significiant base of arguments; no important difference on the shapes of the curves were found between the coplanar model and non coplanar one, and hence the molecule was assumed to have a planar skelton in this case.

Parameter ranges were taken as: C—Cl=1.67~1.75 Å, C—F=1.29~1.37 Å, F—Cl=2.90~3.04 Å. The assumption and the thermal factors were treated in a way similar to the case of *p*-fluorobromobenzene. Fig. 5 and Table 4 show typical curves and their parameters of twenty-one models which have been tested.

Curves A, B, F, G, and H are rejected because they show considerably different shapes in the region q=20~30. Curves C, D and E are mostly acceptable, though curve E is rather a borderline case since max. V and XII are somewhat out of step with the observed ones.

However when we examine them more strictly, they show several difficulties: max. VI is too much weaker than the observed, max. XI is too strong relative to max. X. Spreading the ∠Hal.—C—C over 120°, we can remove these difficulties, and curves K and L show the best agreement with the observations. Even curve J shows the fit better than curve C. Curves I and M are borderline cases.

Quantitative comparisons are given in Table 5. The final structure is C—F=1.30±0.03 Å, C—Cl=1.69±0.02 Å, and ∠F—C—C (adjacent of Cl)=∠Cl—C—C (adjacent of F)=121±1°.

Table 4
Parameters for *o*-fluorochlorobenzene

Model number	C—Cl (Å)	C—F (Å)	Cl—F (Å)	F—C—C (adj. of Cl) Cl—C—C (adj. of F)
A	1.67	1.29	2.90	120°
B	1.67	1.33	2.91	120°
C	1.70	1.29	2.92	120°
D	1.70	1.31	2.92	120°
E	1.70	1.33	2.93	120°
F	1.71	1.29	2.92	120°
G	1.73	1.31	2.94	120°
H	1.73	1.35	2.96	120°
I	1.67	1.29	2.95	121°
J	1.70	1.29	2.95	120°45′
K	1.70	1.29	2.99	121°40′
L	1.70	1.31	2.99	121°30′
M	1.71	1.31	2.99	121°20′

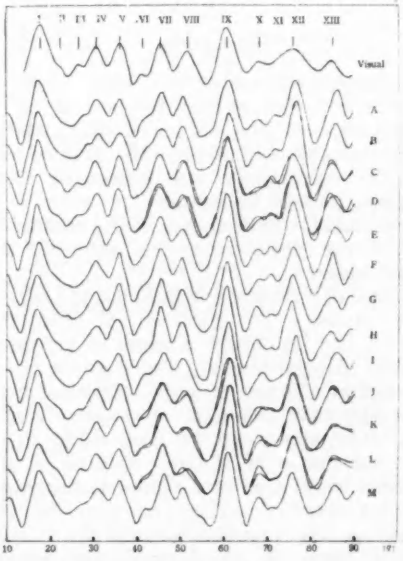

Fig. 5.—Theoretical intensity curves for *o*-fluorochlorobenzene.

10) O. Bastiansen and O. Hassel, *Acta Chim. Scand.*, **1**, 489 (1947).
11) Y. Morino, Discussion on the Inter- and Intramolecular forces, Tokyo, June, 1952.

Table 5

o-Fluorochlorobenzene

Max.	Obs. (q)	$q_{c.}/q_{o.}$ C	J	K
I	17.76	(0.976)	(0.979)	(0.979)
II	(22.28)			
III	26.42	1.001	1.006	1.000
IV	30.56	1.001	1.002	1.004
V	36.29	0.992	0.989	0.989
VI	41.38	/	(1.000)	(1.000)
VII	45.62	1.000	1.001	1.003
VIII	51.98	0.978	0.981	0.981
IX	60.82	1.009	1.007	1.007
X	68.41	(0.994)	(0.996)	(0.994)
XII	76.39	1.002	0.998	0.992
XIII	85.30	0.999	0.999	1.001
Average, 8 features		0.997	0.998	0.996
		0.999	**0.999**	**0.998**
Mean deviation, Δ		0.005	0.006	0.007
Mean square root, $(\Delta^2)^{1/2}$		0.008	0.008	0.008
		D	E	L
Average, 8 features		0.998	0.995	0.997
		1.000	/	**0.998**
Δ		0.009	0.009	0.010
$(\Delta^2)^{1/2}$		0.012	0.010	0.012

Black style numerals indicate the values obtained from temperature-factured curves.

Discussion

We must confess that the value of C—F distance reported earlier by one of us is inadequate.[1] In the earlier work, patterns were detectable only up to $s=15$. It is certain that the impropriety was originated from this experimental limitation.

C—Cl and C—Br distances do not contradict that of the previous works published by several authors.

In case of *o*-fluorochlorobenzene, the reason for a deviation of ∠Hal.—C—C from the value of 120° is chiefly a result of repulsion between halogen atoms. The distance to be expected in absence of such deviation must be smaller than the sum of van der Waals radii, which should be at least 3.0 Å. The slight increment of Hal.—C distance which has been found in several *o*-halogenobenzenes, were not observed. This fact may be explained as the repulsive force is not so sufficiently large as to demand the visible stretching of Hal.—C bonds in this case.

Summary

The molecular structures of *o*-, *p*-fluorochlorobenzene and *p*-fluorobromobenzene have been investigated by the electron diffraction method. The following values have been obtained by the analysis based on coplanar structures; C—F=1.30±0.03 Å, C—Cl=1.68±0.02 Å for *p*-fluorochlorobenzene; C—F=1.30±0.03 Å, C—Br=1.87±0.02 Å for *p*-fluorobromobenzene; and C—F=1.30±0.03 Å, C—Cl=1.69±0.02 Å, and $\angle C_1-C_2-F=\angle C_2-C_1-Cl=121\pm1°$ for fluorochlorobenzene. C—C=1.40 Å, C—H=1.04 Å are assumed throughout the analysis.

The authors wish to express their sincere thanks to Prof. A. Kotera for his continued encouragement to this research. They are also indebted to Mr. M. Yamaha and Mr. M. Igarashi for their helpful discussions and suggestions. A part of the cost of this research has been defrayed from the Scientific Research Encouragement Grant from the Ministry of Education, to which the authors' thanks are due.

Chemical Laboratory, Tokyo Bunrika University, Tokyo

The Structure of Surface Denatured Protein. V. The Surface Film of Diketo-piperazine

Kazutomo IMAHORI

(Received August 8, 1952)

Introduction

Many investigations have been made about the properties of monolayers of proteins. Rideal[1] and Alexander[2] insist that the unfolded polypeptide chain has β-keratine configuration, while Isemura[3] has explained his results by using Mizushima and Shimanouchi's model. But none has regard for the existence of diketopiperazine configuration on the surface. It may not be probable that polypeptide chain has diketopiperazine configuration on the water surface. Yet, the existence of diketopiperazine configuration cannot be denied until the limiting area of diketopiperazine film is determined.

The author has investigated the diketopiperazine monolayer and obtained the value of limiting area from the results of F—A, V—A and η—A curves.

Experimental

Material—Diketopiperazine is prepared from glycine by Dr. Tadao Sugita, in the Institute of Chemistry, Faculty of Science, University of Tokyo, and is recrystallized several times. This is spread on the surface of KCl solution of about 0.2 N concentration from the solution in the mixed solvent of dichloracetic acid and benzene. The spread film is uniform as checked by the constancy of surface potential within the error of 1 mV.

Measuring Apparatuses—Surface pressure was measured by a modified Wilhelmy balance, which has been described in the Part I of this series[4]. Surface potential is measured by the apparatus described in Part III of this series[5]. Viscosity of monomolecular film can be measured by the method of flowing out through a capillary canal[6], by the method of the oscillation of a ring in the monolayer[7] or by the method of rotation of a ring (analogous to a cell of Couette) in the monolayer[8].

The apparatus and the procedure of the present measurements are essentially the same as those described by Joly[6]. A diagram of the apparatus used is shown in Fig. 1. This consisted essentially of a brass tray T, containing a canal C and two Wilhelmy balances W and W'. The canal is 1.1 cm long and 0.062 cm broad, and have door D at its end, which controls the flow of monomolecular film. Harkins[9] gave for this case the following equation,

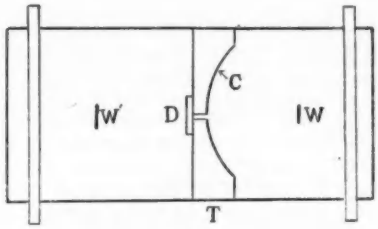

Fig. 1

$$\eta = \frac{\alpha}{Q} \cdot \frac{d^3}{12} - \frac{d \cdot \eta_0}{\pi}$$

where α is the film pressure gradient, Q the quantity of the film which passes through the canal in unit time, d the breadth of the canal and η_0 the viscosity of the substrate.

Thus, the surface viscosity η can be determined by the measurement of the quantity Q.

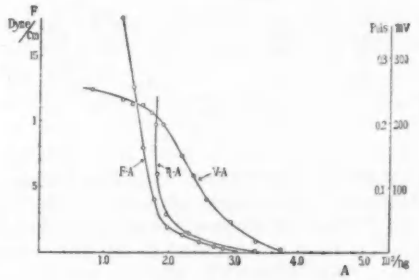

Fig. 2

1) E. K. Rideal, *Proc. Roy. Soc.* (*London*) **A137**, 70 (1932).
2) C. W. N. Cumper and A. E. Alexander, *Trans. Farad. Soc.*, **46**, 240 (1950).
3) T. Isemura and K. Hamaguchi, This Bulletin, **25**, 40 (1952).
4) K. Imahori, This Bulletin, **25**, 7 (1952).
5) K. Imahori, This Bulletin, **25**, 13 (1952).
6) M. Joly, *Kolloid Zeits.*, **89**, 26 (1939).
7) L. Fourt, *J. Phys. Chem.*, **43**, 887 (1939).
8) R. Chaminade, D. G. Dervichian et M. Joly, *Journ. Chim. Phys.*, **47**, 883 (1950).
9) W. Harkins, *J. Chem. Phys*, **5**, 601 (1937), **6**, 53 (1938).

Results

The F—A curve in Fig. 2 shows the plot of the film pressures in dyne per centimeter against the film areas in square meters per milligram. The measurements were done as carefully as possible. The film was compressed slowly with small decrements. Ample time was allowed after each decrease in area for the attainment of equilbrium surface pressure. The result shows that the limiting area of this curve is 1.85 m^2/mg.

The V—A curve in the figure shows the plot of the surface potentials of the film in millivolt against the film areas in square meters per milligram. The curve shows that the limiting area is 1.82 m^2/mg.

The η—A curve in the figure shows the plot of the surface viscosity in pois against the film area in square meters per milligram. All the experiments, represented by the circlets in the figure, were carried out under surface pressure differences below 2.5 dyne per centimeter. In the figure, sudden increase in slope of the curve occured at 1.82 m^2/mg and this shows that the limiting area is 1.82 m^2/mg.

Discussions

The above three curves show that the limiting area of diketopiperazine monomolecular film is 1.82—1.85 square meters per milligram. The mean of the three values is 1.83 m^2/mg (or 34.6 $Å^2$ per one diketopiperazine molecule).

The crystal structure of diketopiperazine has been determined by Corey[10] by X-ray diffraction. From this result, the limiting area per one diketopiperazine molecule is to be 35.5 $Å^2$ when diketopiperazine molecule are orientated flat on the surface (the broad side on) perhaps in such a way as shown in Fig. 3.

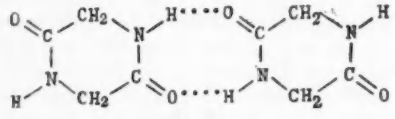

Fig. 3

Comparing this result with that obtained by author's experiment, we can say the following: The diketopiperazine molecules lie flat when they are expanded on the water surface. But when the film is compressed below the limiting area, diketopiperazine molecules probably begin to rise on the surface.

10) R. B. Corey, *J. Amer. Chem. Soc.*, **60**, 1598 (1938).

On the other hand, the author has obtained the limiting area of the horse serum albumin molecule to be about 9820 $Å^2$ [4]. The chemical constitution of the serum albumin molecule has been determined by several authors[11] and it is calculated that one serum albumin molecule contains about 780 amino acid residues. Thus, the mean limiting area per one amino acid residue becomes to be 12.5 $Å^2$. This value is far less than the limiting area of the diketopiperazine film (17.3 $Å^2$/amino acid residue) and, it can be denied that the polypeptide chain of the serum albumin shows diketopiperazine configuration as it is spread on the surface.

The value of 14.7 $Å^2$ is obtained by Isemura[3] for synthetic protein analogues and also by Alexander for the alanine-polymer[2]. And it is obvious that synthetic protein analogues also does not show the diketopiperazine confiuration, when they are spread on the water surface.

As Isemura has insisted, the above value of 14.7 $Å^2$ can be explained most perfectly by using Mizushima and Shimanouchi's E-type model,[12] while one amino acid residue of B-type molecule would cover about 10 $Å^2$. Dr. T. Shimanouchi and the present author has ascertained these two values from the experiments of glycine-polymer monolayer, which will be published in other report.

Anyhow, from these values, the configuration of polypeptide chain of surface denatured serum albumin does not comprise the diketopiperazine ring. Probably, it is the mixture of B-and E-type of Mizushima and Shimanouchi's model[12].

Summary

1. The curves of the surface pressure against area, the surface potential against area, and surface viscosity against area were obtained with diketopiperazine. All the three curves show the limiting area to be about 1.83 m^2/mg or 34.6 $Å^2$ per molecule.

2. Comparing this result with that obtained by Corey, diketopiperazine molecules are thought to lie flat on the surface.

3. The above value is far larger than the limiting areas of native serum albumin or synthetic protein analogues. And the polypeptide chain will not show the diketopiperazine configuration on the surface.

The author wishes to express his hearty thanks to professors S. Mizushima and B.

11) W. Steine & S. Moore, *J. Biol. Chem.*, **178**, 79 (1949), E. Brand et al., *J. Amer. Chem. Soc.*, **67**, 1524 (1945).

12) S. Mizushima & T. Shimanouchi, This Bulletin, **21**, 1 (1948).

Tamamushi for their kind advice and encouragement. The author also owes much to Dr. T. Shimanouchi to whom the author's thanks are due. The expense of this work has been defrayed from the Grant in Aid for Fundamental Scientific Research from the Ministry of Education.

Chemical Institute, College of General Education, University of Tokyo

Intermolecular Charge-Transfer Spectra. I. Halogen-Aromatic Complexes

Hideo MURAKAMI

(Received February 17, 1953)

Introduction

Recently, Mulliken developed the theory of intermolecular charge-transfer spectra[1,2]. According to him, the concept of intermolecular charge-transfer spectra gives a reasonable explanation for many cases, such as halogen-aromatic complexes, organic molecular compounds, hydrated anions, etc. In the present paper, we shall study the characteristic absorption bands (λ_{max}: 2,800 Å~3,300 Å, ϵ_e: 7,000~14,000) of halogen-aromatic complexes, especially the dependence of the absorption intensity on the structure of aromatic components. In the case of methyl derivatives of benzene, experimental results indicate that the true molar extinction coefficient ϵ_e decreases with introducing methyl groups into an aromatic component. On the contrary, the above-mentioned theory indicates the increase of ϵ_e for the same condition as above, and Mulliken himself admits the difficulty of this contradiction. The chief object of the present paper is to solve this puzzle.

When halogen derivatives of benzene are used as aromatic components, the observed values of ϵ_e are mysterious. The reasonable interpretation for these results will also be given.

Absolute Intensity

In the case of hydrated anions, Rabinowitch introduced the idea of electron transfer spectra to explain the characteristic strong absorption band[3]. He attributed it to such an electron transfer from anion to water molecule as follows.

$$X^-\cdot(H_2O) \xrightarrow{h\nu} X\cdot(H_2O)^-$$

As was emphasized by Rabinowitch, the absorption intensity which corresponded to the above process was very large (ϵ~10,000).

It is obvious that anion X^- and molecule H_2O are chemically saturated. Therefore, we cannot expect the usual valence bond between them. Then the distance R between them may be approximately given by addition of their respective van der Waals radius. Consequently, R becomes relatively large compared with the usual covalent bond distances. This situation indicates the small overlapping between orbital functions of two components. Taking this fact into account, the above-described large absorption intensity is somewhat surprising.

Recently, Mulliken gave the quantum mechanical formalism to the idea of electron transfer spectra (in Mulliken's nomenclature, intermolecular charge-transfer spectra), and showed that large absorption intensity was understandable even when the intermolecular distance R was relatively large.

Now, we summarize the essence of Mulliken's theory in the suitable form for the present study. In complex A·B, A and B represents the acceptor and donor respectively. Then, two sorts of wave functions, ψ_0 and ψ_1, are defined. Firstly, ψ_0 is a "no-bond" wave function with respect to covalent bonding, that is

$$\psi_0=\psi(A\cdot B) \qquad (1)$$

Secondly, ψ_1 is a "dative" wave function corresponding to the transfer of an electron from B to A accompanied by the establishment of a weak covalent bond, that is

$$\psi_1=\psi(A^-—B^+) \qquad (2)$$

Using these wave functions, the wave function of the ground state N of any complex A·B is approximated by

1) R. S. Mulliken, *J. Am. Chem. Soc.* **72**, 600 (1950).
2) R. S. Mulliken, *J. Am. Chem. Soc.* **74**, 811 (1952).
3) E. Rabinowitch, *Rev. Mod. Phys.*, **14**, 112 (1942).

$$\psi_N = a\psi_0 + b\psi_1 \qquad (3)$$

In loose complexes, the relation $a^2 \gg b^2$ is expected. Further, we can expect that the overlap integral

$$S = \int \psi_0 \psi_1 dv \qquad (4)$$

is very small*, and neglect it in the following rough approximation.

From Eq. (3), the energy of the ground state is given by the lower root of the seqular equation

$$\begin{vmatrix} W_0 - W & H_{01} \\ H_{01} & W_1 - W \end{vmatrix} = 0 \qquad (5)$$

where

$$W_0 = \int \psi_0 \boldsymbol{H} \psi_0 dv \ , \quad W_1 = \int \psi_1 \boldsymbol{H} \psi_1 dv$$

$$H_{01} = \int \psi_0 \boldsymbol{H} \psi_1 dv \qquad (6)$$

$\boldsymbol{H}$ is the exact Hamiltonian operator for the entire system. The solution of Eq. (5) is given as

$$W = (W_1 + W_0)/2 \pm [(W_1 - W_0)^2 + 4H_{01}^2]^{\frac{1}{2}}/2 \qquad (7)$$

In case of loose complex, we can expect the relation

$$1 \gg 4H_{01}^2/(W_1 - W_0)^2 \qquad (8)$$

Taking this relation into account, we expand the second term of the right hand side of Eq. (7), then

$$\left.\begin{aligned} W_N &\simeq W_0 - H_{01}^2/(W_1 - W_0) \\ W_E &\simeq W_1 + H_{01}^2/(W_1 - W_0) \end{aligned}\right\} \qquad (9)$$

where W_N and W_E represents the energy of normal and excited state respectively. These are familiar second-order perturbation equations, and correspond to Mulliken's equations in which the overlap integrals S are taken as zero. The wave function ψ_E which belongs to the eigenvalue W_E takes the following formula

$$\psi_E = a\psi_1 - b\psi_0 \qquad (10)$$

The ratio of the coefficients a and b is easily given as follows,

$$\pm\rho = b/a \simeq -H_{01}/(W_1 - W_0) \qquad (11)$$

Using Eqs. (3) and (10), the dipole moment μ_{EN} of transition $(\psi_E \to \psi_N)$ is given as

$$\mu_{EN} = -e \int \psi_E \vec{r} \psi_N dv \simeq eab(\vec{r}_B - \vec{r}_A) \qquad (12)$$

where $\vec{r}_B$ and $\vec{r}_A$ represents the radius vector from origin of arbitrary coordinate to the center of two components B and A, respectively. So long as the wave functions ψ_N and ψ_E are normalized, the condition $a^2 \gg b^2$ requires that a is very near to unity and b is relatively small compared with unity. Under such a condition, the dipole moment μ_{EN} is very sensitive to the value of b and, according to Mulliken, a relatively small value of b is sufficient to explain the observed large absorption intensity. At the present stage, however, the reliable and exact determination of the value of b has not been established yet.

Relative Intensity (Analysis of Experimental Results)

In 1938, Aickin, Bayliss and Rees studied the absorption spectra of bromine in solution and observed the new intense absorption bands in the neighbourhood of 2950 Å in case of aromatic solvents[4]. They interpreted these bands, however, as bromine bands which were enormously enhanced by the solvent effect. Later, Benesi and Hildebrand investigated the absorption spectra of iodine in aromatic solvents[5]. The intense absorption bands which were analogous to those of bromine solutions were observed. Moreover, they found that the extinction coefficient of these bands was directly proportional to the iodine concentration using aromatic solvents. This fact indicates the existence of the equilibrium as follows,

$$I_2 + Ar \rightleftarrows I_2 \cdot Ar$$

where Ar denotes the aromatic hydrocarbon, and $I_2 \cdot Ar$ denotes the iodine-aromatic complex.

They considered that the above-mentioned intense absorption bands in the near ultraviolet region were due to only the presence of the complex $I_2 \cdot Ar$, and determined the

* The exact determination of the value of S is somewhat difficult. In case of iodine-benzene complex, Mulliken considered that the upper limit of S is the order of 0.1~0.2. According to our estimate, however, the overlap integral between π-orbital of benzene and σ-orbital of iodine do not exceed 0.02 so long as we assume the usual Slater type functions and the same model of complex as that of Mulliken.

4) R. G. Aickin, N. S. Bayliss and A. L. G. Rees, *Proc. Roy. Soc.* (London), **A169**, 234 (1938).

5) H. A. Benesi and J. H. Hildebrand, *J. Am. Chem. Soc.*, **71**, 2703 (1949).

true molar extinction coefficient ϵ_c of complex by taking into account the equilibrium constant for the above reaction. The results are given in Table 1. Keefer and Andrews performed the same experiment using chlorine, bromine and iodine monochloride instead of iodine and obtained the interesting results as shown in Table 1 and 2[7,8]. From these results, we can extract some noticeable relations as follows:

Table 1
Experimental Values of λ_{max} and ϵ_c

Aromatic Component	I_2-Aromatic Complexes		Cl_2-Aromatic Complexes	
	λ_{max} (A)	ϵ_c	λ_{max} (A)	ϵ_c
Benzene	2970	15400		9090
m-Xylene				6340
Mesitylene	3330	9300		

Table 2
Experimental Values of λ_{max} and ϵ_c

Aromatic Component	Br_2-Aromatic Complexes		ICl-Aromatic Complexes	
	λ_{max} (A)	ϵ_c	λ_{max} (A)	ϵ_c
Benzene	2920	13400	2870	9900
Toluene	3010	10500	2940	9050
t-Butylbenzene			2900	8470
o-Xylene	3130	8200	3030	7720
m-Xylene	3120	10100	3010	9000
p-Xylene	3060	7300	2950	7200
Chlorobenzene	2860	7300	2870	5650
Bromobenzene	2880	7600	2890	5750
Iodobenzene	3100	17000		

a) When toluene or *t*-butylbenzene is used as aromatic component instead of benzene, the true molar extinction coefficient ϵ_c derceases to some extent.

b) When xylene or mesitylene are used instead of benzene, ϵ_c decreases further except in the case of *m*-xylene. In the case of *m*-xylene complex, ϵ_c is almost the same as in toluene complex.

c) When chlorobenzene or brombenzene is used, ϵ_c is small and the same order of *o*-or *p*-xylene. In case of iodobenzene complex, howeuer, ϵ, is larger than that of benzene complex.

d) Now, we compare ϵ_c of Br_2-complex with those of corresponding ICl-complexes. (See Table 2). To extract the interesting regularity, we define the ratio k of ϵ_c as follows.

$$k_1 = \frac{\epsilon_c \text{ of } Br_2\text{-substituted benzene complex}}{\epsilon_c \text{ of } Br_2\text{-benzen complex}}$$

$$k_2 = \frac{\epsilon_c \text{ of ICl-substituted benzene complex}}{\epsilon_c \text{ of ICl-benzene complex}}$$

The values of k_1 and k_2 for various aromatic components are easily calculated using ϵ_c in Table 2, and shown in Table 3. Then, it is obvious that in any case the relation

Table 3
Comparison of k_1 and k_2

Aromatic Component	k_1	k_2
Benzene	1.00	1.00
Toluene	0.78	0.91
o-Xylene	0.61	0.78
m-Xylene	0.75	0.91
p-Xylene	0.54	0.73
Chlorobenzene	0.54	0.57
Bromobenzene	0.57	0.59

$$k_2 > k_1$$

exists without exception.

The main object of this paper is to explain the above-mentioned relations a), b), c) and d) considering the relative configuration of two components from the statistical point of view.

As is described in a) and b), true molar extinction coefficient ϵ_c decreases with introducing metyl groups into the aromatic components. According to Mulliken's theory, the reverse is predicted. As shown in Table 4, the ionization potential of an aromatic molecule decreases with introducing methyl groups[8]. This makes the value of $(W_1 - W_0)$ smaller, and according to Eq. (11), the value of $\rho = b/a$ larger. Consequently, Eq. (12) predicts the increase of dipole moment μ_{EN}, that is, the increase of absorption intensity. At first sight, the contradiction of experimental and theoretical results seems very difficult to solve. We can show, however, that the harmony between them is obtainable by the examination of a model.

Table 4
Lowest Ionization Potential (in ev)[8]

Aliphatic Compound	I. P.	Aromatic Compound	I. P.
Methane	13.1	Benzene	9.24
Ethane	11.6	Toluene	8.92
Propane	11.3	*t*-Butylbenzene	8.5*
Methyl Chloride	11.25	*o*-Xylene	8.3*
Ethyl Chloride	10.89	*m*-Xylene	8.3*
Methyl Bromide	11.17	*p*-Xylene	8.3*

6) R. M. Keefer and L. J. Andrews, *J. Am. Chem. Soc.*, **72**, 4677, 5170 (1950).
7) L. J. Andrews and R. M. Keefer, *J. Am. Chem. Soc.*, **73**, 462 (1951).
8) W. C. Price, *Chem. Rev.*, **41**, 257 (1947).

Ethyl Bromide	10.92 10.24[a]	Chlorobenzene	9.42[b]
Methyl Iodide	9.49	Bromobenzene	9.41[b]
Ethyl Iodide	9.34 9.295[a]	Iodobenzene	9.10[b]

* These value have been estimated by consideration of spectroscopic features other than Rydlberg series, and probably less accurate.

a) W. C. Price, *J. Chem. Phys.*, 3, 365 (1935).

b) J. D. Morrison and H. J. C. Nicholson, *J. Chem.* Pys., **20**, 1021 (1952).

Relative Intensity (Statistical Consideration)

For the relative configuration of two components in the complex, Mulliken assumed the model, in which iodine or bromine molecule rests on the benzene molecule with its axis parallel to the plane of the benzene and its center on the sixfold axis of the benzene. It is obvious that this model is the most compact one, and stable on account of van der Waals interaction. Moreover, according to Mulliken's opinion, the resonance energy $-H_{01}^2/(W_1-W_0)$ between ψ_0 and ψ_1 in the ground state is larger in this model than in the other. (See Eq. (9)). Then, it is an interesting and important problem to compare the magnitude of van der Waals interaction energy with that of resonance stabilizing energy.

Experimentally, Cromwell and Scott measured the heat of formation of iodine-benzene complex.[9] Their results indicate that ΔH is approximately -1.4 Kcal./mol. This value is smaller than the energy in weak hydrogen bond and is the order of magnitude which is understandable as mere van der Waals interaction energy. Further, Ham, Rees and Walsh found out that the infrared spectra of saturated solution of iodine in the purified mesitylene was indistinguishable from that of mesitylene[10]. These results probably indicate that the main interaction is the van der Waals type, and the resonance type (in Mulliken's nomenclature, charge-transfer force) is smaller compared with the former.

If the van der Waals type is predominant and the resonance type is negligible compared with the former, Mulliken's idealized model needs some revision for halogen-substituted benzene complexes. For example, when the aromatic component is monosubstituted benzene, we can consider the two configurations (α) and (β) in Fig. 1, and can expect almost the same stability for them considering van der Waals type interaction. Then it occurs that (α) and (β) type complexes exist in solution with almost equal statistical weight.

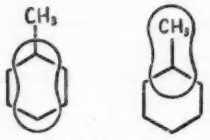

(α) Fig. 1 (β)

In case of model (β), the overlapping between π-orbital of aromatic component and σ-orbital of halogen component is decreased considerably, and the distance between centers of two components is slightly lengthened. These situations make the value of H_{01} smaller and of (W_1-W_0) slightly larger. Remembering Eqs. (11) and (12), we can expect the decrease of coefficient b, and then of dipole moment μ_{EN}.

In the experimental determination of ϵ_c, it was assumed that all the complexes had the same absorption intensity. As is shown before, however, this assumption is not a reasonable one, and the experimental values are nothing but the statistical mean for complexes (such as models (α) and (β)) which have their own various absorption intensities.

a) Bromine-Toluene Complex.—As idealized model, we consider the two relative configurations (α) and (β) which are shown in Fig. 2.

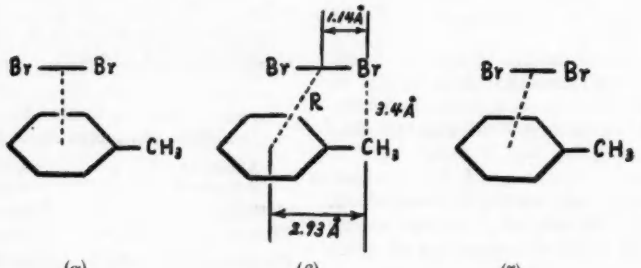

(α) (β) (γ)

Fig. 2

9) T. M. Cromwell and R. L. Scott, *J. Am. Chem. Soc.*, **72**, 3825 (1950).

10) N. S. Ham, A. L. G. Rees and A. Walsh, *J. Chem. Phys.*, **20**, 1336 (1952).

In model (α), all conditions are equal to that of an idealized model for bromine benzene complex which has been postulated by Mulliken, except the decrease of ionization potentical of aromatic component by amount of 0.32 ev. (See Table 4). Since the decrease of ionization potential causes the decrease of (W_1-W_0) by almost the same amount, it is expected that the wavelength λ_{max} at maximum absorption of toluene complex shifts towards the longer side. Taking λ_{max} =2920 Å. of benzene complex as origin, the decrease of (W_1-W_0) by amount of 0.32 ev. predicts λ_{max}=3160 Å. for model (α) of bromine-toluene complex. This is longer than the experimental value 3010 Å. As is easily shown, the absorption intensity of bromine-toluene complex in model (α) is almost the same as that of bromine-benzene complex, that is, $\epsilon_e^{(\alpha)}\sim$13400. (See Table 2).

In model (β), the intermolecular distance R which combines the center of bromine molecule and center of benzene ring is lengthened by the amount of 0.44 Å. This causes the decrease of absolute value of Coulombic energy by the amount of 0.48 ev in excited state. If the effect of polarization is taken into account, this value may become smaller to some extent. The decrease of absolute value of Coulombic energy tends to conpensate the variation of ionization potential and exchange interaction energy. Therefore, we assume that (W_1-W_0) is equal to that of bromine-benzene complex. Then λ_{max} in model (β) is expected to be 2920 Å. (See Table 2). In model (β), as discussed before, the overlapping between π-orbital of benzene ring and σ-orbital of bromine may decrease and this causes the decrease of ϵ_e considerably. The exact calculation of ϵ_e in model (β) is somewhat defficult; then we postulate that the value of ϵ_e in model (β) is the half of that in model (α) as tentative one, that is, $\epsilon_e^{(\beta)}\sim$6700.

Now, we bring up the third assumption that models (α) and (β) have almost equal stability and exist in solution with almost equal statistical weight. Then the molar extinction coefficient of bromine-toluene complex is give by

$$\epsilon_e=(\epsilon_e^{(\alpha)}+\epsilon_e^{(\beta)})/2=10500$$

The observed ϵ_e is just 10500 (See Table 2). On account of the superposition of two bands, the wavelength at absorption maximum becomes to lie in the middle of λ_{max} which are predicted for models (α) and (β), then approximately at about 3040 Å. The observed value is 3010 Å. The same result is obtainable by postulating model (γ) instead of the third assumption. In model (γ), the relative position of bromine to benzene ring is in the middle of models (α) and (β).

b) Bromine-Xylene complexes.—When *o*- or *p*-xylene is used as aromatic component, we can expect the three relative configurations as shown in Fig. 3. Then, as is postulated in bromine-toluene complex, we assume that these configurations have almost the same stability. Using the same values of $\epsilon_e^{(\alpha)}$ and $\epsilon_e^{(\beta)}$ as those used before, we obtain ϵ_e of bromine-xylene complex as follows.

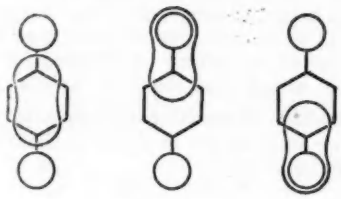

Fig. 3.

$$\epsilon_e=(\epsilon_e^{(\alpha)}+2\epsilon_e^{(\beta)})/3=8933$$

The observed value is 8200 for *o*-xylene complex, and 7300 for *p*-xylene complex.

In case of *m*-xylene complex, the observed value of ϵ_e is very large, that is 10100. This fact indicates that model (α) is more stable than model (β) and predominant statistically in solution. Consequently, we must consider that the benzene ring in *m*-xylene has a larger van der Waals attraction than that in *o*- or *p*-xylene.

According to experimental results of Platt and Klevens, the intensity of $N\rightarrow V$ type transition of π-electron in *m*-xylene is larger than that in *o*- or *p*-xylene.[11] The experimental total oscillator strength f of this transition is 1.46 for *m*-xylene and 1.22$\sim$1.23 for *o*- or *p*-xylene. According to our tentative estimate, this strong $N\rightarrow V$ type transition contributes considerably to the van der Waals interaction, and the larger f value of *m*-xylene may probably sufficient to explain the required larger van der Wasls attraction of benzene ring in *m*-xylene.

c) Bromine-Halogenobenzene Complexes.—When chlorobenzene or bromobenzene is used as aromatic component the observed ϵ_e is very small, and it has the same order with $\epsilon_e^{(\beta)}$ (See Table 2). This requires that model (β) is more stable than model (α), and almost all the complexes exist in the con-

11) J. R. Platt and H. B. Klevens, *Chem. Rev.*, **41**, 301 (1947).

figuration of model (β). If we take into account the interaction between large dipole of C—Cl or C—Br bond and the induced dipole in bromine molecule, the above requirement may probably be understandable.

On the contrary, when iodobenzene is used as aromatic component, the observed ϵ_c is very large. In case of iodobenzene, the ionization potential of substituted iodine (9.295 ev.) is almost equal to that of benzene (9.24 ev.) (See Table 4). Then, being different from other cases, π-electrons in substituted iodine can contribute to intermolecular charge-transfer spectra as well as π-electron in benzene ring. Consequently, the magnitude of H_{01} in model (β) may be equal to or larger than that in model (α). This situation may probably explain the observed large ϵ_c.

d) Iodine Monochloride-Aromatic Complexes.—As is shown in Table 3, there exists the relation,

$$k_2 > k_1$$

This relation requires that the stability of model (α) relative to model (β) is larger in ICl-aromatic complexes than in corresponding Br_2-aromatic complexes. This requirement may be understandable considering the interaction between large dipole of ICl and the induced dipole in the benzene ring.

The above discussions all concern the halogen-aromatic complexes. We can expect the validity of the analogous discussions for the other molecular compounds, such as quinhydron type molecular compounds. The detailed study for these cases will be reported later.

Summary

The intermolecular charge-transfer spectra of halogen-aromatic complexes have been studied theoretically. Especially, the dependence of absorption intensity on the structure of aromatic component has been investigated. To solve the discrepancies between experimental results and Mulliken's theoretical predictions, we have introduced the statistical consideration for the relative configurations between two components. Using some reasonable assumptions, we have obtained the satisfactory agreement between theoretical predictions and experimental results, at least qualitatively.

The author wishes to express his sincere thanks to Prof. S. Akabori for his encouragement and interest in the course of this work, and also to Mr. I. Tanaka and Y. Mori for their valuable discussions.

Faculty of Science, Osaka University, Osaka

Intermolecular Charge-Transfer Spectra. II. Pressure Effect on the Characteristic Absorption Spectra of Molecular Complexes

Hideo MURAKAMI

(Received March 20, 1953)

Previously, Gibson and Loeffler studied the absorption of visible light by solutions of amins in nitrobenzene under large hydrostatic pressures, and observed the significant change of absorption as a function of pressure.[1] Recently, Shuler presented a free electron model to explain the characteristic absorption spectra of molecular complexes, especially the above-mentioned pressure effect on these spectra.[2] According to our opinion, however, Shuler's theory is not a suitable one for the explanation of the present problem, at least in its original form. In the following discussion, we show that the kinetic consideration of Gibson and Loeffler combined with Mulliken's theory[3] may probably be sufficient to explain the observed pressure effect.

Discussion on Shuler's Theory

The essence of Shuler's theory can be summarized as follows. When two one dimensional conjugated molecules, A and B, ap-

1) R. E. Gibson and H. Loeffler, *J. Am. Chem. Soc.* **62**, 1324 (1940); See also, **61**, 2877 (1939).
2) K. E. Shuler, *J. Chem. Phys.*, **20**, 1865 (1952).
3) R. S. Mulliken, *J. Am. Chem. Soc.*, **74**, 811 (1952).

proach sufficiently close, the potential for π-electrons can be expressed by the idealized model as shown in Fig 1. Then, the pene-

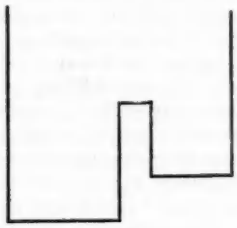

Fig. 1—One-dimensional unsymmetrical potential model for molecular complex.

tration of the central potential barrier by π-electrons produces a splitting of energy levels in the resulting two minimum potential. It was difficult, however, to obtain these splittings quantitatively for the unsymmetrical potential as described above, and Shuler assumed the simplified symmetrical potential as shown in Fig. 2. For this model, each

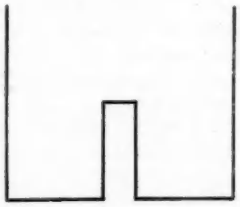

Fig. 2.—Simplified symmetrical potential model which is assumed by Shuler for molecular complex.

original energy level of the free molecule splits into two, and this situation is shown in Fig. 3. On account of the assumption of

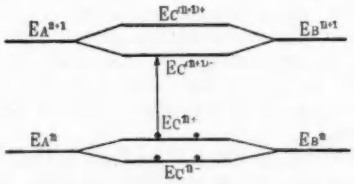

Fig. 3.—Splitting of energy levels by complex formation in case of symmetrical potential

symmetrical potential, one has the simple relationship

$$E_A^n = E_B^n \qquad (1)$$

for all the energy levels of the conjugated molecular partners. Taking the splitting of each level into account, the energy levels E_C of the complex which correspond to the energy levels E_A^n and E_B^n of A and B can be expressed as follows:

$$E_C^{n+} = E_A^n + \epsilon^n \qquad (2)$$

$$E_C^{n-} = E_A^n - \epsilon^n \qquad (3)$$

where $2\epsilon^n$ is the delocalization energy for the n the level. If E_C^{n+} is the highest filled level of the complex, the main absorption band is then due to the transition

$$E_C^{n+} \longrightarrow E_C^{(n+1)-}$$

where

$$E_C^{(n+1)-} = E_A^{(n+1)} - \epsilon^{(n+1)} \qquad (4)$$

and the wavelength λ_C of this absorption peak is given by

$$\lambda_C = \frac{hc}{\Delta E} = \frac{hc}{[E_A^{(n+1)} - E_A^n] - [\epsilon^{(n+1)} + \epsilon^n]} \qquad (5)$$

Now, Shuler postulated that the effect of pressure reduced the width and height of central potential barrier corresponding to the closer approach of both components. This situation produces an increase of delocalization energy ϵ on account of easier penetration by π-electrons through the barrier. Consequently, as is seen in Eq. (5), the increase of ϵ produces an increase of λ_C, so long as one assumes the constancy of $[E_A^{(n+1)} - E_A^n]$. Thus, Shuler's theory predicts the shift of main absorption band towards the longer wavelength side at higher pressure.

We must emphasize, however, that the assumption of symmetrical potential is not adequate to amine-nitrobenzene complexes. In these cases, the potentials are rather unsymmetrical as shown in Fig. 4. And so, the condition of Eq. (1) becomes no longer valid. Then, Eqs. (2), (3), (4) and (5) lose their validity. According to Mulliken's theory, the characteristic absorption band of molecular complex (A B) corresponds essentially to the transition, as follows.

$$(A\,B) \longrightarrow (A^- - B^+)$$

That is, one electron is transferred from B to A in the process of optical transition. In a free electron model, this situation should be expressed by the transfer of a π-electron from level N_B to level $(M+1)_A$ as shown in Fig. 4. Further, in the case of an unsymmetrical model, the delocalization energy may be mainly due to the small amount of penetration of π-electron from level N_B to

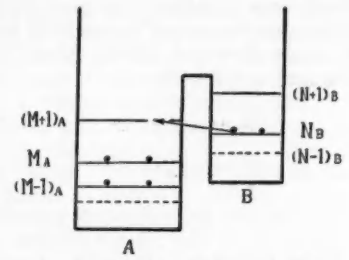

Fig. 4.—Expected relative height of energy level in case of unsymmetrical potential. (In the present case, component A and B corresponds to nitrobenzene and dimethylaniline respectively).

level $(M+1)_A$ through the potential barrier. Thus, the application of Shuler's model may probably be limited to the self-complex such as benzene-benzene complex.

Discussion on Absorption Intensity

The typical experimental results of Gibson and Loeffler are shown in Fig. 5 for 50% solution of dimethylaniline in nitrobenzene at 45°. The results are given as transmission curves. Curve 1 and 3 is the case of solution in 0.5 cm. cell at 1 bar and 1000 bars respectively. Curve 2 and 4 is the case of solution in 0.9 cm. cell at 1 bar and 1000 bars respectively. It must be emphasized that these curves are nothing but a very small portion of the complete absorption band, and the behaviours at the region of absorption maximum under the influence of pressure are not observed. Then, we cannot conclude directly the shift of absorption bands towards the longer side so long as the data are limited to the above mentioned ones.

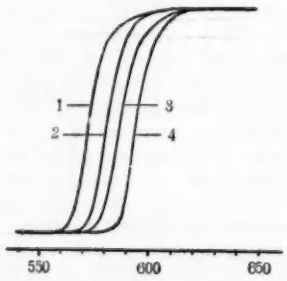

Fig. 5.—Transmission curves for 50% solution of dimethylaniline in nitrobenzene at 45°
1, solution in 0.5 cm cell at 1 bar;
2, solution in 0.9 cm cell at 1 bar;
3, solution in 0.5 cm cell at 1000 bars;
4, solution in 0.9 cm cell at 1000 bars.

Moreover, the comparison between curves 1 and 2 suggests that the pressure effect is mainly due to the intensification of light absorption. In case of curve 2, the absorbing layer is increased 1.8-fold in thickness compared with curve 1. Consequently, we can expect that the degree of light absorption is also increased by the same amount. This situation appears in Fig. 5 as if the absorption band is pushed towards the longer wavelength side, although the location of the absorption band should be the same in either case. If we assume that the pressure effect is only due to the intensification of light absorption, the distance between curves 1 and 3 or curves 2 and 4 requires that the absorption intensity is 2.5~3.5-fold increased under the pressure of 1000 bars, at least in the region of the observed wavelength.

At the present stage, we cannot give any conclusion whether the wavelength at absorption maximum shifts towards the longer or shorter side, or remains at the same position under the effect of pressure. On the other hand, however, we can give a rather definite explanation of the intensification of light absorption, as follows.

Gibson and Loeffler assumed that the absorption of visible light by the solution was proportional to the average time the active groups of unlike molecules spent very close to each other, i.e., to the probability of finding two unlike molecules at very short distances apart and suitably oriented in the solution. Using kinetic consideration and some empirical relations which were obtained by them, they showed that the above hypothesis was sufficient to explain the intensification of light absorption due to the increase of pressure at constant temperature or the elevation of temperature at constant volume. Then, the remaining task is to base the hypothesis of Gibson and Loeffler by Mulliken's theory on intermolecular charge-transfer spectra.

According to Eq. (12) in Part I, the dipole moment of charge-transfer spectra is approximated by the formula

$$\mu_{EN} \simeq e a_0 (\vec{r}_B - \vec{r}_A) \qquad (6)$$

were

$$b/a \simeq -H_{01}/(W_1 - W_0) \qquad (7)$$

As has been discussed in Part I, dipole moment μ_{EN} is sensitive to the value of H_{01}. Since absorption intensity f_{EN} is proportional

to the square of μ_{EN}, f_{EN} is much more sensitive to the value of H_{01}. Further, as can easily be seen from Eq. (6) in Part 1, the value of H_{01} is very sensitive to the overlap between the wavefunctions (in the present case, between that of π-electron systems) of both components. The degree of overlap depends very much on the distance and relative orientation between both components. Consequently, the increase of the probability of finding two unlike molecules, A and B, at very short distances apart and suitably oriented in a solution makes the absorption intensity much larger. Thus, the hypothesis of Gibson and Loeffler is based by the theory of intermolecular charge-transfer spectra.

The author wishes here to express his sincere gratitude to Prof. S. Akabori for his interest and encouragement throughout the study of this series.

Faculty of Science, Osaka University, Osaka

Physicochemical Properties of the Surface of Aqueous Solutions VI. Breaking of the Solid Surface

By Hideo KIMIZUKA

(Received May 14, 1953)

In one of our preceding papers, the study on the mechanical properties of the surface of a solution[1] was carried out in relation to the foam stability and a further investigation was continued on the mechanical behavior of the surface[2]. As to the foam stability, however, it may be pointed out that the formation of the coherent adsorbed layer though closely related is not an exact explanation for the stabilizing action of the foam, because the mechanical behaviors thereby investigated was that of the surface film suffering no destruction. On the other hand, some complicated phenomena such as an irreproducibility in the surface tension value[3], and the membrane effect were observed when the surface tension was measured with a solution forming a solid film. So a further study on the mechanical property of the film near the yield point, where so-called time dependent phenomena[4,5] were frequently observed, was attempted to obtain a more plausible explanation for these phenomena.

1) H. Kimizuka and T. Sasaki, This Bulletin, **24**, 230 (1951).
2) H. Kimizuka and T. Sasaki, This Bulletin, **25**, 318 (1952); H. Kimizuka, ibid, **26**, 30, (1953).
3) du Noüy, "Surface Equilibria of Biological and Organic Colloids" *J. Am. Chem. Soc.*, Monograph Series No. 27, Chemical Catalog Comp. Inc., New York (1926).
4) W. F. Busse, E. T. Lessig, D. L. Loughborough and L. Larric, *J. App. Phys.*, **13**, 715 (1942).
5) H. Kubota, *Oyo Butsuri* (*J. App. Phys.*), **17**, 236 (1948).

Experimental and Result

In the present study, the solutions used were chosen so that the liquid might form a solid film[2]. In the first place, a distribution of the life-time of the aqueous film was observed under a constant tension using du Noüy's tensiometer. A platinum ring of the tensiometer, 1.5 cm. in diameter, was just touched to a fresh surface of 1% saponin solution contained in a shallow glass vessel, 6 cm. in diameter and 1.3 cm. in depth. A constant tension was applied to the ring and the breaking time, t, elapsed before the detouchment of the ring from the surface was measured. The experiments were carried out at 28±1°C. The results showed that N, the number of breakings which occurred after a time t, was empirically approximated by the equation,

$$N = N_0 e^{-mt} \qquad (1)$$

where N_0 and m are constants excepting the case in the region of the smaller time. The results of similar experiments under diffrent tensions were shown in Fig. 1. For water, ethyl alcohol and its aqueous solution, m was either zero or infinity.

A measurement of the breaking time as a function of stress was carried out by means of the torsion ring method. The apparatus[2]

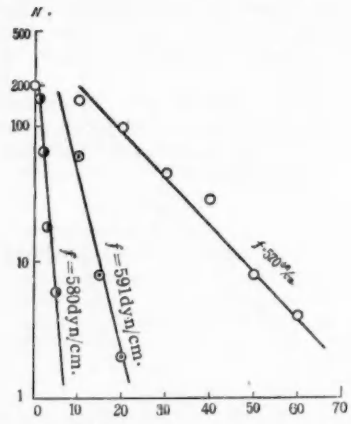

Fig. 1. Distribution of breaking time with constant tension. Saponin solution (10g./l.).

used was essentially the same as described already, but in this case a suspension wire with a torsion constant, κ, of 5.35 dyn. cm. and a platinum ring with diameter of 2.0 cm. was used and the inner cylinder was removed. The breaking time, τ, elapsed before the sudden increase in a strain of the surface, $d\theta$ was measured under a constant torsional force, f ($=\kappa\theta_0$, θ_0 being a torsion angle) for 1 g./l. saponin solution aged for one hour. The temperature of this and all of the following experiments was 10±1°C. One of the results is shown in Fig. 2. The following relation can then be found to hold as shown in Fig. 3 a,

$$log\tau = a - bf \qquad (2)$$

where a and b are constants.

The torsion ring method was also applied for the measurement of yield value. Immediately after a breaking of the surface by rotating the top of torsion wire with the

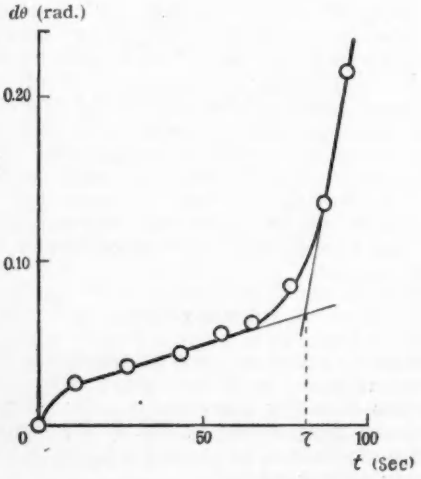

Fig. 2. Strain~time curve near rupture of absorbed layer of saponin solution (1g./l.) aged for 1 hr. $f=\kappa\theta_0=22.8$ dyn. cm.

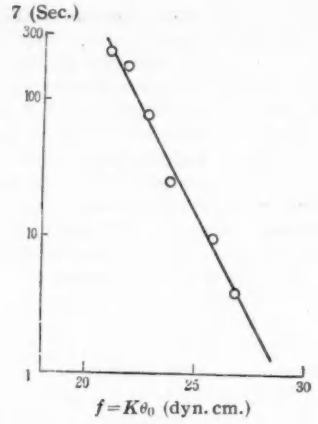

Fig. 3 a. Breaking time as a function of stress. Saponin solution (1g./l.).

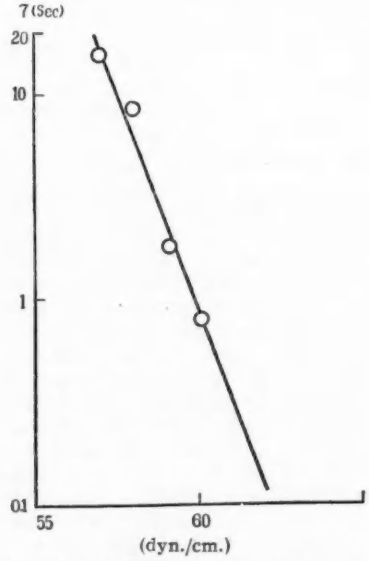

Fig. 3 b. Breaking time as function of stress. Saponin solution (10g./l.).

angle of θ_r under the condition of $\tau \fallingdotseq 0$, the top was returned to the initial position and θ_a, an angle at which the motion of the ring was stopped, was measured. Thus we obtained the values $\kappa\theta_r$ and $\kappa\theta_a$ which were considered to correspond to the yield value of breaking and solidifying respectively. The membrane effect[1], M, was measured by the capillarimeter with a radius of 0.0284 cm. Now it can easily be seen that $\kappa\theta_r$ and $\kappa\theta_a$ should correspond to M_r and M_a respectively, where M_r and M_a represent the membrane effect acting on the receding and advancing meniscii in the capillary tube. Here the true surface tension is assumed to be situated between the two apparent surface tensions and $M=M_r+M_a$. Both the measurements of the yield value and the membrane effect were carried out for the surfaces of solutions containing various substances aged for one hour. The result is shown in Fig. 4, in which the ordinate represents M; the abscissa, $F_0=\kappa(\theta_r+\theta_a)$.

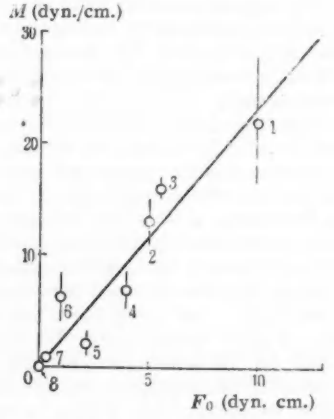

Fig. 4. Membrane effect versus yield value of adsorbed layer diagram for solutions. 1, 0.25 g./l. saponin solution; 2, 0.10g./l. saponin solution; 3, 1g./l. egg albumin solution; 4, 10g./l. peptone solution; 5, 5g./l. polyvinyl alcohol solution; 6, 5×10^{-3} M./l. night blue solution; 7, 5g./l. gum arabic solution; 8, water.

A method for the measurement of the surface tension was devised as follows. A platinum ring of the du Noüy's tensiometer was just touched to the surface of a solution, which was pulled upward by the applied force, and a rise of liquid meniscus was measured. Under such a condition, the principal section of the free liquid surface is represented as shown by a curve AB in Fig. 5. In this figure, A shows a cross section of the

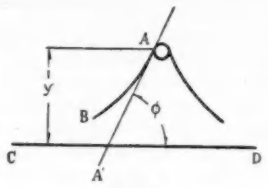

Fig. 5.

platinum ring and AA' is a tangent to the curve AB at the point of contact A, and makes an angle ϕ with the horizontal surface of liquid. Then a rise of meniscus y is given by the equation[6],

$$\rho g y^2 = 2\sigma(1-\cos\phi), \qquad (3)$$

where ρ is the density of liquid; g, the gravity constant and σ, the surface tension. Now if f is a force exerted by the ring per unit length,

$$f=\sigma \sin\phi. \qquad (4)$$

A simple calculation* using Eqs. (3) and (4) leads to the expression,

$$\lim_{y\to 0}\frac{df}{dy}=(\rho g\sigma)^{\frac{1}{2}}$$

or

$$\sigma=\frac{1}{\rho g}\left(\lim_{y\to 0}\frac{df}{dy}\right)^2 \qquad (5)$$

This relation holds fairly well for ethyl alcohol solutions with varying concentrations as shown in Fig. 6, where σ is measured by the usual method. In the case of the surface exhibiting the nature of a solid film, σ in Eq. (5) should be replaced by σ' of the following equation,

$$\sigma'=\sigma+Ed\zeta, \qquad (6)$$

where E is the elastic constant and $d\zeta$, an increase in surface area with relation to y. Since the condition of $y\to 0$ corresponds to that of $d\zeta\to 0$, σ' is equal to σ in such a case and again the Eq. (5) is valid, namely the equation gives a true surface tension even when the surface film becomes somewhat

6) F. C. Chapman and N. Davy, "Properties of matter", Blackie & Son Ltd., London and Glasgow, (1936) p 104.

* If we assume further the condition of $f=\sigma$ and therefore $\phi=\pi$ 2 in this calculation, $\sigma=\frac{1}{2}\rho g y_0^2$ results, where y_0 is y when $\phi=\frac{\pi}{2}$, a maximum rise of the meniscus. This equation was confirmed by the experiment using ethyl alcohol solution with varying concentration. The result is shown in Fig. 8.

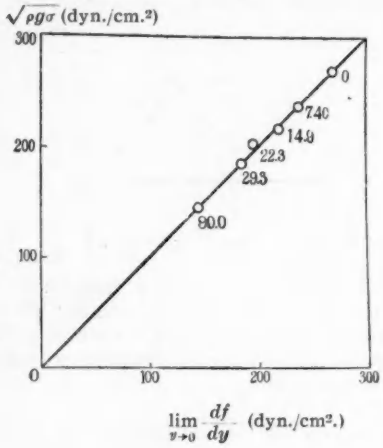

Fig. 6. Relation between $\lim_{y\to o}\frac{df}{dy}$ observed and $\sqrt{\rho g\sigma}$ calculated. Number listed at each point represents the concentration (%) of aqueous ethyl alcohol solution.

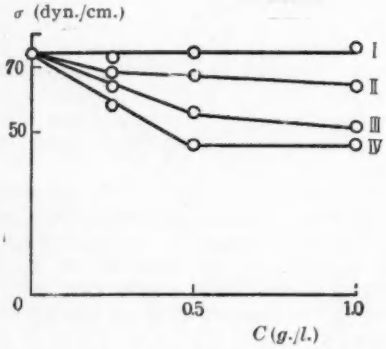

Fig. 7. Surface tensions of saponin solution. Each curve shows the values of surface tension measured by the ring method (II), present method (III) and capillary method (I and IV which correspond to receding and advancing meniscii respectively.).

solid in nature. Thus the present method was adopted for the measurement of surface tension of the saponin solution aged for one hour. The values obtained for various concentrations were plotted in Fig. 7, together with those of apparent surface tension obtained by the capillary rise method with receding and advancing conditions, and the ring method.

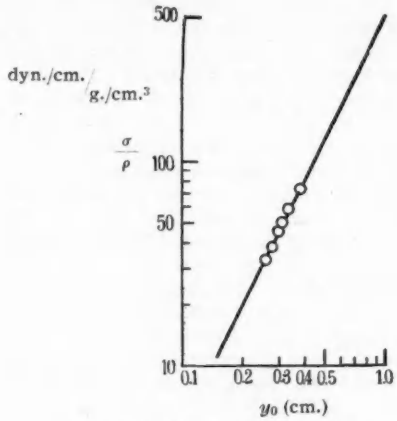

Fig. 8. Ethyl alcohol solution.

Discussion

It has frequently been pointed out for the measurement of surface tension of such a solution as saponin solution that the reproducible results could hardly be obtained even when the experimental conditions such as temperature, concentration and time of ageing were carefully controlled[3]. Among the other factors which are responsible for such a fluctuation, the breaking of the solid film hereby formed can be considered most important. In fact, if the measurement is carried out by means of du Noüy's tensiometer, the measured "surface tension" may actually be the force required for the breaking of the surface film. Results obtained as shown in Fig. 1 evidently show this fact. Kubota[5] obtained a similar result for the breaking of glass which he accounted for by introducing the probability of breaking, m, which was independent of time. Now it was confirmed that in the case of common liquids, m sharply changed from zero to infinity as the external force increased, whereas in the case of saponin solution m changed gradually from zero to infinity.

We should like further to refer to the equations (1) and (2). The phenomena expressed by these equations are liable to conflict with each other. As shown in Fig. 1, however, the deviation from the constancy of the value of m was observed in the region of shorter time, and in fact a frequency of occurrence of breaking showed a maximum in this range of time. A time, τ, at which the maximum frequency was observed was again related with the corresponding stress, f, by the equation (2). This was shown in Fig. 3b.

This relation was further confirmed by the measurement of the thin film withdrawn from the surfaces of 1% solutions of saponin and egg albumin, which was not given here. A possibility may further be considered that the surface tension effect would also be the cause of this phenomenon, but the result of the torsion ring method may exclude such a possibility, since here the surface area is kept constant and the motion of the ring is free from the action of surface tension. Thus the coincidence of the results of both techniques gives us the confirmation that they can be explained by the same mechanism, the breaking of a solid film. A similar relation was also observed for the breaking of high polymer[4] and was also treated theoretically[7]. These fact together with our former result[2] lead us to the opinion that the rupture of an aqueous saponin film rather resembles the breaking of a solid body such as glass or high polymer, and should not be treated as the rupture of the ordinary liquid film. Thus the breaking of the surface film, proved to occur in some range of stress, may result in the irreproducibility of apparent surface tension, if we do not specify the time required for the rupture of film, for instance, to be sufficiently small. A number of explanations[8] for the foam stability have already been presented, but they all neglected to take into account of this fact.

As shown in Fig. 4, the membrane effect was proportional to the yield value of the solid film, which was valid for the several solutions. This will be a confirmation of the view presented in a preceding paper[9] that the membrane effect is a measure of the strength of the surface.

As pointed out before, the irregularity of surface tension is due to the rupture of solid film, so a method free from such an influence is required for a measurement of true surface tension. The technique devised proved to be applicable for common liquids as shown in Fig. 6, which showed a good agreement with the result obtained by the usual method for ordinary solutions. On the other hand, the apparent surface tension of saponin solution measured by the usual method was somewhat higher than that by the present method as shown in Fig. 7. This probably means that the usual method involves an inevitable rupture of surface film. Fig. 7 also showed that the true surface tension is situated between two apparent surface tensions measured previously by a capillarimeter[9].

7) A. Tobolsky and H. Eyring, *J. Chem. Phys.*, **11**, 125 (1943).
8) T. Sasaki, *Kagaku no Ryoiki*, **5**, 16 (1951).
9) H. Kimizuka and T. Sasaki, *Memoirs of the Faculty of Science, Kyushu University, Ser. C*, **1**, 197 (1950).

Summary

(1) The rupture of aqueous saponin film was studied by measuring the variation of the frequency of the breaking with tension as well as by measuring the breaking time as a function of stress. The results showed that the irreproducibility of the observed data upon surface tension was due to the breaking of the solid film and this mechanism was also responsible for the nature of the stability of such a foam as that produced by saponin, which was also considered to consist of solid film.

(2) A new method for the measurement of surface tension, applicable to the solution forming a solid adsorbed layer, was presented.

(3) It was shown that the membrane effect is a breaking stress of the adsorbed layer.

In conclusion, the author expresses his hearty thanks to Prof. T. Sasaki for his kind guidance and encouragement throughout this study and he is also indebted to Dr. T. Tanaka of this University for his kind suggestion and criticism. A part of the cost of this research has been defrayed from the Scientific Research Expenditure of the Ministry of Education given to Professor Sasaki.

Department of Chemistry, Faculty of Science, Kyushu University, Fukuoka

Synthesis and Dielectric Polarization of 9-Anthranol

By Kenkichi NUKADA and Yoshié BANSHO

(Received June 23, 1953)

Introduction

K. H. Meyer reported in 1911 on the synthesis of 9-anthranol, which is the simplest substance in leuco-compounds of anthraquinone series, and also on its behaviour in several organic solvents.[1] He observed that 9-anthranol exhibited strong fluorescence in some solvents and explained that there might exist in solution a chemical equilibrium between anthrone and 9-anthranol, the reaction velocity

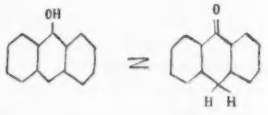

9-Anthranol Anthrone

Fig. 1

and equilibrium constant of which depended on solvent. Bäckström et al. pointed out an iodine titration method for the quantitative analysis of 9-anthranol.[2] Le Fèvre et al. investigated the dielectric behaviour of the same substance and its methyl ether. However, the above-mentioned authors could not prepare pure 9-anthranol. The present authors have established the best condition of synthesis of 9-anthranol and measured the dipole moment of it by the solution method. The reproducibility was satisfactory.

Experimental

Synthesis

The original procedure of Meyer[1] and the modified one of Bäckström and Beatty[2] have been traced, but the purity of 9-anthranol prepared in this way was unsatisfactory. The authors have synthesized 9-anthranol of high purity by improving these two methods. They have found that it was important to operate the synthesis continually in a stream of nitrogen (to prevent oxidation) and to maintain the temperature as low as possible (to prevent isomerisation) during the preparation. The result of synthesis had good reproducibility.

Anthrone was prepared from anthraquinone (Org. Syn. Coll. vol. 1, p. 60) and recrystallised twice from mixed solvent of benzene and petroleum ether (3:1). m.p. 154.7°C.

The apparatus is shown schematically in Fig. 2, and the procedure is as follows:

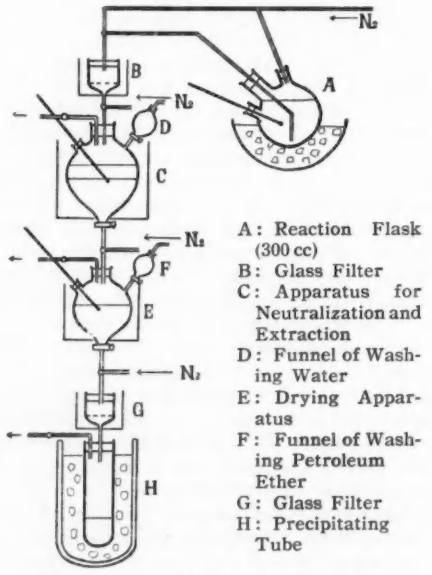

Fig. 2. Apparatus for Synthesis of 9-Anthranol

3.0 g. of fine powdered anthrone was boiled in 180 g. of 10% aqueous solution of sodium hydroxide for about ten minutes in a stream of nitrogen, and as soon as the boiling was over, 300 g. of ice pieces were added and the flask was cooled rapidly by an ice sodium chloride bath set outside. When the temperature of the solution lowered to −5°C, the flask was arranged as indicated in Fig. 2, A, and cooled to maintain this temperature.

Apparatus for neutralization and extraction, C, which contained 120 cc. of toluene, 300 cc. of distilled water, 300 g. of ice pieces and 15 cc. of 98% sulphuric acid, was cooled from outside by solid carbon dioxide to maintain −5°C. The solution of sodium salt of 9-anthranol was poured directly into C in a stream of nitrogen and shaken; the

1) K. H. Meyer, *Ann.*, **379**, 37 (1911).
2) H. Bäckström and H. Beatty, *J. Phys. Chem.*, **35**, 2549 (1949).
3) C. L. Angyal and R. J. W. Le Fèvre, *J. Chem. Soc.*, **1950**, 562.

precipitated 9-anthranol was extracted in upper toluene layer. Then by the pressure of nitrogen the water layer was removed, the toluene layer was washed with 200 cc. of distilled water and the water layer was removed similarly. The yellow emulsion was sent into a drying apparatus F which contained 80 g. of fresh calcined and oxygen-free anhydrous sodium sulphate, and was shaken at −5°C. 20 cc. of petroleum ether (b.p. 60~70°C.) was cooled beforehand at ca. −70°C. in a precipitating tube H which was immersed in a solid carbon dioxide-methanol bath; the clear dried 9-anthranol toluene solution was then poured into petroleum ether through the glass filter G by the suction and the pressure of nitrogen. Sodium sulphate was washed with 60 cc. of petroleum ether (b.p. 60~70°C) and solution in H was diluted simultaneously. The pale yellow precipitate of 9-anthranol was deposited immediately and the precipitation was accomplished in an hour. The precipitate was filtered in a stream of nitrogen as rapidly as possible, washed with 50 cc. of petroleum ether (b.p. 45~50°C), then taken in a vacuum desiccator and sucked by a vacuum pump for half an hour at 0°C to remove petroleum ether contained in crystal. Then the product was dried for about ten hours over phosphorous pentoxide in a vaccum at the same temperature. The yellow fine crystal of 9-anthranol was enclosed in ampouls in a stream of nitrogen. yield: 1.5—1.7 g.

Infrared spectrum of 9-anthranol suspended in Nujol was measured and a strong absorption band of OH group was observed.

Notice

1) Water and toluene used in the synthesis were distilled in a stream of nitrogen, so that they were free from oxygen.

2) It was necessary to cool all the apparatus, A to G, at −3 ~ −5°C by small pieces of solid carbon dioxide.

3) All the transfusions of liquid were made in a closed apparatus by the suction or under the pressure of nitrogen, and the whole time of preparation was within half an hour.

4) Oange-yellow to red crystal was deposited, if the temperature rose or the air leaked into the apparatus. The product prepared in this way could not be used as a sample for the measurement of dielectric constant because the reproducibility of results was unsatisfactory.

Behaviour in Solvent

9-Anthranol was dissolved in several solvents and the times t's required for the complete disappearance of fluorescence of solutions were measured. (Table 1). According to Meyer,[1] t was a function of the reaction velocity of tautomerism.

In ethanol, dioxane and ether t's were large and the reactions were supposed to be slow. However in carbon disulphide, carbon tetrachloride, acetone and pyridine no fluorescence appeared and the reactions were supposed to be very fast. In benzene t was large and as the number of methyl groups of benzene ring increased, t decreased. In petroleum ether, n-heptane and cyclohexane t's were large but practically these solvents could not be used in the dielectric measurement because the solubilities in these were very small.

As the suitable solvents the authors then chose benzene, dioxane and toluene for the following experiments.

Table 1

The Times Required for the Complete Disappearance of Fluorescence at 7°C.

Solvent	Solubility	t (hours)
Benzene	+	22
Toluene	+	10
m-Xylene	+	5
Chlorobenzene	+	0.5
Methanol	+	6.5
Ethanol	+	ca. 50
n-Buthanol	+	7
i-Amyl Alcohol	+	17
Ether	+	24
Dioxane	++	ca. 60
Petroleum Ether (b.p. 40~60°C.)	−	24
n-Heptane	−	24
Cyclohexane	−	23
Acetic Acid	+	1
Chloroform	+	0.2
Carbontetrachloride	+	No fluorescence
Carbon Disulphide	+	"
Acetone	+	"
Pyridine	++	"

The symbols are: ++ very great, + ordinary, − very small.

Dielectric Measurements

Solvent: All the solvents were purified according to the methods in "Organic Solvents".[4]

Density: Ostwald-type pycnometer was used.

Instrument: Usual Heterodyne-beat type oscillator designed and constructed by one of the authors (Nukada) was used to measure dielectric constants of solutions.[5] Capacities of sample cells were from 50 pF to 80 pF.

The synthesized sample had to be stored in nitrogen atomosphere at low temperature and to be dissolved in solvents as quickly as possible. When the purity of a sample was low or the temperature of solution too high, 9-anthranol changed into anthrone and the fluorescence of the solution vanished rapidly.

4) A. Weissberger and E. Proskauer, "Organic Solvents", Oxford University Press, 1935, p. 106, 107, 140.

5) e.g. see J. W. Baker and L. Groves, *J. Chem. Soc.*, 1939, 1144.

Table 2

The Dielectric Constants and the Densities of 9-Anthranol in Several Organic Solvents.*) **) ***)

i) Solvent: Benzene, 6.3°C.

ω	ε_{12}	v_{12}
0.01297	2.345	—
0.00885	—	1.1164
0.00485	2.325	1.1178
0.00165	2.318	1.1190

$\varepsilon_1=2.313$ $v_1=1.1193$
$\alpha=23.0$ $\beta=-0.397$
$p_{20}=0.634$ $P_{20}=123$ cc
$\mu=1.72$ D

ii) Solvent: Benzene, 15°C.

ω	ε_{12}	v_{12}
0.02197	—	1.1240
0.01654	2.338	—
0.01299	2.330	—
0.00877	2.317	1.1281
0.00860	2.315	—
0.00520	2.309	1.1295
0.00386	2.304	—
0.00234	—	1.1303
0.00165	2.299	—

$\varepsilon_1=2.294$ $v_1=1.1309$
$\alpha=26.7$ $\beta=-0.332$
$p_{20}=0.73$ $P_{20}=142$ cc
$\mu=1.99$ D

iii) Solvent: Dioxane, 15°C.

ω	ε_{12}	v_{12}
0.01424	2.336	0.9578
0.01044	—	0.9588
0.00380	2.306	0.9605
0.00229	2.303	0.9610

$\varepsilon_1=2.298$ $v_{12}=0.9614$
$\alpha=26.7$ $\beta=-0.264$
$p_{20}=0.63$ $P_{20}=122$ cc
$\mu=1.82$ D

iv) Solvent: Benzene-Dioxane Mixture, 15°C (Mol fraction B : D = 10 : 1)

ω	ε_{12}	d_{12} (g/cc)	P_2 (cc)
0.01555	2.352	0.9089_2	162
0.01296	2.341	0.9076_8	159
0	2.295	0.9028_5	—

$P_{20}=161$ cc $\mu=2.20$ D

v) Solvent: Benzene-Dioxane Mixture, 15°C (Mol fraction B : D = 100 : 1)

ω	ε_{12}	d_{12} (g/cc)	P_2 (cc)
0.02150	2.350	0.8979_9	138
0.00914	2.313	0.8935_7	132
0	2.291	0.8911_8	—

$P_{20}=135$ cc $\mu=1.91$ D

vi) Solvent: Toluene, 15°C.

ω	ε_{12}	d_{12} (g/cc)	P_2 (cc)
0.02117	2.444	0.8788	115
0.01605	2.440	0.8776	128
0.00826	2.426	0.8767	134
0.00409	2.409	0.8728	132
0	2.398	0.8713	—

$P_{20}=133$ cc $\mu=1.88$ D

*) The symbols used in this Table are the same as those of Halverstadt and Kumeler.[7] ε_{12}: dielectric constant of solution, $v_{12}(=1/d_{12})$: specific volume of solution (cc/gr), ω: concentration (weight percent), P_2: solute molar polarization, P_{20}: solute molar polarization at infinite dilution, p_{20}: solute specific polarization at infinite dilution: $\alpha=\frac{d\varepsilon_{12}}{d\omega}$, $\beta=\frac{dv_{12}}{d\omega}$, ε_1: dielectric constant of solution at infinite dilution, v_1: specific volume at infinite dilution, μ: dipole moment (Debye unit).

The values of α, ε_1, β and v_1 were calculated utilizing the statistical method of least squares.

**) In calculation of the orientation polarization the authors have assumed that the sum of electric polarization and atomic one was equal to the molar refraction MR_D for sodium D line. For 9-anthranol $MR_D=58$ cc.

***) μ were calculated as

$$\mu=0.0128\times\sqrt{(P_{20}-MR_D)T}$$

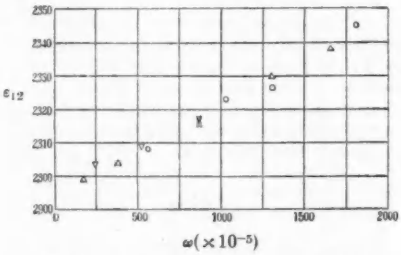

Fig. 3. Relation between ω and ε_{12}
Solvent: Benzene. 15°C.
Symbols △, ▽ and ○ represent the results of several experiments under the same condition.

Results

Dielectric constants and densities of several solutions were measured at various concentrations. (Table 2).

All the $\omega\sim\varepsilon_{12}$ curves became straight lines except for toluene solution.[6]

The dipole moments of 9-anthranol in benzene and dioxane solutions were calculated by Halverstadt-Kumler's equation[7] and the moments in other solutions by the usual method.[8] The results are in Table 3. Since in solutions there exists a chemical equilibrium

6) Fig. 3 shows the result of several measurements under the same experimental condition. Unlike the case of other samples, (e.g. anthrone in benzene, Denys, I. Coomber and J. R. Partington, *J. Chem. Soc*, **1938**, 1444,) the curves were not fine straight lines. This deviation means probably the unstability of 9-anthranol in solvents.

7) I. F. Halverstadt and W. D. Kumler, *J. Am. Chem. Soc.*, **64**, 2988 (1942).

8) P. Debye, "Polare Molekeln". Leibzig, 1929.

between 9-anthranol and anthrone, values in Table 3 do not mean the "exactly true value of dipole moment of 9-anthranol" but should be regarded as a "nearly true one", because in such solvents the velocity constants are small. Le Fèver et al. measured the dipole moment of 9-anthranol methyl ether. (1.5 D). Noting a difference of 0.4~0.5 D between phenol and its methyl ether, they supposed that 9-anthranol had a moment of 1.9~2.0 D.[3] The authors' result agrees with this supposition.

Table 3

The Dipole Moments of 9-Anthranol in Several Organic Solvents

Solvent	Temp	Moment (Debye Unit)
Benzene	6.3°C	1.72 D
Benzene	15 °C	1.99 D
Benzene : Dioxane (100 : 1)	15 °C	1.91 D
Benzene : Dioxane (10 : 1)	15 °C	2.20 D
Dioxane	15 °C	1.82 D
Toluene	15 °C	1.88 D

In benzene-dioxane mixture, the moment values are comparable with Nagakura and Baba's result on phenol.[9]

In toluene $\omega \sim \varepsilon_{12}$ curve was not a straight line.

It may be reasonable to explain the stabilisation of 9-anthranol by the assumption that in benzene[10] and dioxane[11] OH-group of 9-anthranol makes weak combination with solvent and the potential barrier between anthrone and 9-anthranol becomes higher, hydrogen atom of 9-anthranol's OH is thus hindered from shifting to the position "10" of anthracene ring. The results in Table 1 also support this asumption except for acetone and pyridine, in which the stabilisation of 9-anthranol by the combination O···H—O and N···H—O can be expected, but the causes of these exceptions are not plain now.

9) S. Nagakura and H. Baba, *J. Am. Chem. Soc.*, **74**, 5693 (1952).

10) There is a coupling of π-electrons of benzene with proton of OH-group in solute molecule. (W. Lütte and R. Mecke, *Z. Elektrochem.* **53**, 241 (1949).)

11) In dioxane a hydrogen bond between solvent and solute may exist.

Summary

1) The condition of synthesis to obtain pure 9-anthranol was established.

2) Times required for the complete disappearance of fluorescence of solution were measured and assumed to be measures of reaction velocities of tautomerism from 9-anthranol to anthrone. In ethanol, ether, dioxane and benzene the reaction velocities were small.

3) Dielectric constants of 9-anthranol in benzene, dioxane, benzene-dioxane mixtures and toluene solutions were measured. Reproducibility was satisfactory. In the said solvents 9-anthranol was relatively stable and $\omega \sim \varepsilon_{12}$ curves were straight lines except in toluene.

4) The stability of 9-anthranol in solvent was supposed to be increased, by an interaction between π-electrons of solvent and proton of solute O—H group in the case of benzene, or by O···H—O combination in the case of dioxane.

The authors' thanks are due to the kind guidance of Mr. Y. Mashiko and Mr. E. Koike, the Technical Officials of this Institute, and Assistant Prof. S. Nagakura, Tokyo University and to the advices in experiment of Mr. S. Saeki and Mr. K. Fujii, this Institute.

The Government Chemical Industrial Research Institute, Tokyo

Rheology of Coal. VI. The Micelle Structure in Relation to Anomalies of Rheological Properties of A Bituminous Coal

By Katsuya INOUYE and Hideo TANI

(Received August 25, 1952)

Introduction

The linear relationships between ash concentration in volume percentage and some rheological properties of coals[1,2,3] have made one of the authors (K. I.) propose a theory on the structure of coals, especially for caking coals, in which the coal molecules "solvate" around ash particles as a filler in formation of a micelle-like structure.

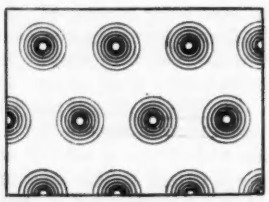

Fig. 1-a. Model of the Structure of Caking Coals.

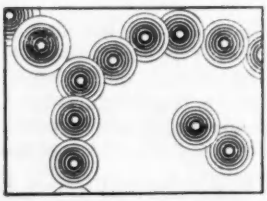

Fig. 1-b. Scaffolding Structure of Micellar Spheres.

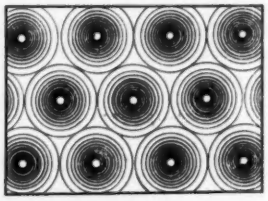

Fig. 1-c. Close-packed state.

The "free" molecules freed from solvation forces act as a plasticizer when the whole system is carbonized. The model would thus appear able to illustrate the cause of caking properties which means and necessitates the mobile condition of the system in caking temperature range, according to the theory, by the "plasticizer effect" of the matrix of micellar system, notwithstanding whether or not the *intra*-micellar changes have to occur. Fig 1-a illustrates the structural model of strongly-caking coal. The concentration of blackening means the strength of intermolecular forces, and the circles represent ash particles as skeletons. High concentration around the circles means strong solvation. For weakly or non-caking coals, the concentration around ash is low and at the same time blackening of the background must be strong; in such conditions thermal mobility of the whole system at higher temperatures cannot be accomplished.

The validity of this model with micelle and matrix may be well demonstrated by using carbon black as rigid micelle spheres and bakelite "A" as more freely combined matrix[4]. This black mixture, preferably with addition of a small amount of alcohol, when "carbonized" up to say 120°C, fuses (cakes) and remarkably swells, resulting in a very porous hard substance which very much resembles coke.

In this paper, the authors make mention of discussing the anomalous behavior of a Japanese bituminous coal, Takashima, in its rheological properties to discuss the model structure by an actual example.

Elasticity, Viscosity and Strength

Takashima bituminous coal, mined in Kyushu, Japan, having the average volatile matter of approximately 38% (d. a. f.), has been distinguished in the authors' experiments by wide distribution of ash concentration between various specimens from 1 to 20 in weight %.

1) Elasticity; Prat I of this study, K. Inouye, *J. Colloid Sci.* **6**, 190, (1951).
2) Internal Viscosity; Part II, K, Inouye, This Bulletin, **26**, 84, (1953).
3) Breaking Strength; Part V, K. Inouye and H. Tani, This Bulletin, **26**, 359, (1953).
4) K. Inouye, Unpublished experiments.

The modulus of elasticity values by resonant frequency method previously reported[1] and further data showed that the variation curve of elastic constant with ash concentration has some ranges of entirely different inclination, as shown in Fig 2. It is noteworthy that a minimum of the elastic moduli exists at $\phi=2$, and also that the elasticity decreases again in the range of 8~10% of ϕ. (ϕ is the ash content in volume percentage, dry basis.)

The experiments of internal viscosity from measuring the vibrational decrement at audiofrequencies[2], which suggested that the same relationships as in the Young's modulus experiments exist also in the viscosity data, led to an interesting fact of Fig. 2 that for Takashima coal a minimum at $\phi=2\%$ and second maximum at $\phi=10$ were recognized for the internal viscosity also.

Furthermore, the strength for rupture of the rectangular specimen[3] showed a variation of the strength factors with ϕ in nearly the same form, as illustrated in Fig. 2. The statistical correlation of the breaking strength upon ash concentration[3] has already suggested that the correlation must be considered for every individual range of ash concentration.

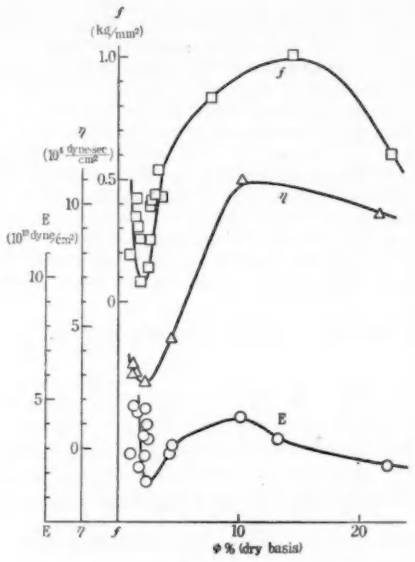

Fig. 2. Varication of Rheological Properties with Ash Concentration.
E: Young'g Modulus
: Internal Viscosity
f: Breaking Strength

An Interpretation of Variations in Rheological Properties

It is recognized in the rubber science that the loading with carbon black to improve mechanical properties of rubber causes perturbation of the stresses and strains set up in the body, and hence this leads to an increase in the elastic and viscosity constants, i, e., a stiffening of the solid, in linear relationships with carbon content.[5,6] Tensile strength, for instance, increases by the loading. However, the changes of strength are considered to be not in linear relationship with loading but in varying manner according to the ranges of loading. E. Guth[6] suggested that the decrease of the tensile strength of rubber-carbon black system for small loadings is caused by the stress concentrations occurring around the carbon particles when the stress is applied, and the increase of the strength for greater loadings by the tendency of the carbon black particles (perhaps of the "solvated" micellar spheres) to form chains and finally some type of network. This increase with loading continues up to the point where the suspension becomes a dilution of carbon by rubber. He made mention of carbon content for the first range as up to 10% by volume, for the second 10 to 30%.

Such descriptions are apparently very suggestive for the present case of coal, by the close similarity of the fundamental characteristics, in spite of the numerical differences. The minimum of Young's modulus, internal viscosity coefficient and breaking strength at 2% of ash content by volume appears to correspond to the state where the micelle spheres, in which the ash particles as nuclei solvate coal molecules, first contact each other to form a scaffolding structure, as schematically illustrated in Fig 1-b. In other words, the modellic picture as Fig. 1-a, homogenious in distribution of the micelles, may not represent the actual structure, because if all micellar spheres could touch each other even at the ash concentration of 2% by volume, the dimension of a micellar sphere must be very large.

If the maximum of the rheological properties at approximately 8 to 10% by volume of ash means the point where the micellar spheres exist in a closed-packing state, as Fig. 1-c, the total internal surface of the micellar system is calculated as,

$$S=\frac{m(\text{area of a sphere})}{m(\text{volume of a sphere})d}$$
$$=m4\pi R^2/m(4/3)\pi R^3 d$$
$$=3/Rd,$$

where S is the total specific surface area per one gramme of the coal, m the number of micellar spheres per gramme, R the radius of the sphere and d is the true density. Hence the radius of the micelle can be obtained if the specific internal surface area of the sample with 10% of ash content by volume is known. A specimen with 10.13% of ϕ was examined at first for Young's modulus (4.19×10^{10} dyne/cm²) and internal viscosity coefficient (1.1×10^{5} dyne. sec/cm²) to ascertain

5) H. M. Smallwood, *J. Appl. Phys.*, **15**, 758, (1944).
6) E. Guth, *J. Appl. Phys.*, **16**, 20, (1945).

to assume as the appropriate sample for this purpose, and then powdered. The range of particle size of 30 to 60 Tyler mesh was chosen to measure the specific surface area by the iodine adsorption method at 25.0°C[7]. Using the obtained value of specific area, 9.51×10^4 cm²/g (dry basis), and the density measured in methanol at 25.0°C, 1.24, R was calculated as 2,540Å. As the value of ϕ of this sample is 10.13%, the radius of the ash particle is estimated as 1,160 Å; the value of the radius of "filler" particle in coal is in the same order, but slightly larger, as those of some kinds of carbon blacks[8]. The value of the micellar radius may mean, on the other hand, that solvation forces or internal pertubation caused by ash particles reach in the space of radius of approximately 2,500 Å. However, it may not be true that the dimension of ash particles is always constant overall the ranges of ash concentration, but varying dimensions according to the ash content and therefore to the variation of micellar structure itself are more probable.

Shigen-Gijyutsu-Shikenjo
(Resources Research Institute)
Saitama-Kawaguchi, Japan

(7) K. Inouye, *J. Fuel Soc. Japan*, **29**, 112, (1950).

(8) J. Sameshima, H. Akamatsu, K. Inouye, S. Kawamura, R. Matsuura, H. Hamada and K. Tamaru, *Rev. Modern Colloid Sci. Japan*, Vol. **1**, 250, (1948). R. B. Anderson and P. H. Emmett, *J. Appl. Phys.*, **19**, 367, (1948)

On the Ring-opening Reactions of the Furan Compounds. III. On the Condensation of Furfural with Methyl Ethyl Ketone by Alkali

By Hiroshi MIDORIKAWA

(Received March 20, 1953)

In the case of condensation of furfural with methyl ethyl ketone by alkali, there are two possibilities, as illustrated in the accompanying equation:

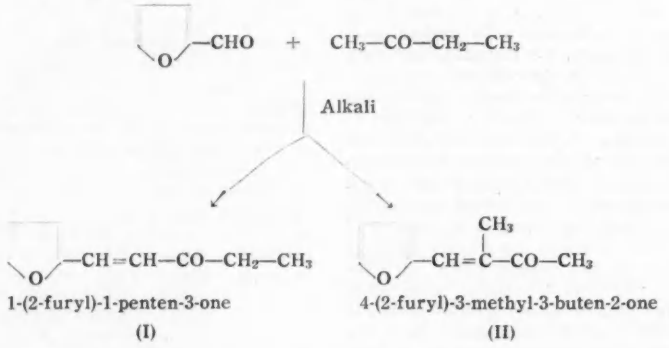

1-(2-furyl)-1-penten-3-one (I)

4-(2-furyl)-3-methyl-3-buten-2-one (II)

Kashiwagi[1] and the other[2] indicated that the condensation product was II. But they gave no satisfactory confirmation of its structure.

On the other hand, Hunsdiecker[3] and the others[5] reported that the condensation product which they assumed to be I afforded γ,ζ-dioxopelargonic acid by ring-opening in alcoholic hydrochloric acid. The work done to date seems to be not yet clear.

In the present experiment, the condensation was carried out at reaction temperatures 0° and 60°.

At reaction temperature 0°, furfural underwent principally the aldol condensation with methyl ethyl ketone. The resulting aldol was easily dehydrated with acetic anhydride or dilute hydrochloric acid to yield the unsatu-

1) I. Kashiwagi: This Bulletin, **2**, 310 (1927).
2) D. M. Al'vin Gutzatz: *C. A.*, **30**, 3591 (1936).
3) H. Hunsdiecker: *Ber.*, **75B**, 447 (1942).

ated ketone, which gave a semicarbazone of foliated crystals melting at 212~4°. This unsaturated ketone was smoothly oxidised to α-methyl-2-furanacrylic acid III by sodium hypochlorite. It is undoubted, therefore, that this unsaturated ketone is II and the reaction sequence is shown as follows:

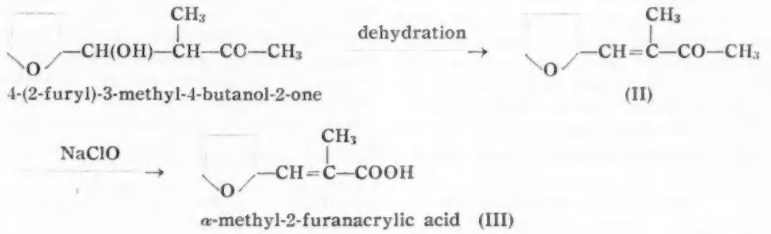

4-(2-furyl)-3-methyl-4-butanol-2-one

(II)

α-methyl-2-furanacrylic acid (III)

From the condensation product at reaction temperature 60° was obtained a mixture of two semicarbazones, which consisted of a larger part of needles melting at 182~4° and a smaller part of foliated crystals melting at 212~4°. The latter was identical with the semicarbazone of II. This condensation product, on sodium hypochlorite oxidation, afforded III in a very poor yield. It seems certain that the semicarbazone of needles melting at 182~4° is that of I. Furthermore, this condensation product, on ring-opening in alcoholic hydrochloric acid, gave a dioxocarboxylic acid in a fairly good yield.

On the other hand, the condensation product at reaction temperature 0°, after dehydration with acetic anhydride, gave the same dioxocarboxylic acid by ring-opening in alcoholic hydrochloric acid as the condensation product at reaction temperature 60°, but its yield was very poor.

From these results, it may be inferred that the dioxocarboxylic acid was γ,ζ-dioxopelargonic acid arising from the ring-opening of I as illustrated below, and the condensation product at reaction temperature 0° contained a small amount of I accompanying 1-(2-furyl)-1-pentanol-3-one, and II failed to give a dioxocarboxylic acid by ring-opening in alcoholic hydrochloric acid.

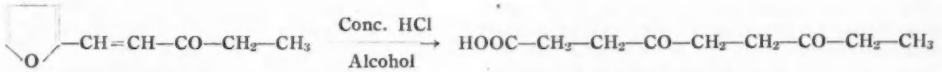

(I)

γ,ζ-dioxopelargonic acid

The semicarbazones obtained here were converted to the 2,4-dinitrophenylhydrazones respectively. It is interesting that the 2,4-dinitrophenylhydrazone of red needles (m.p. 184~5°) and the one of carmine rhombic plates (m.p. 212~3°) were detected to be those of II. The former was obtained directly from the condensation product at reaction temperature 0°, and the latter from the unsaturated ketone obtained by dehydration of this condensation product. These two 2,4-dinitrophenylhydrazones on recrystallisation did not shift to each other, which may be those of cis- and trans-isomers of II.

The semicarbazones of I and II, together with their 2,4-dinitrophenylhydrazones, are shown in the accompanying table.

	Semicarbazone	2,4-dinitrophenylhydrazone
1-(2-furyl)-1-penten-3-one	colourless needles, m.p. 182~4°	red needles m.p. 205~6°
4-(2-furyl)-3-methyl-3-buten-2-one	colourless leaflets, m.p. 212~4°	carmine rhombic plates, m.p. 212~3°
		red needles, m.p. 184~5°

Detection of the 2,4-dinitrophenylhydrazones obtained from the condensation product at reaction temperature 25° indicated the presence of I, II and 4-(2-furyl)-3-methyl-4-butanol-2-one.

Experimental

Condensation at 60~5°.—A solution of furfural (12 g.) and methyl ethyl ketone (24 g.) in water (200 cc.) was mechanically stirred at 60~5° and 5% aqueous caustic soda (20 cc.) was at once run in. After stirring for 1.5 hrs., the reaction mixture was neutralised with dil. sulfuric acid, the oily layer separated, and the aqueous solution extracted twice with benzene. The separated oil and the benzene extract were combined. The benzene solution was dried over calcium chloride and the benzene removed. From the remaining oil was collected a fraction (10 g.) distilling at 128~9°/22 mm.

	H	C
Anal. Calcd. for $C_9H_{10}O_2$:	6.71%	71.96%
Found:	6.72%	71.31%

This fraction gave a mixture of two semicarbazones which consisted of a larger part of needle crystals (m.p. 182~4°) and a smaller part of foliated crystals (m.p. 212~4°). The former was more soluble in methanol than the latter.

The needles (this was considered to be 1-(2-furyl)-1-penten-3-one semicarbazone)

	H	C	N
Anal. Calcd. for $C_{10}H_{13}O_2N_3$:	6.32%	57.94%	20.28%
Found:	6.27%	57.90%	20.08%

The foliated crystals (4-(2-furyl)-3-methyl-3-buten-2-one semicarbazone)

	H	C	N
Anal. Calcd. for $C_{10}H_{13}O_2N_3$:	6.32%	57.94%	20.28%
Found:	6.42%	58.12%	19.85%

The semicarbazone of needle crystals was converted to a 2,4-dinitrophenylhydrazone of carmine needle crystals (m.p. 205~6°).

	H	C	N
Anal. Calcd. for $C_{15}H_{14}O_5N_4$:	4.27%	54.53%	16.96%
Found:	4.05%	54.43%	17.09%

The semicarbazone of foliated crystals was converted to a 2,4-dinitrophenylhydrazone [of carmine rhombic crystals (m.p. 212~3°).

	H	C	N
Anal. Calcd. for $C_{15}H_{14}O_5N_4$:	4.27%	54.53%	16.96%
Found:	4.10%	54.84%	17.14%

Aldol Condensation at 0~3°.—Into a stirred solution of furfural (15 g.) and methyl ethyl ketone (20 g.) in water (350 cc.) was at once introduced 10% aqueous caustic soda (10 cc.) at 0~3°, after stirring for 4.5 hrs. at 0~3°, the reaction mixture was neutralised with dil. sulfuric acid, the oily layer was separated and the aqueous solution extracted twice with ether. The separated oil and the ether extract were combined. Fractionation of the ether solution, after drying over calcium chloride for a brief time, gave a pale yellow oil (10 g.), b.p. 117~8°/10mm., which was considered to chiefly contain 4-(2-furyl)-3-methyl-4-butanol-2-one.

	H	C
Anal. Calcd. for $C_9H_{12}O_3$:	7.19%	64.24%
Found:	6.79%	65.13%

This fraction afforded a 2,4-dinitrophenylhydrazone of unsaturated ketone $C_9H_{10}O_2$, which was recrystallised from pyridine-methanol; microscopic carmine needles; m.p. 184~5°. This was considered to be the 2,4-dinitrophenylhydrazone of 4-(2-furyl)-3-methyl-3-buten-2-one.

	H	C	N
Anal. Calcd. for $C_{15}H_{14}O_5N_4$:	4.27%	54.53%	16.96%
Found:	4.14%	55.03%	16.93%

Dehydration of Aldol.—The foregoing aldol (6 g.) was gently refluxed with acetic anhydride (6 g.) for 3 hrs. Fractionation of the reaction mixture gave a yellow oil (4 g.), b.p. 124~5°/20 mm.

	H	C
Anal. Calcd. for $C_9H_{10}O_2$:	6.71%	71.96%
Found:	6.43%	71.00%

This fraction gave the semicarbazone of foliated crystals (m.p. 212~4°) and the 2,4-dinitrophenylhydrazone of rhombic crystals (212~3°).

The aldol was also dehydrated by heating with 5% hydrochloric acid on the water-bath for a short time, giving the same semicarbazone and 2,4-dinitrophenylhydrazone.

Oxidation by Sodium Hypochlorite.—Anhydrous sodium carbonate (7 g.) and bleaching powder (10 g.) were mixed in water (30 cc.) After a brief time, the resulting calcium carbonate was filtered off, the filtrate was diluted to 40 cc. with water and 1 g. caustic soda was added.

The oil (1 g.) obtained by the dehydration of the aldol was suspended in the sodium hypochlorite solution (8 cc.) prepared above and the vessel was kept for two days in water at room temperature, with occasional shaking. Then, the reaction mixture was acidified with dil. hydrochloric acid to yield α-methyl-2-furanacrylic acid (0.35 g.) It was recrystallised from hot water; colourless needles; m.p. 116~7°; lit.[4] m.p. 116°.

	H	C
Anal. Calcd. for $C_8H_8O_3$:	5.29%	63.13%
Found:	5.34%	63.15%

4) I. Kashiwagi: This Bulletin, **2**, 318 (1927).

The condensation product at reaction temperature 60~5° gave a trace of α-methyl-2-furanacrylic acid under the same conditions.

Ring-opening in Alcoholic Hydrochloric Acid.—The condensation product (2 g.) at reaction temperature 60~5° was refluxed with alcohol (4 cc.) and conc. hydrochloric acid (1.5 cc.) on the water-bath for 3 hrs. The reaction mixture, after addition of water, was evaporated to dryness on the water-bath. The residue was extracted with a sufficient quantity of boiling water; the extract, after decolourising with active charcoal, was evaporated up. The dioxocarboxylic acid which was considered to be γ,ζ-dioxopelargonic acid was obtained as a crystalline mass (0.35 g.) on cooling and recrystallised twice from ligroin; colourless hexagonal plates; m.p. 83~4; lit.[5] m.p. 84~5°.

	H	C
Anal. Calcd. for $C_9H_{14}O_4$:	7.58%	58.03%
Found:	7.55%	57.54%

The dehydration product from the aldol gave a very small amount of colourless tabular crystals by the same procedure; m.p. 83~4°. The mixed melting point of the specimen with the foregoing dioxocarboxylic acid showed no depression.

Condensation at Ordinary Temperature(25°).—A mixture of furfural (10 g.), methyl ethyl ketone (20 g.), 10% aqueous caustic soda (10 cc.) and water (250 cc.) was stirred for 5 hrs. at about 25°. By the same procedure as described above, a pale yellow oil (8 g.) distilling at 131~5°/22 mm. was obtained, which gave a mixture of the three species of 2,4-dinitrophenylhydrazone mentioned above. These 2,4-dinitrophenylhydrazones were separable from the mixture by virtue of their pyridine solubility. The 2,4-dinitrophenylhydrazone of m.p. 212~3° was the least soluble and that of m.p. 185~6° was the most soluble.

5) F. L. Breusch and E. Ulusoy: *C. A.*, **42**, 5850 (1948).

Summary

It seems that furfural can react with methyl ethyl ketone in two ways by alkali.

In the condensation at 0~3°, the main product was 4-(2-furyl)-3-methyl-4-butanol-2-one. This aldol was easily dehydrated to 4-(2-furyl)-3-methyl-3-buten-2-one, which was oxidised to α-methyl-2-furanacrylic acid by sodium hypochlorite.

In the condensation at 60~3°, the main product was the furfurylidene ketone, which gave the semicabazone melting at 182~4° and the dioxocarboxylic acid by ring opening in alcoholic hydrochloric acid. It is presumed that this ketone is 1-(2-furyl)-1-penten-3-one, and the dioxocarboxylic acid resulting from it is γ,ζ-dioxopelargonic acid.

It is also interesting that two species of 2,4-dinitrophenylhydrazone were obtained with respect to 4-(2-furyl)-3-methyl-3-buten-2-one.

The author wishes to thank Messrs. K. Furuhashi and K. Muto for micro-analyses.

Scientific Research Institute
Komagome, Tokyo

Studies on the Chemical Constitution of Agar-agar. XV.[1] Exhaustive Mercaptolyses of Agar-agar[2]

By Choji ARAKI and Susumu HIRASE

(Received April 22, 1953)

Agar-agar, a gel-forming polysaccharide extracted from certain species of red sea weeds, has long been known to produce D-galactose on acid-hydrolysis. C. Araki, one of the present authors, revealed that 3,6-anhydro-L-galactose besides D-galactose is a constitutional monosaccharide, on the bases that he isolated agarobiose[3] (4-D-galactopyranosyl-3,6-anhydro-L-galactose) from partial hydrolysis products of agar, and that he could obtain 2-methyl 3,6-anhydro-L-galactose dimethylacetal[4] from methylated agar as well as 3,6-anhydro-L-galactose dimethylacetal[5] from agar itself by the methanolysis method. Jones and Peat were of the opinion that 3,6-anhydro-L-galactose might arise secondarily from L-galactose-6-sulfate during some chemical operations[6]. Further evidence, however, which excludes the possibility of the latter opinion, is now made available by the mer-

1) Part XIV: C. Araki, *J. Chem. Soc. Japan*, **65**, 725 (1944). Works on this subject are reviewed by C. Araki in "A Summary of Organic Chemical Investigations on Agar-agar", Memoirs of the Faculty of Industrial Arts, Kyoto Technical Univ., **2**(B), 17 (1953), written in English.

2) Read at the Ordinaty Meeting of the Kinki Branch of the Chemical Society of Japan in September, 1950.

3) C. Araki, *J. Chem. Soc. Japan*, **65**, 533, 627 (1944).

4) C. Araki, *J. Chem. Soc. Japan*, **61**, 775 (1940).

5) C. Araki, *J. Chem. Soc. Japan*, **65**, 725 (1944).

6) W. G. M. Jones and S. Peat, *J. Chem. Soc.*, **1942**, 225.

captolysis of agar.

Mercaptolysis[7], substantially hydrolysis followed by simultaneous mercaptalation, has proved in a few cases[8] to be successful in isolating aldose components as their crystalline mercaptals. This has led the authors to apply the procedure to establish the constitutional sugars of agar.

Mercaptolysis of agar was accomplished by dissolving it in concentrated hydrochloric acid with ice-cooling and by stirring the solution with addition of ethylmercaptan for forty eight hours. Neutralization of the reaction mixture followed by evaporation produced well-known crystalline D-galactose diethylmercaptal, which was also identified by oxidation to mucic acid and acetylation to characteristic pentaacetate.

A filtered solution from crystals mentioned above was then extracted with ether in Soxhlet's percolator. Ether extracts yielded crystalline 3,6-anhydro-L-galactose diethylmercaptal, and small amounts of crystalline DL-galactose diethylmercaptal and of xylose diethylmercaptal-containing sirup. 3,6-Anhydro-L-galactose diethylmercaptal, which gave crystalline tri-*p*-nitrobenzoate, was identified by conversion to free sugar and then to crystalline diphenylhydrazone[5] and phenylosazone[5]. Further confirmative evidence was provided by comparison with the authentic specimen prepared for the first time. DL-Galactose diethylmercaptal, also a new compound, giving crystalline pentaacetate, was confirmed by its optical inactivity, its oxidation to mucic acid and by the preparation of an authentic sample.

As the residue obtained by evaporation of the solution, from which the monosaccharide derivatives mentioned above had been removed, seemed to comprise oligosaccharide diethylmercaptals, it was submitted to a second mercaptolysis for forty eight hours to yield monosaccharide units. Crystalline diethylmercaptals of D-, 3,6-anhydro-L- and of DL-galactose were isolated again. The non-crystalline residue of the second mercaptolysis products was further effected by the third mercaptolysis, the same products being isolated in a crystalline state. In the last two cases, no xylose derivative could be found. Thus repeated exhaustive mercaptolyses of agar furnished crystalline specimens of diethylmercaptals of D-galactose, 3,6-anhydro-L-galactose and of DL-galactose in yields of 30.2 %, 24.4 % and 1.0 % to agar employed, respectively.

It may not be a matter of surprise that such an acid sensitive sugar as 3,6-anhydro-L-galactose was out of perfect degradation in the presence of a strong mineral acid, inasmuch as 2-desoxy-aldohexose, which has been accepted as an acid-sensitive sugar equal to 3,6-anhydro-aldohexose, affords its stable mercaptal[9] under the similar condition. With regard to DL-galactose, one of the authors reported that he could not find it in the hydrolysate of agar extrated from *Gelidium amansii*[10], but afterwards it was isolated from an agarous substance of *Camphaephora Hypraeides*, J. Ag[11]. As commercial agar, employed in this investigation, is generally prepared by extracting a mixture of *Gelidium amansii* and several other species of sea weeds, it may be possible to assume that DL-galactose derivative isolated above arises from other species than *Gelidium amansii*. Xylose was also detected[12] in the hydrolysis products of commercial agar, but further evidence will be necessary for its conclusive identification.

From these results it is concluded that 3,6-anhydro-L-galactose as well as D-galactose is a chief constitutional sugar in the agar molecule, just as one of the authors has stated. Moreover, it may be of interest that derivatives of D-galactose and 3,6-anhydro-L-galactose can be isolated approximately in equal yield. This suggests that these two sugars are involved in almost equal amounts in the molecule of agar. But it would be still difficult to conclude that these two sugars comprise the main bulk of the molecule, as the exhaustive experimental conditions employed above have made it impossible to deal with the whole material quantitatively.

Experimental

Unless otherwise stated, concentration and evaporation of the solution were carried out under reduced pressure below 40°. Analyses for the thioethoxyl group are according to the method of the present authors[13]. All m.ps. are uncorrected.

7) M. L. Wolfrom, L. W. Georges and J. C. Sowden, *J. Am. Chem. Soc.*, **60**, 1026 (1938); M. L. Wolfrom, D. R. Myers and E. N. Lassettre, ibid., **61**, 2172 (1939).

8) I. R. Hooper, L. H. Klemm, W. J. Polglase and M. L. Wolfrom, *J. Am. Chem. Soc.*, **68**, 2120 (1946); **69**, 1052 (1947); P. W. Kent, *Nature*, **166**, 442 (1950).

9) W. G. Overend, M. Stacey and J. Stanek, *J. Chem. Soc.*, **1949**, 2481; W. G. Overend, F. Shafizadeh and M. Stacey, *J. Chem. Soc.*, **1950**, 671.

10) C. Araki, *J. Chem. Soc. Japan*, **58**, 1214 (1937).

11) C. Araki, Collection of Treatises in Commemoration of the 45th Anniversary of Kyoto Technical College, pp 69 (1948).

12) S. Hirase and C. Araki, Memoirs of the Faculty of Industrial Arts, Kyoto Technical Univ., **1**, 19 (1952).

13) The method will be published elsewhere.

I. Mercaptolysis of agar-agar.—Commercial powdered agar (60.0 g., dry weight 49.1 g.), placed in a three-necked flask fitted with a mechanical stirrer, dropping funnel and calcium chloride tube, was dissolved in concentrated hydrochloric acid (*d* 1.20, 200 g.) by stirring and ice-cooling; the agar dissolved gradually in 40 mins. into a deep brown solution. Ethylmercaptan (80 g.) was then added from the dropping funnel with vigorous stirring in three portions so that the temperature did not exceed 10°. After addition, the stirring was continued for 48 hrs., maintaining the temperature at 10~12°. The reaction mixture was neutralized by pouring it on excess lead carbonate suspended in water (1 l.). Precipitates of the excess lead carbonate and lead chloride formed were removed by filtration and washing with cold water (1 l.). The combined filtrate and washings were saturated with hydrogen sulfide,

Operations for Mercaptolysis Products of Agar-agar.

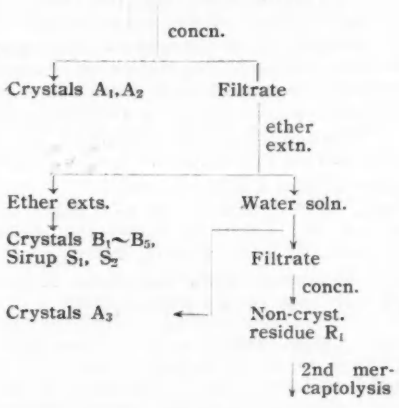

the precipitate of lead sulfide being removed by filtration. The filtrate was then neutralized with silver carbonate after removal of hydrogen sulfide in vacuo, and filtered before and after a second treatment with hydrogen sulfide. The solution thus obtained was operated as shown in the accompanying diagram and as described below.

II. Isolation and confirmation of D-galactose diethylmercaptal.—The neutralized solution obtained above was concentrated until it gave rise to crystalline magma. The crystals (A_1) were filtered, washed with cold water and dried; yield 7.25 g., m.p. 139~140°, $[\alpha]_D^{15}$ −4.3° in water. The second crop of the crystals (A_2) was obtained by concentrating the combined filtrate and washings mentioned above to about 200 cc., and allowing it to stand overnight in an ice-box; yield 1.95 g., m.p. 140~141°, $[\alpha]_D^{15}$ −4.6° in water. Crystals A_1 and A_2 were combined and recrystallized from alcohol. Pure D-galactose diethylmercaptal was obtained as prismatic needles, m.p. 141~142°, $[\alpha]_D^{15}$ −4.65° in water (*c* 0.680), −3.99° in pyridine (*c* 1,003). Its m.p. was not depressed on admixture with an authentic sample (m.p. 142°)[14].

Anal. Found: C, 41.65; H, 7.99; SC_2H_5, 42.75. Calcd. for $C_{10}H_{22}O_5S_2$: C, 41.93; H, 7.74; SC_2H_5, 42.68%.

Oxidation of the crystals mentioned above with nitric acid (*d* 1.15) yielded mucic acid, m.p. 212°, not depressed on admixture with an authentic specimen (m.p. 214°).

Pentaacetyl D-galactose diethylmercaptal[15]: m.p. 76~77°, $[\alpha]_D^{18}$ +11.31° in chloroform (*c* 2.210).

III. Isolation and confirmation of 3,6-anhydro-L-galactose diethylmercaptal.

a) Isolation:—Combined filtrate and washings from A_2, described in **II**, were concentrated to about 150 cc., and extracted with ether in a Soxhlet's percolator.

The first extract (20 hrs.) on cooling gave crystals (B_1, 6.95 g.), m. p. 102~5°, $[\alpha]_D^{12}$ +11.0° in water. The ethereal filtrate from B_1 on evaporation furnished further crops of crystals (B_2, 1.17 g.), m.p. 102~5°, $[\alpha]_D^{12}$ +10.8° in water. The mother liquor from B_2 was concentrated to a sirup (S_1, 1.20 g.), $[\alpha]_D^{12}$ −1.6° in water.

The second extract (30 hrs.) afforded crystals (B_3, 0.58 g.), m.p. 109~116°, $[\alpha]_D^{12}$ +1.7° in water, filtrate from which on evaporation gave further crystals (B_4, 0.22 g.), m.p. 102~5°, $[\alpha]_D^{12}$ +13.3° in water. Mother liquor from B_4 was concentrated to a sirup (S_2, 0.45 g.), $[\alpha]_D^{12}$ −6.1° in water.

The third extract (70 hrs.) gave crystals (B_5, 0.75 g.), m.p. 115~121°, $[\alpha]_D^{12}$ −2.5° in water. Ethereal filtrate from B_5 left nothing on evaporation.

The crystals B_1, B_2 and B_4, showing the same properties, were combined and recrystallized from ethyl acetate (40 cc.), yielding almost pure 3,6-anhydro-L-galactose diethylmercaptal (5.20 g.), m.p. 104~7°, $[\alpha]_D^{25}$ +12.1° in water. An additional product (2.61 g., m.p. 103~6°, $[\alpha]_D^{25}$ +11.8° in water), was recovered by evaporating the mother liquor. A pure substance was obtained after several recrystallizations from ethyl acetate containing a small amount of petroleum ether (b. p. 40~70°), forming silky needles with m.p. 110~111° and $[\alpha]_D^{14}$ +14.09° in water (c 1.636), −21.11° in ethanol (c 1.041) and −26.25° in pyridine (c 1.638). Its m.p. was not depressed on admixture with the authentic specimen, the preparation of which is described in **III—d.** It was readily soluble in water, methanol, ethanol and pyridine, moderately soluble in ether, acetone, ethyl acetate and chloroform, and practically insoluble in benzene and petroleum ether. It gave a Seliwanoff's ketose reaction.

14) E. Fischer, *Ber.*, **27**, 678 (1894); R. M. Hann, W. D. Maclay and C. S. Hudson, *J. Am. Chem. Soc.*, **61**, 1270 (1939).
15) M. L. Wolfrom, *J. Am. Chem. Soc.*, **52**, 2467 (1930).

Anal. Found: C, 44.48; H, 7.68; SC_2H_5, 45.65. Calcd. for $C_{10}H_{20}O_4S_2$: C 44.75; H, 7.51; SC_2H_5, 45.55 %.

b) Tri-*p*-nitrobenzoyl 3,6-anhydro-L-galactose diethylmercaptal:—To a solution of 3,6-anhydro-L-galactose diethylmercaptal (0.50 g.), isolated above, in pyridine (10 cc.) was added *p*-nitrobenzoyl chloride (1.20 g.). The reaction mixture, after being allowed to stand 2 days, was treated in the usual manner. Recrystallization of the product from ethanol containing a small amount of ethyl acetate furnished colorless fine needles of tri-*p*-nitrobenzoate (0.50 g.), m.p. 140~142°, $[\alpha]_D^5$ +18.48° in chloroform (c 0.974).

Anal. Found: N, 5.64; S, 8.91. Calcd. for $C_{31}H_{23}O_{13}N_3S_2$: N, 5.86; S, 8.96 %.

c) 3,6-Anhydro-L-galactose:—To a solution of 3,6-anhydro-L-galactose diethylmercaptal (5.32g.) in water (50cc.), held in a three-necked flask equipped with a mechanical stirrer, finely powdered lead carbonate (15 g.) and a solution of mercuric chloride (11 g.) in water (200 cc.) were added. Rapid stirring was maintained for 3 hrs. at room temperature. The reaction mixture was then filtered, a small amount of lead carbonate being placed in a filter flask. The filtrate was concentrated to about 20 cc. in the presence of lead carbonate. Unaffected mercaptal and excess mercuric chloride were removed by exhaustive extraction with ether until nothing came into the extract. The remaining water solution was concentrated to dryness by repeatedly adding absolute ethanol and distilling it off. The residue was dissolved in absolute ethanol, insoluble lead compounds were removed by filtration, and the filtrate was concentrated to a glassy solid of 3,6-anhydro-L-galactose (2.90 g.), $[\alpha]_D^{25}$ −39.4° (initial) in water (c 1.75), −25.2° (24 hrs., constant). It reduced cool Fehling's solution, showed strong Seliwanoff's reaction, and restored the color to Schiff's reagent.

Diphenylhydrazone[5]: m.p. 154°, $[\alpha]_D^{14}$ − 34.31° (initial) in methanol (c 1.370), −24.09° (24 hrs.).

Phenylosazone[5]: m.p. 217°, $[\alpha]_D^{15}$ −75.38° (initial) in pyridin-methanol (2:3) (c 0.738), −53.48° (24 hrs.).

d) 3,6-Anhydro-L-galactose diethylmercaptal from corresponding dimethylacetal:—A solution of 3,6-anhydro-L-galactose dimethylacetal (2.50 g.) in concentrated hydrochloric acid (2.5 g.) was shaken for 1 hr. with ethylmercaptan (1.6 g.) with ice-cooling. Small pieces of ice were added to induce crystallization, and separated crystals of the mercaptal were filtered, washed with small portions of ice-water, and dried over potassium hydroxide in vacuo; yield 2.37 g., m.p. 105~8°. Several recrystallizations from ethyl acetate containing a small amount of petroleum ether (b. p. 40~70°) gave silky needles, m.p. 110~111°, $[\alpha]_D^{15}$ +14.36° in water (c 1.253), −21.03° in ethanol (c 1.617) and −26.32° in pyridin (C 1.140).

Anal. Found: C, 44.49; H, 7.73; SC_2H_5, 45.43. Calcd. for $C_{10}H_{20}O_4S_2$: C, 44.75; H, 7.51; SC_2H_5, 45.55 %.

IV. Isolation and confirmation of DL-galactose diethylmercaptal.

a) Isolation:—Crystals B_3 and B_5, described in **III-a,** were considered to be mixtures from their ill-defined m.ps. These were combined and divided into two components by fractional crystallizations from acetone. From the less soluble fraction, D-galactose diethylmercaptal (0.48 g.) was obtained, m.p. alone and mixed m.p. 139~140°, $[\alpha]_D^{12}$ −4.40° in water. DL-Galactose diethylmercaptal was accumulated in the more soluble fraction. The crude crystals (0.55 g.), m.p. 123~5°, were purified by further recrystallizations from ethanol, forming prismatic needles, m.p. 127°, $[\alpha]_D^{15}$ ±0° in water (c 0.676) and pyridine (c 0.711). Its m.p. was not depressed on admixture with an authentic specimen, of which preparation is described in **IV-c.**

Anal. Found: C, 41.71; H, 7.84; SC_2H_5, 42.75. Calcd. for $C_{10}H_{22}O_5S_2$: C, 41.93; H, 7.74; SC_2H_5, 42.68 %.

The substance gave mucic acid on oxidation with nitric acid (d 1.15), m.p. 212°, undepressed when mixed with an authentic sample (m.p. 214°).

b) Pentaacetyl DL-galactose diethylmercaptal:—The crystals (0.20 g.) obtained above were acetylated with pyridine and acetic anhydride in the usual way. The product was recrystallized by dropping water to its methanolic solution, forming prisms (0.28 g.), m.p. 112~113°, $[\alpha]_D^{17}$ ± 0° in chloroform (c 0.954).

Anal. Found: C, 48.17; H, 6.71; SC_2H_5, 24.51; CH_3CO, 43.85. Calcd. for $C_{20}H_{32}O_{10}S_2$: C, 48.37; H, 6.50; SC_2H_5, 24.61; CH_3CO, 43.33 %.

c) DL-Galactose diethylmercaptal from dulcitol:—Dulcitol (5.0 g.) was oxidized with 3 % hydrogen peroxide according to literature[15] on the subject. The reaction product, however, was converted to diethylmercaptal, without direct isolation of DL-galactose, by the action of concentrated hydrochloric acid (2 g.) and ethylmercaptan (2 g.). The mercaptal obtained was purified by recrystallizations from ethanol, yielding prismatic needles (0.80 g.), m.p. 125~127°.

Anal. Found: C, 41.72; H, 7.95; SC_2H_5, 42.43. Calcd. for $C_{10}H_{22}O_5S_2$; C, 41.93; H, 7.74; SC_2H_5, 42.68 %.

V. Detection of xylose diethylmercaptal.

A small portion of each of sirups S_1 and S_2, the separation of which is described in **III-a,** was treated with mercuric chloride and mercuric oxide to yield free sugar. Both of resulting products were shown to be mixtures of xylose and 3,6-anhydro-L-galactose by paper chromatography. Hence, S_1 and S_2 were combined and extracted with cold benzene. Extract on solvent removal gave a colorless sirup (1.40 g.), $[\alpha]_D^{17}$ −7.7° in water, SC_2H_5 46.89 (calcd. for $C_9H_{20}O_4S_2$: 47.64 %). An attempt to crystallize xylose diethylmercaptal or its acetate was unsuccessful.

16) C. Neuberg and J. Wohlgemuth, *Z. physiol. Chem.*, **36**, 219 (1902).

VI. Second mercaptolysis.

The residual water solution from ether extraction, described in **III-a,** was diluted with water to 200 cc. after the removal of ether in vacuo, and allowed to stand in an ice-box for a week. A small amount of crystals of D-galactose diethylmercaptal was deposited; yield 0.90 g., m.p. and mixed m.p. 137~139°, $[\alpha]_D^{15}$ −4.9° in water. The filtrate was concentrated to a sirup, which was dried by repeated additions of absolute methanol followed by evaporation, yielding an amorphous solid (R_1); yield 29.0 g., $[\alpha]_D^{13}$ −7.5° in water, SC_2H_5 22.62 % (hexobiose and hexotriose diethylmercaptals require SC_2H_5 27.2 and 22.6 %). It did not reduce a hot Fehling's solution, the observation excluding the possibility of the existence of ketose components.

R_1 was dissolved in concentrated hydrochloric acid (120 g.) and stirred with ethylmercaptan (40 g.) at 10~12° for 48 hrs. The reaction products were treated quite in the same manner as before; the yields of crystalline diethylmercaptals of D-galactose, 3,6-anhydro-L-galactose and of DL-galactose were 8.09 g., 7.29 g. and 0.23 g., respectively. No sirup containing xylose derivative could be found. The residue (R_2), corresponding to R_1 in the first series, was obtained as amorphous solid (12.7 g.), $[\alpha]_D^{21}$ −6.8° in water, SC_2H_5 22.10 %. This did not reduce a hot Fehling's solution.

VII. Third mercaptolysis.

R_2 obtained above was again submitted to mercaptolysis with concentrated hydrochloric acid (60 g.) and ethyl mercaptan (30 g.) at 10~12° for 48 hrs. The procedure was essentially the same as in the preceding two cases, except for being carried out on a smaller scale. The yields of crystalline dietylmercaptals of D-galactose, 3,6-anhydro-L-galactose and of DL-galactose isolated herein were 4.88 g., 4.22 g. and a trace, making the total yield 23.55 g., 19.85 g. and 0.78 g., respectively. No xylose derivative was found in this case. The residue (R_3), corresponding to R_1 in the first series, was brown a sirup (3.1 g.), $[\alpha]_D^{24}$ −1.7° in water, SC_2H_5, 21.05 %.

The authors wish to express their thanks to Mr. K. Arai for the microanalyses for carbon, hydrogen and nitrogen, and to Mr. K. Yamanouchi for his assistance in this work. This research has been aided by the Grant for Scientific Research from the Ministry of Education.

Institute of Chemistry,
Faculty of Industrial Arts,
Kyoto Technical University, Kyoto

Electronic Remarks on the Origin of the Anomalous Color of Some Organic Iron. III. Complex Salts

By Kôzô Sone

(Received May 18, 1953)

Introduction

The absorption spectra of chelate compounds of Fe (II) were studied by the present author[1] and he came to the conclusion that unsaturated intramolecular chelate rings formed between Fe and chelating organic compound would probably act as the new chromophore to produce the new absorption bands in the visible region. The several compounds of Fe (III) containing ligands such as acetylacetone[2] or 8-quinolinol were found also to show a similar intense absorption band as Fe (II) compounds. Other examples of such an intense absorption bands, those of Fe (III) chelate compounds of 1-nitroso-2-naphthol and nitrosophenylhydroxylamine will be reported in this paper.

The Fe (III) complexes of NCS^- and N_3^- ions[3] and the enolic and phenolic substances[4] all show intense, distinct bands in the visible region and from the fact that these bands are also completely different from the band of Fe^{+++} ion or from those of the ligands, it is likely that these bands also belong to the

1) K. Sone, This Buletin, **25**, 1 (1952); *J. Am. Chem. Soc.* in press.
2) K. Sone, I. Miyake, H. Kuroya, K. Yamasaki, *J. Chem. Soc. Japan*, **69**, 70 (1948).
3) A.v. Kiss et al., *Z. anorg. allg. Chem.*, **244**, 98 (1940); J. Badoz-Lambling, *Bull. soc. chim. France*, **1950**, 1195.
4) F. Wesp and W.R. Brode, *J. Am. Chem. Soc.*, **56**, 1037 (1934); H. Henecka, *Ber.*, **81**, 179 (1948); see also H. Henecka, "Chemie der Beta-Dicarbonyl-Verbindungen", p. 110, Springer-Verlag, Berlin, 1950.

same kind as those absorption bands of the above mentioned chelate complexes.

From all these facts it seems clear that the Fe^{+++} ion posesses a peculiarly high ability to produce anomalously deep-colored organic complexes. Indeed it was pointed out by Yoe[5] that among about 5000 organic substances studied, about 1200 were found to produce intensely colored complexes with iron, while no other metal showed such a high ability for color production.

In the present article, discussions will be made on this problem from the standpoint of the electronic theory of organic chemistry and it will be shown that by the application of this theory a number of features of these colorations can be explained satisfactorily.

Experimental

A Beckman model DU spectrophotometer and a Coleman universal spectrophotometer were used in the spectral measurements. The results of absorption spectra were shown in Fig. 1 in which the ordinate expresses the value of molecular extinction coefficient ε calculated by the familiar formula $\varepsilon = \frac{\log I_0/I}{c.d.}$

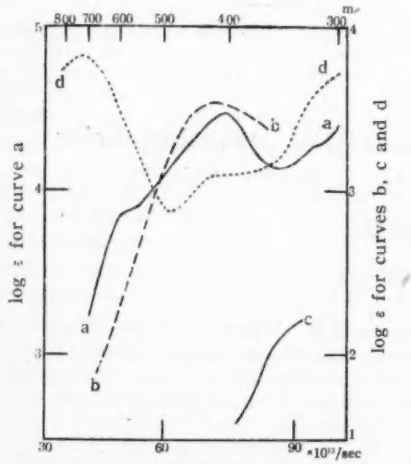

Fig. 1.—Curve a: Tris (1-nitroso-2-naphthol) iron in chloroform, b: Tris (nitrosophenylhydroxylamine) iron in chloroform, c: Ammonium salt of nitrosophenylhydroxylamine (cupferron) in water, d: Colloidal solution of Prussian blue.

The tris (1-nitroso-2-naphthol) iron (III) was prepared after Ilinsky and Knorre[6]. Chloroform solutions of the above complex and of tris (nitrosophenylhydroxylamine) iron (III) were used for spectral measurements. Concentrations used were 1/1500 mole for tris (1-nitroso-2-naphthol) iron and 1/5000 mole for tris (nitrosophenylhydroxylamine) iron respectively.

Colloidal solution of Prussian blue prepared by mixing aqueous solutions of $K_4[Fe(CN)_6]$ and iron alum was also studied. The final concentration of Fe^{++} and Fe^{+++} were 1/2000 and 1/4000 mole respectively. The ε value was calculated for one atom of Fe^{+++}.

Discussion

The tris (nitroso-naphthol) iron has a band at 407 mμ. The longer wave length side of this band shows a hump at ca. 600 mμ. This means the probable existence of a new band in this region which is responsible for the dark color, almost black of this iron complex. This color is in contrast with the nitrosonaphtholates of other metals such as Co, Cu and Pd which are mostly red or brown.

The iron (III) complex of nitrosophenylhydroxylamine which contains 3 molecules of the ligand shows a strong band at 420 mμ which is quite different from the absorption of the ligand itself (Fig. 1, curve c.). The color of this iron complex is red which is in contrast with complexes of other metals. For example, complexes of Cr, Ni and Co are green and pink[7] and similar to their hydrated ions in the color.

The number and shapes of the anomalous absorption bands in the above-mentioned Fe (III) complexes are considerably different in each case, and therefore it will be rather difficult to give a general treatment to explain their origins. In addition, it is also known from magnetochemical observations[8] that the Fe-ligand coordinate bonds in the dipyridyl and phenanthroline complexes are of covalent character, while most of the other complexes with anomalous absorption only contain ionic linkage. Therefore there certainly exists a considerable difference between the electronic structures of these two types of complexes. Nevertheless, it is fairly clear that by the combination of the Fe (III) ion and all these organic ligands some completely new electron transitions which were absent beforehand become possible.

In regard to the origin of the appearance of such transition, it can be pointed out that the redox transition between the Fe^{++} and

5) J. H. Yoe, *Anal. Chem.*, **20**, 393 (1948).
6) M. Ilinsky and J. Knorre, *Ber.*, **18**, 2728 (1885).
7) V. Anger, L. Lafontaine, C. Caspar, *Compt. rend.*, **180**, 376 (1925).
8) B. Werbel, V.H. Diebler and W.C. Vosburgh, *J. Am. Chem. Soc.*, **65**, 2329 (1943); A.E. Martell and M. Calvin "Chemistry of the Metal Chelate Compounds", **1952**, p. 214

Fe^{++} ions occurs with relative ease in contrast with the other heavy metals, such as Co, Ni and Cu which have strong tendencies to keep their most stable valence states. This indicates that the energy difference between these two valence states is relatively small.

Now if an organic ligand which can cause the anomalous absorption with Fe (III) and which generally contains conjugated double bonds and is therefore rich in the mobile π-electrons, approaches the Fe^{+++} ion, the electronic structure (B) shown below becomes possible,

$$\underset{(A)}{Fe^{+++} + :R} \longleftrightarrow \underset{(B)}{Fe^{++} + \cdot R} \qquad (1)$$

i.e., one electron is partially transferred from :R to Fe^{+++}, producing a Fe^{++} ion and a free radical $\cdot R$ derived from the ligand.

These two structures (A) and (B) will make possible the condition of mutual resonance and therefore the structure (B) will, to a certain extent, contribute to the resonance of the whole system containing Fe^{+++} and R^- together.

The present author assumes that the establishment of this resonance system (1) and the occurrence of electron transitions between the new energy states produced by such resonance could be the true origin of the anomalous absorption bands of the above-mentioned Fe (III) complexes.

The assumption of the existence of such a resonance system may be supported by the following facts of organic chemistry. Dewar[9] described that when some aromatic amines are oxidized by $FeCl_3$, the first step is the reaction of the type

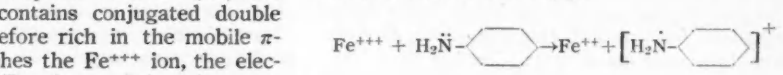

which looks quite analogous to the above mentioned resonance formula, and from this fact it is also very probable that this reaction proceeds through the formation of an intermediate complex,

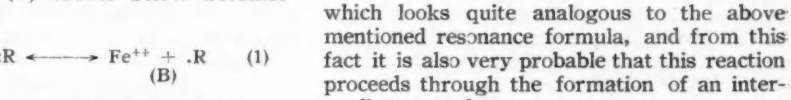

in which the two electronic states corresponding to the (A) and (B) given above are in resonance. Similar assumption of the one-electron transfer is generally accepted also to explain the oxidation and oxidative decomposition of phenols, facts which are important for the later discussions.

From these considerations, it will be quite reasonable to assume that, in the well-known

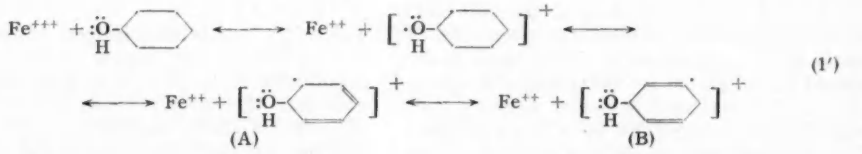

(1′)

reaction of the Fe^{+++} ion and phenol, the Fe^{+++} ion will show some properties of the Fe^{++} ion, and the phenol molecule will acquire some properties of the free radicals as shown schematically in (1′). Under this assumption, a number of experimental data on the Fe^{+++} ~phenol reaction can be explained satisfactorily.

(1) When an anionoid, or electron-donating group (alkyl, halogens, NH_2, OH etc.) is substituted in the benzene nucleus of phenol, the electron transfer from the phenolic OH to the Fe^{+++} ion will be more or less facilitated, thus promoting the contribution of the structure (B) in the resonance system (1′), and therefore increasing the mobility of the whole π-electron system, shifting the absorption band to the longer wave length, and making the phenol molecule highly reactive owing to its free-radical character enhanced by the substituted group.

(2) When a cationoid, or electron-attracting group (CHO, COOH, NO_2 etc.) is substituted, the electron transfer from OH to Fe^{+++} will become rather difficult, shifting the band towards the shorter wave length and thereby stabilizing the ligand molecule from reacting away.

These conclusions coincide completely with the experimental data of Wesp and Brode[4]. According to them,

(1) In the alkyl-, halogen-, NH_2- and OH-substituted phenols, the position of the band is generally shifted to longer wave length from the position found for the unsubstituted phenol and, in the case of its *o*- and *p*-derivatives, the produced colored complexes are very unstable, changing rapidly into the Fe^{++}

9) M.J.S. Dewar, "The Electronic Theory of Organic Chemistry", 1949, p. 248; L. Fieser and M. Fieser, "Organic Chemistry", 1950, p. 677.

ion and resinous substances which are formed from the oxidative polymerization of the respective phenols. With *m*-derivatives the band shifts are much less, or even in the opposite direction and the complexes are somewhat more stable.

These facts can be explained if the following two assumptions are made. Namely, (i) the coordinated phenol molecule with some enhanced free radical character polymerizes into the resinous matter, leaving the iron which is now in the Fe (II) state; (ii) since the m-substituent is difficult to resonate with the OH group, it cannot greatly influence the resonance of the whole system in such a way as the o- and p-substituents do.

It might be added that the same kind of band shift and instabilization of complexes occurs in the case of thiophenol, whose SH group is much more deformable than the OH group of phenol.

(2) In the case of the CHO-, COOH- and NO_2-substituted phenols the band is shifted to the shorter wave length than in the case of phenol, and the resulting complexes become very stable.

Wesp and Brode also observed that the Fe (III) complexes of naphthols are generally colored in blue or green, and thus absorb light at longer wave length than phenols, and this fact is explained easily if the greater mobility of the π-electrons in the naphthalene ring compound with benzene ring is taken into account.

Recently Henecka[4] measured the absorption spectra of the color reactions of two series of enolic substances with Fe^{+++}. The structures of their complexes are, respectively,

(A) acetylacetone type,

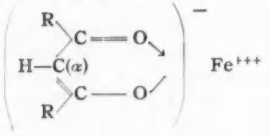

and (B) acetoacetate type.

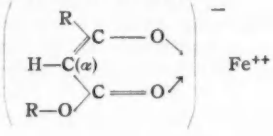

From his experimental data it can be observed that: (1) the absorption maximum for a compound of type (A) is generally located at a shorter wave length than that of the corresponding compound of type (B) with silmilar substituent groups, (2) when the H atom on the α-position in both types is replaced by alkyl, Cl-, or OR-group (i.e. anionoid group), the band is shifted to the longer wave length, while RCO-, RO_2C- or CN-group (i.e. cationoid groups) shifts the band in the opposite direction. It is very remarkable that these relationships are quite analogous to those observed by Wesp and Brode for the phenols. The relationship (1) can be readily understood because the compound of type (B) is that of type (A) substituted with an anionoid OR group.

In this way, the general characteristics of the Fe^{+++}~phenol and enol colorations can be explained adequately, and other anomalous colorations of the Fe (III) complexes can be considered in analogous manners. There exist some experimental evidences which support this point of view; for example, Linhard and Weigel[10] indicated that the strong absorption band at 300~330 mμ shown by the rhodanato- and azido-complexes of Co (III) originates from the following electron transition:

$$\left[Co^{(+++)}\ X^{(-)}A_5\right]^{++} \xrightarrow{h\nu} \left[Co^{(++)}\ X\ A_5\right]^{++}$$

($A = NH_3$, $X^- = NCS^-$ or N_3^-)

which is virtually an electron transfer from the ligand to the central metal. If their arguments are correct it will be fairly probable that the strong bands at 450~500 mμ of the Fe^{+++}~NCS^- and Fe^{+++}~N_3^- complexes are also of the same origin, i.e., they are derived from the electron transfers which are closely related to the resonance of type (1). The change between the Fe (III) and Fe (II) in this case, however, would occur much more easily than that between the Co (III) and Co (II) in the ammine complexes, and this will cause the absorption band of Fe^{+++} complex appear in the longer wave length, as is observed experimentally.

It is also conceivable that the anomalous colors of the Fe (II) chelates, which the author formerly considered to be due to the special ring formation[1], might be in fact, due to the resonance of the type

$$Fe^{++} + :R \longrightarrow Fe^{+++} + :R^-$$

i.e. the reverse of that assumed for the Fe (III) complexes[11]. The possibility of the

10) M. Linhard and M. Weigel, *Z. anorg. allg. Chem.*, **267**, 113, 121 (1951).

11) Interesting remarks concerning such colorations were made by P. Krumholz (*Nature*, **167**, 570 (1951).

production of deep colors as the result of the resonance between the metallic complex ion and the organic molecules was also indicated by the study of Kröhnke[12] on some deeply colored organic ferrocyanides, and further examples of similar anomalous colorations of iron complexes are found in the books of Feigl[13].

It may be added that some of the absorption spectra of anomalously colored complexes such as $Fe^{+++}\sim NCS^-$ or $Fe^{++}\sim$phenanthroline complexes show apparent similarities to that of the Prussian blue solution, which certainly contains a resonance system between the Fe^{++} and Fe^{+++} ions through the coordinated CN^- ions. (cf. Fig. 1, curved). These apparent similarities seem to give further support to the point of view discussed throughout this article.

The author wishes to express his thanks to Prof. K. Yamasaki for his guidance, and also to Mr. M. Kobayashi of Tokyo University and to Mr. K. Nakanishi of Nagoya University for their valuable advice and suggestions.

Aichi College of Liberal Arts
(Aichi-Gakugei-Daigaku)
Higashiku, Nagoya

12) F. Kröhnke, *Ber.*, **83**, 35 (1950).
13) F. Feigl, "Chemistry of Specific, Selective and Sensitive Reactions", New York, 1949.

An Improved Accurate Film Balance*

By Kiyoshi INOKUCHI

(Received May 29, 1953)

Introduction

Measurement of low film pressure is a matter of increasing importance for the study of monomolecular layers. The apparatus for measuring film pressures generally falls into three types, i.e., dipping slide type, two-dimensional aneroid type, and float balance type. The dipping slide method, introduced by Dervichian[1], and Harkins and Anderson[2] is uniquely simple and yields reliable value when properly used. Bull[3], and Abribat et al.[4] recently used this type of apparatus for the monolayers of various macromolecules, such as proteins or long chain polymers, and obtained the molecular weight of the film molecules. The main drawback of this method, however, lies in the fact that the measurements become unreliable whenever the decreasing film pressures are involved. It requires, moreover, careful choice of materials for dipping slide, since a small change of contact angle of the slide owing to the deposition of monolayer may introduce large errors.

The aneroid type of balance, originated by Marcelin,[5] was recently modified by Puddington[6] and Kalousek.[7] The feature of this type is the fact that the movable float, indispensable for the float balance, is eliminated, and the construction is comparatively simple. The principal objection to this type, however, may be the difficulty of obtaining the absolute calibration for it, and the difficulty of removing the contamination which may, more or less, occur inside the enclosed area.

On the other hand, the float balance has an advantage over the above two methods, since it eliminates their objections and permits wide application. Although the disadvantage of this type lies in the comparatively laborious technique for preventing leakage at both ends of the float, it is a matter of technique which could be overcome in some way. Adam

* Presented at the Symposium on Colloid Chemistry of the Chemical Society of Japan, Nov. 1951, Tokyo.
1) D. G. Dervichian, *J. Phys. Radium*, **6**, 221, 429 (1935).
2) W. D. Harkins and T. F. Anderson, *J. Am. Chem. Soc.*, **59**, 2189 (1937).
3) H. B. Bull, ibid., **67**, 4, 5 (1945).
4) M. Abribat and J. Pouradier, *Compt rend.*, **227**, 1101 (1948).
5) A. Marcelin, *Ann. physique*, **4**, 505 (1925).
6) I. E. Puddington, *J. Colloid Sci.*, **1**, 505 (1946).
7) M. Kalousek, *J. Chem. Soc.*, **1949**, 894.

and Jessop's[8] apparatus, an adaptation of Langmuir's[9] balance for low pressure measurement, is too complicated in construction and laborious in operation. Sensitive float balances were presented by Marcelin,[10] Moss and Rideal,[11] and Guastalla,[12] and have proved their merits for measuring extremely low pressure. These apparatus, however, are not extensively used because of their unfavorable design for routine work. Thus, a generally accessible apparatus is now wanted, which enables film pressures of the order of millidynes per cm. to be accurately measured with ease of operation. The present paper deals with an improved apparatus and technique for use which meet all the requirements stated above.

Construction

The apparatus to be described is of float balance type. The elevation views of the construction are illustrated in Fig. 1. The apparatus provides a vertical torsion wire (1), which suspends a torsion weight (2). Below the torsion weight, a cramp (3) for the wire is provided, which can be raised or lowered by turning the knob (4). This cramp fixes the weight at raised position and protects the torsion wire from accidental shock when the

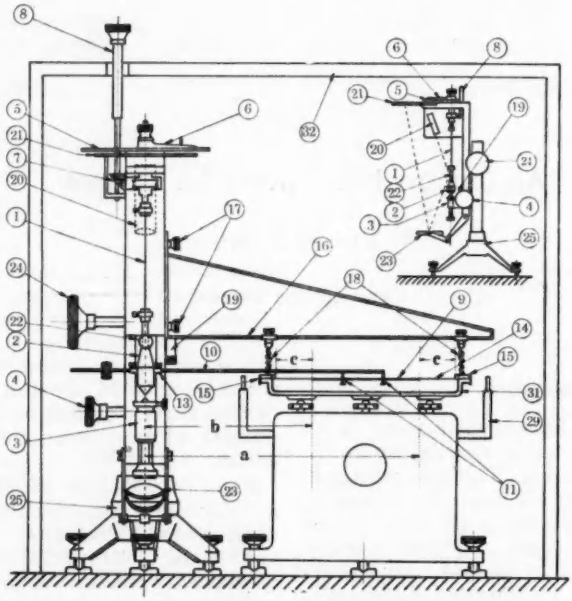

Fig. 1.—Elevation views of construction

apparatus is out of measurement. Lowering the cramp makes the torsion weight free and sets the apparatus ready for use. At the top of the apparatus, a reading scale (5) is provided with a pointer (6), which is coaxial to the torsion head. The torsion head is connected to the knob (8) through the gear-wheel (7). Thus, the rotation of the torsion head is transmitted finely by the manual movement of this knob from the outside of the cabinet (32). The torsional angle of the torsion head can be read down to 0.1 degree by means of the vernier of the pointer.

On the surface of water, a paraffin-waxed mica strip (called a float (9) hereafter) is placed. The float is supported by the arm (10) which extends above the surface of water in parallel with the length of the float. The connection of the float with the supporting arm is as follows. The arm has two needles (11), which penetrate the float through two holes respectively. The holes are so loosely bored that the float can be moved freely according to the change of water level, but they are tight enough to follow the horizontal movement of

8) N.K. Adam and G. Jessop, *Proc. Roy. Soc.*, **110A**, 423 (1926).
9) I. Langmuir, *J. Am. Chem. Soc.*, **39**, 1848 (1917).
10) A. Marcelin, *Ann. physique*, **4**, 481 (1925).
11) S. A. Moss and E. K. Rideal, *J. Chem. Soc.*, **1933**, 1525.
12) M. J. Guastalla, *Cahier de physique* **10**, 36 (1942).

the float. The end of the supporting arm is fixed to the torsion weight (2) by the small stopper (13).

The leakage of the film past the ends of the float is prevented by thin silk threads (14) treated with paraffin or vaseline. The metal blocks (15) which ride on the rims of the trough (31) serve the purpose to fix the threads on the rims rapidly and surely with simple technique. At the side of the apparatus, a frame (16) of L-form is equipped being fixed by the screws (17). From the horizontal arm of this frame hang two short chains (18), which suspend the above metal blocks in such a way that the metal blocks just mount on the rims of the trough when the apparatus is just in condition for measurement. When it is necessary to wash the float, it is removed from the position (13) and attached to the clip (19) of the frame (16), which is removable from the system as a whole.

The apparatus also provides the optical system in order to visualize the fine dislocation of the float and to carry out the measurement rapidly in continuous work. A bulb and the convex lens with a slit, both assembled in a container (20), are attached behind the scale (5). Outside the scale, a frosted glass (21) with adjustable scale is attached on which the light image is projected. The torsion weight also provides a small mirror (22) which is movable with the rotation of the float. The other mirror (23), equipped at the lower part of the apparatus is about 4 cm. in diameter and the reflecting plane is adjustable to all direction by manuplation. The path of the light is arranged in such a way that the light image of the slit is reflected via both the moving mirror (22) and the fixed mirror (23) on the frosted glass (21).

By turning the knob (24), the apparatus can be raised until the float leaves the surface of the water. In such position, the apparatus can be turned around the vertical axis of the stand (25). By turning it to the right, the apparatus is made parallel to the length of the trough.

Performance

Operation of apparatus.—The supporting arm of the float is fixed to the clip (19) of the frame, and thin silk threads, treated with paraffin or vaseline, are set across the gaps between both ends of the float and the metal blocks so as to make nearly semicircles. The frame (16) is then dismantled from the apparatus and the floating barrier is allowed to be washed under the tap water. After the washing is over, the frame is reassembled to the apparatus. The apparatus is so set that the length of the float becomes parallel to that of the trough. The supporting arm of the float is removed from the clip of the frame and fixed to the stopper of the torsion weight. After cleaning of water surface, the apparatus is so turned that the length of the float is at right angles to the trough. By turning the knob (4), the cramp (3) is lowered in order to let the weight be free; then, by turning the knob (24), the apparatus is lowered slowly down until the float, as well as threads, is allowed to swim on the surface of the water and the metal blocks come to ride on the rims of the trough (Fig. 2.).

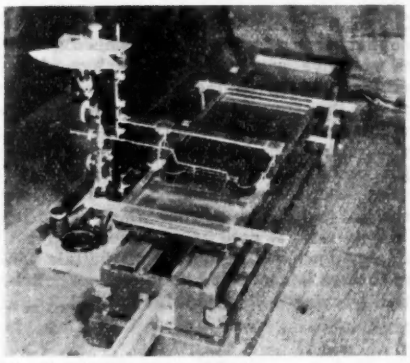

Fig. 2.—Apparatus ready for measurement.

The position of the pointer (6) is set to zero; the light image on the adjustable scale is brought to zero position by manuplating the mirror (23). The film-forming substance is now spread on the surface of water. Since the dislocation of the float due to the film pressures deflects the light image on the frosted glass, zero adjustment is conducted by turning the knob (8) so that the image returns to zero position of the scale. The film pressures exerted here, can be calculated from the readings of the angles thus distorted.

Determination of Film Pressures.—When the torsional angle of α radians is required to bring the dislocated float to zero position, the following equation will hold between the film pressures and the torsional angles

$$\int_{b-e/2}^{a+e/2} F x dx = \frac{F}{2}(a^2-b^2+ac+bc)=\alpha k \quad \text{.....[1]}$$

where F represent the film pressures in dyne per cm., k, the torsion constant of the wire, x, the distance from the torsion wire, a, the distance from the torsion wire to the distant end of the float, b, that to its nearer end, and c, the distance of the gaps at both ends of the float, respectively (see Fig. 1). From the equation [1], follows

$$F=\frac{2\alpha k}{(a+b)(a-b+c)} \quad \text{.....[2]}$$

When the measuring of a, b, and c, are 20.0 cm., 12.0 cm. and 3.0 cm. respectively, using torsion

wire of phosphor bronze of 0.273 mm. in diameter and 8.0 cm. in length gives the sensitivity of 0.273 dynes per cm. per scale degree and the measurable upper limit of about 40 dynes per cm. For lower pressures, the thinner wires are employed. The wire of 0.101 mm. in diameter and 8.0 cm. in length was found suitable for lower pressure measurement, giving the sensitivity of 0.004 dynes per cm. per scale degree and the measurable upper limit of about 0.7 dynes per cm. The torsion constant of the wire was obtained from the period of swing of a torsion weignt whose moment of inertia is possible to compute.

Cleaning of Water Surface.—Sweeping with a moving barrier, made of a paraffined glass rod, does not give perfectly clean surface of water, since the rubbing of the glass rod against the rims of the trough may more or less cause scratching of the paraffin surface. So, a rubbingless barrier is desired in which no scratching might occur. The suggestion is given by the method described by Guastalla.[12] The principle is that a band of talc powder which is sprinkled on the surface, is used as a barrier to arrest the contamination, and the driving of the talc powder thus formed is conducted by air-jet. The scheme of the sweeping is illustrated in Fig. 3. A long glass

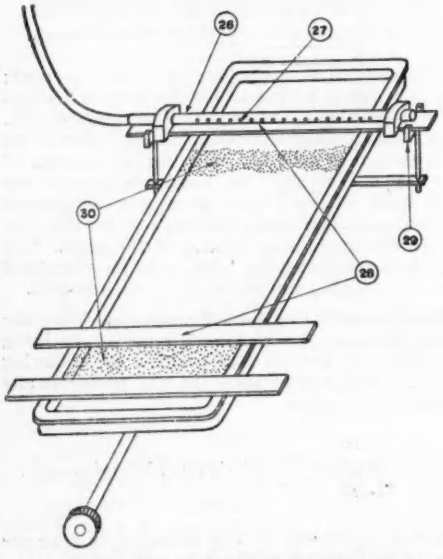

Fig. 3.—Schematic illustration of sweeping of water surface by talc blowing method.

tube (26), with fine orifices (27) along its length, is mounted on the movable glass rod which is held by a rod carrier (29) a short distance above the surface. Talc powder, purified by washing with water, alcohol, and benzene, and then heated properly, is spread on the surface at one side of the trough in the form of a band. Compressed air, filtered by cotton plug and purified by bubbling through the column of water, is sent out from the orifices of the glass tube. The movement of the glass rod with the above glass tube is conducted so that the air stream from the orifices blows off the talc barrier (30) to the opposite side of the trough. When the impurities are collected into the corner of the trough, the glass rod is lowered so as not to be in contact with water, in the order to prevent the talc powder from floating back. Such operation is repeated until the surface pressure attains a constant value.

Prevention of Leakage past the Threads by Sprinkling Talc Powder.—When the measurements are performed in a high pressure region, the operation which is recommended is that a small amount of purified talc powder is sprinkled around the solid-thread connections before the spreading of materials. This operation, though not always necessary, is useful for eliminating the possibility of leakage around the threads, and guarantees the measurement of high pressures up to 30 dynes per cm. or more.

Example

Fig. 4 shows an example of the force-area curve of myristic acid at the air-water interface, measured with this apparatus. The

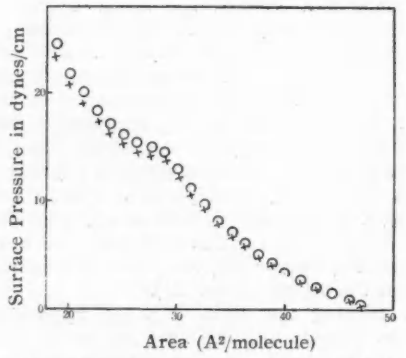

Fig. 4.—Force-area curve of myristic acid on 0.01 N hydrochloric acid at 18.0C°. Circles indicate the pressures determined by this apparatus, while crosses, the pressures by dipping slide method.

results obtained were in good accordance with that of Harkins.[13] The results, moreover, were referred to the one with simultaneous measurement using the dipping slide method. A fairly good agreement was obtained between the two methods. In details, however, it was found that the pressures obtained with the dipping slide method were

13) W. D. Harkins, "Physical Chemistry of Surface Films" p. 112, Reinhold Publ. Co. (1952).

** Purest sample (m.p. 54,5°C) given through the courtesy of Dr. H. Fukuba of the Nutritional Chemical Laboratory of this University, to whom the author's thanks are due.

consistently a little lower than those with this apparatus, and such a trend was emphasized in the higher pressure region, especially above the kink point of the curve. Harkins and Anderson[2] obtained just the same trend with pentadecylic acid and lecithin when they compared the values from both methods of dipping slide and of float balance, and they attributed this discrepancy partly to the errors made in the calibration of film balance. It is, however, noteworthy that the same tendency was obtained under the present experimental condition, where a different type of balance was used. This fact may suggest that this discrepancy may not be of accidental nature as they say, but of something essential associated with the instrumentation. It is rather reasonable to think that the discrepancy is due wholly to the increasing contact angle of the dipping slide owing to the deposition of the monolayer substance.

Summary

An improved apparatus and technique for measuring low film pressures, have been described. Although the apparatus bears resembalance to the Marcelin's balance, the following improvements were achieved in order to enable the low pressure measurement to be generally accessible.

(1) The main construction is laid beside the trough, unlike the usual apparatus whose construction is placed above the surface of water. This design is well suited for minimizing the chance of contamination which more or less occurs on the surface during assembling or operation of the instrument.

(2) Since one of the disadvantages of this type balance lies in the possibility of leakage at the solid-thread connections, especially at the connection between rims of the trough and thread, properly designed metal blocks are used to ensure the perfect connection with simple technique.

(3) An important point in the design of the apparatus is that it should be capable of easy dismantling and reassembling, so that the operation of cleaning can be easily conducted. This requirement is satisfied by the use of a carrier for the float and threads which is easily removable from the main construction of the apparatus.

(4) The float is so designed that the connection between the float and the supporter is an independent bearing, when the float is allowed to be in contact with the water surface. Owing to such construction, the change of water level during run does not matter.

(5) The optical system, which makes the deflection of the floating barrier visible, is equipped with the apparatus. Since the frosted glass, on which the light image is projected, lies just beside the reading scale, observations can be made with no unnecessary delay.

These designs meet well the requirements for measuring low film pressures. Continuous use for eighteen months has shown the apparatus to be very convenient and reliable.

The author wishes to express his hearty thanks to Prof. Taro Tachibana for his helpful advice and encouragement.

Department of Chemistry,
Faculty of Science,
Ochanomizu University, Tokyo

The Catalytic Action of Organic Peroxides on the Polymerization of Ethenoid Compounds. II. The Activity of Substituted Benzoyl Peroxides on the Polymerization of Vinyl Acetate

By Matsuji TAKEBAYASHI, Tadao SHINGAKI and Yasumasa ITO

(Received May 29, 1953)

In the previous work[1] of this series it was established that the activity of symmetrical *m*- and *p*-substituted benzoyl peroxides on the mean velocity of polymerization of styrene is inversely proportional to the square root of the dissociation constants of the corresponding substituted benzoic acids,* and that the rate of polymerization is in a parallel relation

1) M. Takebayashi and T. Shingaki, This Bulletin, **26**, 137 (1953).

*) The mean velocity of polymerization was measured after eighteen hours at 60° C.

to the rate of decomposition of the peroxides. The present paper is concerned with a comparative investigation of the activity of the peroxides on the polymerization of vinyl acetate and of styrene.

The polymerization of vinyl acetate has been carried out with 1/30 mol. of vinyl acetate and 1/3000 mol. of symmetrical *m*- and *p*-substituted benzoyl peroxides at 40°C. and 60°C. in the absence of air, and the effect of peroxides on the rate of polymerization has been measured. The results obtained are summarized in Table 1. In Fig. 1, the overall velocity (v_{Rr}) of polymerization is plotted against the square root of the dissociation constants (K) of the corresponding substituted benzoic acids.

Table 1

Rate of Polymerization of Vinyl Acetate

Substituted benzoyl peroxide	Rate of polymerization (%)		$v_{Rr}\times10^3$, mol./l., min.	
	at 40°C., for 18 hrs.	at 60°C., for 2 hrs.	at 40°C.	at 60°C.
p,p'-Dimethoxy	99.9	98.3	9.91	87.8
m,m'-Dimethoxy	45.2	87.1	4.49	77.8
p,p'-Dimethyl	49.8	96.8	4.94	86.5
m,m'-Dimethyl	37.0	91.4	3.67	81.6
Unsubstituted	46.2	92.0	4.58	82.2
p,p'-Dichloro	31.4	83.8	3.12	74.8
m,m'-Dichloro	6.6	16.8	0.66	15.0
p,p'-Dicyano	4.1	9.0	0.41	8.0
m,m'-Dicyano	3.4	5.9	0.34	5.3
p,p'-Dinitro	0.7	2.4	0.07	2.1
m,m'-Dinitro	1.0	3.6	0.10	3.2
None	0.0	0.3		

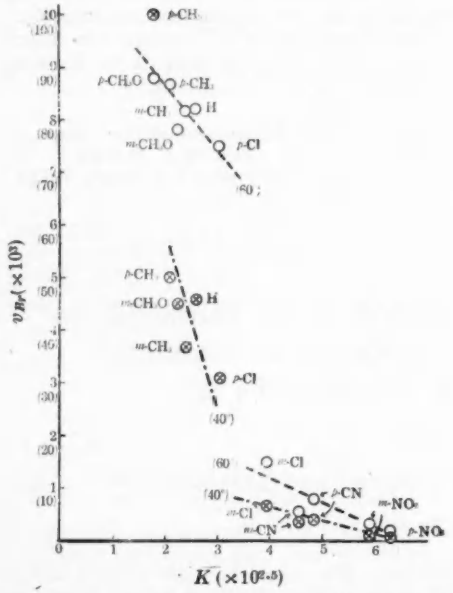

Fig. 1.—Polymerization of vinyl acetate in the presence of substituted benzoyl peroxides at 40°C. and 60°C.

* The numbers in parentheses are those for the data at 60°C.

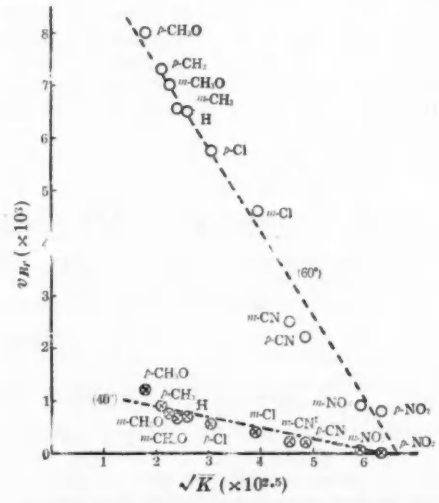

Fig. 2.—Polymerization of styrene in the presence of substituted benzoyl peroxides at 40°C. and 60°C.

Table 2

Rate of Polymerization of Styrene

Substituted benzoyl peroxide	Rate of polymerization (%) at 40°C., for 70 hrs.	Rate of polymerization (%) at 60°C.,* for 18 hrs.	$v_{Pr} \times 10^3$, mol./l., min. at 40°C.	$v_{Pr} \times 10^3$, mol./l., min. at 60°C.
p,p'-Dimethoxy	59.1	99.8	1.18	7.98
m,m'-Dimethoxy	36.9	85.7	0.74	6.85
p,p'-Dimethyl	44.3	91.6	0.89	7.32
m,m'-Dimethyl	33.1	82.0	0.66	6.56
Unsubstituted	35.1	81.5	0.70	6.52
*p,p'*Dichloro	28.6	71.9	0.57	5.75
m,m'-Dichloro	22.3	57.3	0.45	4.58
p,p'-Dicyano	10.3	28.3	0.21	2.26
m,m'-Dicyano	9.7	31.5	0.19	2.52
p,p'-Dinitro	1.4	10.1	0.03	0.81
m,m'-Dinitro	3.1	11.2	0.06	0.89
None	1.1	1.5		

* The data at 60°C. are quoted from the previous paper.

Comparing the results with those obtained in the polymerization of styrene, which are shown in Table 2 and Fig. 2, remarkable differences are recognized in the activity of peroxides and the velocity of polymerization.

In the polymerization of vinyl acetate the peroxides are divided into two groups according to their activities, the one containing effective peroxides, such as dimethoxy-, dimethyl-and *p,p'*-dichloro-benzoyl peroxides,and the other less effective ones, such as *m,m'*-dichloro-, dicyano-, and dinitro-benzoyl peroxides. And the activity of peroxides in each group is nearly inversely proportional to $\sqrt{K}$ at the experimental conditions (Fig. 1), while in the polymerization of styrene the same relation has been satisfied for all peroxides used (Fig. 2).

The polymerization of vinyl acetate proceeded more rapidly than that of styrene, as had been reported.[2] This tendency was observed to be remarkable in the presence of effective peroxides, where the velocity of polymerization of vinyl acetate was found to be about six[3] and over ten times as large as that of styrene at 40°C. and 60°C., respectively. While in the presence of less effective peroxides, the velocity of polymerization of vinyl acetate was observed to be only about two and three times as large as that of styrene at 40°C. and 60°C., respectively.

In the next place, the authors investigated the kinetic order of the thermal decomposition of the peroxides in vinyl acetate at 40°C. and 60°C. by the iodometric method according to the direction of Swain and his co-workers.[4] The decomposition was observed to be of first order at 40°C., but not always exactly so at 60°C. perhaps because of the fact that the polymerization proceeded so rapidly that the condition of decomposition of the peroxides was changed to some extent during the reaction. The rate constant (k_1) is given in Table 3, and that (k_1') in styrene is added in it for the sake of comparison.

Table 3

Rate Constant of Decomposition of Substituted Benzoyl Peroxides

Substituted benzoyl peroxide	$k_1 \times 10^4$, min.$^{-1}$ at 40°C,	$k_1 \times 10^4$, min.$^{-1}$ at 60°C.	log (k/k_0) at 40°C.	log (k/k_0) at 60°C.	$k_1' \times 10^4$, min.$^{-1}$ at 60°C.
p,p'-Dimethoxy	7.36		0.25		17.7
m,m'-Dimethoxy	3.91	34	−0.02	0.0	12.0
p,p'-Dimethyl	4.60		0.05		12.7
m,m'-Dimethyl	2.99	34	−0.14	0.0	11.3

2) For examples: G. V. Schulz and E. Husemann, *Z. physik. Chem.* (B) **39**, 246 (1938); A. C. Cuthbertson, G. Gee and E. K. Rideal, *Proc. Royal Soc.* A, **170**, 300 (1939); G. M. Burnett, *Quarterly Revs.* **4**, 292 (1950).

3) Only in the presence of *p,p'*-dimethoxy-benzoyl peroxide, the polymerization velocity of vinyl acetate was found to be about nine times as large as that of styrene at 40°C.

4) C. G. Swain, W. H. Stockmayer and J. T. Clarke, *J. Am. Chem. Soc.*, **72**, 5426 (1950).

Unsubstituted	4.14	34	0.00	0.0	11.05
p,p'-Dichloro	2.14	18	−0.30	−0.27	9.9
m,m'-Dichloro	1.61	3.2	−0.41	−1.03	8.1
p,p'-Dicyano	0.70	1.8	−0.77	−1.28	4.6
m,m'-Dicyano	0.69	1.8	−0.78	−1.28	4.8

The data given in Table 3 indicate that the greater the electron-repelling effect of substituents, the more rapidly the peroxides decompose in vinyl acetate as well as in styrene, and that the effective peroxides decompose about two to three times more rapidly in vinyl acetate than in styrene at 60°C., while less effective ones decompose about two or three times more slowly, suggesting the solvent effect. Fig. 3 shows the relation between the velocity of polymerization of vinyl acetate and log (k/k_0), where k_0 and k are the rate constants of benzoyl peroxide and substituted benzoyl peroxides, respectively.

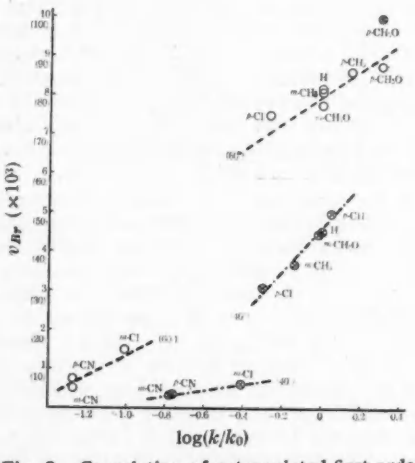

Fig. 3.—Correlation of extrapolated first order rate constants with v_{Br} in vinyl acetate at 40°C. and 60°C.

* The numbers in parentheses are those for the data at 60°C.

The results indicate also that the peroxides are divided into two groups according to their activities, contrary to the results obtained in the polymerization of styrene, and that the activity of peroxides in each group is nearly proportional to log (k/k_0). The above facts lead us to the reasoning that the velocity of polymerization is affected not only by the rate of decomposition of peroxides but also by the activity of radicals derived from peroxides.

Considering that the thermal decomposition of peroxides in vinyl acetate is an uni-moiecular reaction, the radicals acting as the initiator of the polymerization are suggested to be various kinds of benzoate radical RCOO and of aryl radical R, produced by loosing carbon dioxide from the radical RCOO. Then the authors measured the amount of carbon dioxide generated from the peroxides (2/3000 mol.) in vinyl acetate (2/30 mol.).

In the experiments at 40°C. for eighteen hours, carbon dioxide was not generated from all the peroxides except *p,p'*-dimethoxy-benzoyl peroxide. Therefore, it is supposed that the radical acting as the initiator is chiefly RCOO, except in the case of *p,p'*-dimethoxy-benzoyl peroxide. The effects of various kinds of radical RCOO, which should be produced from the peroxides, on the velocity of polymerization were estimated per mol. of RCOO as shown in Table 4.

Table 4

Effect of the Radical RCOO on the Polymerization

Substituted benzoyl peroxide	Extent of decomposition (%)	Amount (M) of RCOO ($\times 10^{-4}$ mol.)	v_{Br}/M (mol./l., min.)
*m,m'*Dimethoxy	34	2.3	0.19
p,p'-Dimethyl	39	2.6	0.19
m,m'-Dimethyl	28	1.9	0.19
Unsubstituted	36	2.4	0.19
p,p'-Dichloro	21	1.4	0.21
m,m'-Dichloro	16	1.0	0.06
p,p'-Dicyano	7	0.5	0.08
m,m'-Dicyano	7	0.5	0.07

The data in Table 4 lead us to the conclusion that there are two groups in the activity of the radical RCOO. From *p,p'*-dimethoxy-benzoyl peroxide 5×10^{-4} mol. of carbon dioxide was produced. The conspicuous effect of the peroxide on the velocity of polymerization is supposed to depend on the activities of *p*-methoxy-benzoyl and *p*-methoxy-phenyl radicals besides the large rate of decomposition of the peroxide.

In the experiments at 60°C. for two hours, on the contrary, carbon dioxide was generated from effective peroxides, not from less effective ones. The result also suggests that two types of radical, RCOO and R, react as the initiator in the presence of effective peroxides, while the radical RCOO reacts chiefly

in the presence of less effective ones. The amounts of carbon dioxide generated are listed in Table 5.

Table 5

Amount of Carbon Dioxide Generated from Peroxides at 60°C.

Substituted benzoyl peroxide	Amount of carbon dioxide ($\times 10^{-4}$ mol.)
p,p'-Dimethoxy	6.8
m,m'-Dimethoxy	3.0
p,p'-Dimethyl	4.5
m,'m-Dimethyl	3.2
Unsubstituted	3.3
p,p'-Dichloro	2.7

The data are in a similar order to those found for the velocity of polymerization at 60°C. in the presence of effective peroxides.

Experimental

Materials.—The vinyl acetate employed was washed several times with water[5], dried over anhydrous sodium sulfate, and fractionated in the atmosphere of nitrogen just before use. b.p. 72°C. All substituted benzoyl peroxides were prepared and purified as described in the previous paper.[1]

Polymerization of Vinyl Acetate.—A peroxide (1/3000 mol.) and vinyl acetate (1/30 mol.) were taken in the reaction tube, the tube cooled in a mixture of solid carbon dioxide and alcohol, and sealed off in a vacuum. The sealed tube was immersed in a thermostat of 40°C. or 60°C. for the reaction time, then removed and cooled in an ice-salt-bath. Unchanged vinyl acetate was driven off in a vacuum and the weight of poly-vinyl acetate was measured. In another experiment, the reaction products were dissolved in acetone and the polymer was precipitated by adding water to the solution. The weight of polyvinyl acetate was almost equal to that of the case mentioned above.

Decomposition of Peroxides.—Owing to the high-volatility of vinyl acetate, the apparatus and experimental procedure were somewhat modified compared with those in the case of the decomposition in styrene. The main part of the apparatus is shown in Fig. 4.

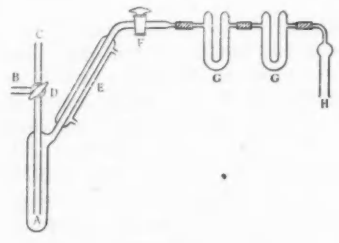

Fig. 4

A is the reaction tube of 22 mm. diameter and 35 cc. capacity, B the inlet tube for nitrogen, C the tube for evacuation, E the cooler with cold water, and G the soda-lime tube for the absorption of carbon dioxide produced. During the reaction a soda-lime tube H was attached to G.

A mixture of peroxide (2/3000 mol.) and vinyl acetate (2/30 mol.) was taken in A and tube A was cooled in solid carbon dioxide and alcohol. After the cock F was closed and the reaction tube evacuated through C, the cock D was closed. Then the tube A was immersed in a thermostst of 40°C. or 60°C. for the reaction time. When the requied time was over, A was cooled again at -30~35°C. in a mixture of solid carbon dioxide and alcohol, the cock F opened, passing pure nitrogen through B into the whole apparatus, and the weight of carbon dioxide absorbed in G was measured. The amount of carbon dioxide was verified by the blank test.

Summary

(1) The activity of symmetrical *m*- and *p*-substituted benzoyl peroxides on the rate of polymerization of vinyl acetate has been investigated at 40°C. and 60°C. in the absence of air.

(2) The peroxides have been divided into two groups according to their activities. The activity of peroxides in each group is nearly inversely proportional to the square root of the dissociation constants of the corresponding substituted benzoic acids in the experimental conditions.

(3) The thermal decomposition of the peroxides in vinyl acetate has been observed to be of first order at 40°C., but not always exactly so at 60°C.

(4) In the decomposition of the peroxides at 40°C., carbon dioxide was not generated from all the peroxides excluding *p,p*-dimethoxybenzoyl peroxide; while in the decomposition at 60°C., carbon dioxide was produced from effective peroxides, such as dimethoxy-, dimethyl-, and *p,p'*-dichloro-benzoyl peroxides.

(5) It has been confirmed that the velocity of the polymerization is affected not only by the rate of decomposition of the peroxides but also by the activity of radicals derived from the peroxides.

(6) The results have been compared with those obtained in the polymerization of styrene.

The authors express their hearty thanks to the Ministry of Education for a grant.

Chemical Laboratory, South College, Osaka University, Osaka

5) S. Okamura, "*Kobunshi-tembo*," **2**, 125 (1950).

LETTER

Separation of Selenium and Tellurium by Means of Cation Exchange Resin

Fumio AOKI

(Received September 4, 1953)

In the cource of studying the analysis of high purity selenium the writer faced the need of separating selenium from tellurium. Reduction of selenite by sulphur dioxide is not only tedious but also unreliable when the amount of tellurium is less than the order of milligram.

A new method by Johnson and Kwan[1] is found to be difficult to perform. Yoshino[2] pointed out that selenium (as selenite) passes through cation exchange resin except when a large amount of iron is present, but he did not mention the behavior of tellurium.

The writer has observed that selenium can be separated from tellurium by applying the solution on a cation exchange resin column.

Experimental

(1) Test solutions:—(a) 99.95% selenium was dissolved in nitric acid, evaporated to dryness, sublimed twice, and the resultant selenium dioxide was dissolved in water. (b) 99.5% tellurium was dissolved in nitric acid, evaporated to dryness, dissolved in the least possible amount of nitric acid; then filtered, and the filtrate was evaporated to drive off most of nitric acid.

The precipitated tellurous acid was washed with hot water, and finally dissolved in the least possible amount of nitric acid. Concentration of each solution was determined gravimetrically.

(2) Resin column:—10 ml. of Amberlite IR 120 (60 mesh) was used as HR type.

(3) Procedure:—25 ml. of slightly acid (<0.05 N) solution, containg 50 to 1000 γ of either selenium or tellurium or both, was dropped on the resin column at the rate of 2 ml./min., followed by 100 ml. of water, 100 ml. of 0.3 N hydrochloric acid and 100 ml. of 3 N hydrochloric acid. Every 25 ml. portion of the passed solution was examined for selenium and tellurium. The examination was made by the stannous chloride reduction method.

(4) Results:—Selenium was found in the first and second portions of the passed solution and in the third portion it was only faintly detected. In the fourth and fifth portions neither selenium nor tellurium seemed to be present. Tellurium appeared from the sixth to the ninth portion.

When the original solution contains iron, lead or copper in comparable amount to selenium or tellurium, heavy metals are separated as well as selenium and tellurium. Heavy metals are, of cource, found in the portions later than the tenth.

Government Chemical Industrial Research Institute, Tokyo-Hatagaya

1) R. A. Johnson, F. A. Kwan: *Anal. Chem.*, **23**, 661 (1951).
2) Y. Yoshino: *J. Chem. Soc. Japan*, **71**, 577 (1950).